# A Mathematical Model for Fractured Reservoirs Using Anomalous Diffusion and Multi-Continuum Approach

By

©Md Mostafijul Karim

A Thesis

Submitted to the School of Graduate Studies

In partial fulfillment of the requirement for the degree of

**Master of Engineering**

**Faculty of Engineering and Applied Science**

Memorial University of Newfoundland

**MAY 2019**

St. John's Newfoundland

# Abstract

An accurate analysis of the characteristic behavior of a fractured reservoir is challenging due to the complex reservoir formation; furthermore, the irregular flow patterns in the discrete domains add to the computational complicacy. The study aims to develop a mathematical model for the fractured reservoir through the utilization of the anomalous diffusion approach and the multi-continuum approach. Firstly, the study reviews both the concepts in details to make a better understanding of the limitations, formulations and the application criteria. A comparative study is done to determine the relative impacts of two approaches in the reservoir at different flow periods. Consequently, a linear model is developed for the reservoir flow towards a hydraulically fractured horizontal well at the transient condition. The derivation considers a modified tri-linear model with different arrangements of the matrix and fractures. The solution is derived in the Laplace domain, and numerically it is inverted to the real-time domain by the Stehfest algorithm. The study shows that the continuum-based approaches differ for the different fracture network, inter-flow condition, continuum-number, and the interface transfer function whereas the anomalous diffusion approach captures the heterogeneity of the reservoir by the fractional time or space derivative. The evidence from the comparative study suggests that a combination of the continuum approach and the anomalous diffusion is recommended as an alternative approach for the modelling of fluid flow in a fractured reservoir. In the developed model, the influence of the super-diffusion in the hydraulic fracture is remarkable as it alters the pressure response during the whole life of the reservoir. However, the sub-diffusion impact increases with the time and is significant at the late stage. The study also shows that Macro-fracture permeability regulates the pressure drop in the reservoir as it is the primary conduit in the inner reservoir. The combination of the approaches and the logical distribution of the flow conditions are shown as the better alternative to the conventional method.

**To**

***My Parents***

**(Abbu & Ammu)**

# Acknowledgement

I would like to express my greatest appreciation and respect to my supervisor Dr. Syed A. Imtiaz for his valuable guidance, generous support and encouragement throughout my research. Thanks to his assistance, insightful instruction and constructive feedback that make my research better.

I would like to express my gratitude and respect to my former supervisor Dr. M Enamul Hossain, for giving me the opportunity to be a part of his research group. I am thankful to him for his guidance, support, inspiration, and valuable instruction in my research.

I would like to thank all the faculty members and the staffs of Process Engineering department at Memorial University of Newfoundland for their support.

In addition, I would like to thank Moya Crocker, Tina Dwyer, and Collen Mahoney for creating a friendly environment and their cordial cooperation, continuous support during my program.

Thanks, and gratitude goes to my all of my research colleagues for their assistance, support, cooperation, and for making a family environment that gives the mental strength to conduct my research.

I would like to thank Natural Sciences and Engineering Research Council of Canada (NSERC); Research & Development Corporation of Newfoundland and Labrador (RDC), and Statoil Canada Ltd., for providing financial support to accomplish this research under Statoil Chair in Reservoir Engineering at the Memorial University of Newfoundland, St. John's, NL, Canada.

My greatest gratitude goes to my parents and to my family members.

# Table of Contents

# List of Figures

# List of Tables

# Chapter 1 Introduction

A naturally fractured reservoir contains a significant portion of the world's fossil fuel reserve. According to the Schlumberger market analysis (2007), more than sixty percent of the world's proven oil reserve and forty percent of the gas reserve are conserved in the fractured carbonate reservoir. Although carbonates and shales are the most common formation of the fractured reservoir, it also belongs to the sandstone, cherts, and the igneous or metamorphic rocks. The fluid that travels through the fractured reservoir pursues a complex path and the production performance of the reservoir also traces this complexity. The fluid flow modelling is a vital tool for the reserve estimation, characterization, and the production optimization of a reservoir. This study aims to develop a linear mathematical fluid flow model for fractured reservoirs and intends to make a better prediction on the reservoir performance. The following discussion states the problem statement, key ideas, objectives, procedures, contributions, and the organization of this research.

## 1.1 Problem Statement

A fractured reservoir can be defined as a formation of altered matrices and fractures. The fluid travels a complex path in such a reservoir. The fracture and the matrix have different flow parameters; therefore, the pressure response at the well contains the contributions of both. The fluid transfer between two adjacent domains depends on the relative storability of the domain and the transfer surface at the mutual boundary of the domains. The modelling of the fluid flow in a fractured reservoir, thus, requires the proper evaluation of the flow at each distinctive regions of the reservoir. Fluid flow condition, either transient or the semi-steady state, is another concern for the modelling.

For the volumetric reservoir, pressure diffusion is the dominant mechanism for the fluid flow. In the classical diffusion, the pressure gradient is a local character; hence, the value of the pressure gradient at a point is considered an instantaneous property and depends on the pressure value at the vicinity of that position. Classical diffusion also assumes a Brownian motion of the particles, and the diffusion process follows the exponential law. Conversely, the anomalous diffusion occurs when the particles have a non-Gaussian distribution. The mean square displacement of the individual particle follows a power law instead of a proportional relationship with time (Fomin et

al., 2011; Raghavan, 2011; Chen and Raghavan, 2015). The particle is treated as a continuous time random walker (CTRW), which can randomly jump or wait (Montroll and Weiss, 1965; Fulger et al., 2008). The waiting time of the particle at the interval of two successive movements is not a constant one. Depending on the time and space event the waiting time is shorter or longer. When the space event dominates the flow, it accelerates the particle movement, and super-diffusion occurs (Montroll and Weiss, 1965). When the flow path restricts the flow, conversely, the waiting time becomes longer, and the time effect controls the flow, which causes sub-diffusion (Caputo, 1998).

Transient flow is the dominant flow condition for the fractured reservoir flow. Gringarten et al., (1974) proposed the following formula to predict the time when boundary dominated flow (Pseudo-steady state) is developed around a vertical fracture with an infinite conductivity

$$t \geq \frac{1.14 * 10^4 \, \phi c_t \mu x_F^2}{k} \tag{1.1}$$

Naturally fractured reservoir has very low permeability (k). Thus, in case of a substantial fracture length ($x_F$) the transient condition is elongated for a longer time. Raghavan et al. (1997) have shown that the transient condition is the prevailing flow condition when the fluid flows toward a fractured horizontal well and it can be prolonged to the most of its production-life. According to the Sharma and Aziz (2004), higher compressibility of the reservoir fluid makes a delay in initiating the boundary dominated flow up to 10 days. In general, the pressure transient tests run for a duration of 1 to 2 days. Therefore, the reservoir fluid is flowing at the transient condition during the determination of the reservoir parameters. The assumption of the transient fluid flow condition, thus, is more appropriate for flow modelling of the fractured reservoir.

A transient pressure response curve ($t_D \; vs \; p_D$) of the homogeneous reservoir has a constant slope because the reservoir-drainage area consists of a single formation. On the other hand, for a fractured reservoir the curve shows a slope change at the early stage and at the late stage. The change of the pressure-depletion trend at a particular time depends on the individual continuum parameters which are being drained at that time (Abdassah and Ershaghi, 1986). Depending on the depletion criteria, the slope is steeper or flatter than the homogeneous response. According to the dual or triple continuum approaches the slope of the curve depends on the relative storability

and the inter-porosity flow parameter of the different continuum. Nevertheless, an anomalous-slope change is observed in case of the hydraulically fractured reservoir that cannot be explained by the multi-continuum approach.

The proper analysis of the pressure depletion for a reservoir is essential for its characterization and the production optimization. A misinterpretation of the pressure transient test data causes an inaccurate prediction about the reservoir performance. Additionally, the proper evaluation of the reservoir parameters and the pressure responses are essential for the production design and reserve estimation. For instance, highly permeable fractures may feed the well at the early stage that causes a high production rate and makes an overestimation in the reserve calculation.

Dual porosity concepts have introduced a new continuum in the homogeneous reservoir to correlate the slope change with the inter-porosity flow of the continuums and remarks that the individual portion in the response curve reflects the domination of the separate continuum (Warreen and Root, 1968). Abdassah and Ershaghi (1986) have considered a new continuum in the model, either a fracture or a matrix, and relates the slope of the response curve with the storability ratio and the inter-porosity flow parameters. They work with both of the strata model and the block model. Jalali and Ershagi (1987) have modified the triple porosity model and extended it to the dissimilar matrix types. Al-Ghamdi and Ershagi (1996) have studied a model with dissimilar fractures and with a radial flow condition. Alahmadi (2010) has proposed a linear triple porosity model and follows the El-Banbi (1998) linear flow solution for a fractured horizontal well. The proposed model reservoir consists of matrix and two set of orthogonal fracture, the micro-fracture and the macro-fracture. Brawn (2009) has developed a tri-linear model for the hydraulically fractured horizontal well and assumes linear flow for all regions; the outer reservoir, the stimulated inner reservoir, and the hydraulic fractured. Ozcan (2014) has modified the tri-linear model by considering anomalous diffusion in the inner reservoir. Furthermore, Albinali (2016) has studied another modification of the tri-linear model by assuming anomalous flow both in the inner reservoir and in the outer reservoir.

Dual and triple porosity models use the intrinsic properties of the reservoir; those are difficult to determine for a fractured reservoir. Moreover, the flatter slope of the pressure response curve at an early time cannot be explained by the dual or triple porosity model. On the other hand, tri-

linear models consider the reservoir geometry in more details and the assumption of the anomalous diffusion eliminates the requirements of the extra intrinsic properties. However, the determination of the anomalous coefficient contains a significant uncertainty. The anomalous behavior of the fractured zone due to the space event within the hydraulic fracture is out of consideration in the previous studies (Brawn, 2009; Ozcan, 2014; Albinali, 2016).

This study aims to eliminate these limitations and proposes a combination of the continuum approach and the anomalous diffusion. Furthermore, this research handles the impacts of the time and space separately at different regions of the reservoir with the proper anomalous diffusion equations.

### 1.2 Key Ideas

The study considers a modified Tri-linear structure (TLM) to develop a mathematical flow model that follows a logical combination of anomalous and conventional flow. The combination is based on the following arguments:

1. Sub-diffusion is occurred in the outer reservoir, an area beyond the tip of the hydraulic fracture and the unstimulated zone in a fractured reservoir. Due to the internal structure, this area has the higher resistance to the fluid flow. Consequently, the time effect becomes a dominant factor in the overall flow that causes a slower-flow than the usual.
2. Fluid flow follows conventional diffusivity law in the inner reservoir and this area is approximated by a multi-continuum structure. The inner reservoir is a stimulated zone between two hydraulic-fracture and contains a number of induced fractures. The construction of the inner reservoir can be approximated by the core data, well log data, and the other methods of formation evaluation. Thus, the orientation and the density of the fractures and the physical properties of the matrixes and the fractures can readily be determined for the inner reservoir.
3. Super-diffusion process takes place in the hydraulic fracture. The stimulation process creates a better conductive region in the hydraulic fracture because it creates and connects the fractures and enlarges the existing fractures. Therefore, the space events control the flow in this region and make a faster flow than the natural.

### 1.3 Purpose Statement

The objectives of the study are:

- **a.** To review the fundamentals of anomalous diffusion process in the fluid flow; additionally, analyzing the formulation and definition of the basic concept of anomalous diffusion, known as memory concept, from different standpoint to distinguish the memory effect from the other types of non-local impact in the fluid-flow.
- **b.** To review the fluid flow models for the fractured reservoir and investigate their assumptions, formulations, and limitations.
- **c.** To conduct a comparative study on the different flow models for the fractured reservoir to determine the appropriate approach.
- **d.** To develop a linear mathematical flow-model for naturally fractured reservoirs and solve the model analytically in case of hydraulically-fractured horizontal well.
- **e.** To analyze the pressure response of the solution for finding the effect of different regions of the drainage area on the overall pressure response at the bottomhole of the well and the conditions for production optimization.

### 1.4 Procedure Statement

The study makes a comparison between the anomalous diffusion method (Chen and Raghavan, 2015) and the linear triple porosity approach (El-Banbi, 1998; Ahmadi and Wattenbarger, 2011). The comparative analysis considers characteristic distinct physical structure for each approach and derives the analytical pressure solution in Laplace domain. To compare the responses of the approaches, it maintains the dimensional consistency in the physical models.

The tri-linear reservoir model (Brawn, 2009; Ozcan, 2011) is the basic structure for the development of the multi-continuum anomalous model. Either a conventional or a modified, continuity equation represents the flow type in separate region. The pressure solution is derived in the Laplace domain and the coupling between the two adjacent regions is done by appropriate boundary conditions. Caputo's (Caputo, 1969) definition and properties of the fractional derivative are used to solve the sub-diffusion equation whereas the basic properties of the mittag-Leffler function (Hombole *et. al.,* 2011, Fomin *et. al.,* 2010) are used for the solution of the super-diffusion process. The linear flow solution in the inner reservoir follows the procedures of

El-Banbi (1998), Brawn, 2009, and Ozcan, 2011. The solution is numerically inverted to the time domain based on the Stehfest algorithm (1970). The pressure response is generated and analyzed by MATLAB_R2016a.

### 1.5 Contribution of the Study

This study investigates different approaches for the fluid flow modelling of a naturally fractured reservoir, inspects the particular physical arrangements, analyses the contrasts among the different models, and examines the mathematical formulations and their limitations.

This study also discusses the current concept of memory in different fields and critically analyses the representative mathematical tools for each corresponding model. The idea of anomalous diffusion in the petroleum engineering is critically reviewed.

To determine the better representative model of the fractured reservoir, the study conducts a comparative analysis on two standard approaches for the fluid flow modelling of a naturally fractured reservoirs: the anomalous diffusion and the multi-continuum approach.

The adaptation of the triple porosity model in the inner reservoir region in a Tri-linear model to capture the heterogeneity in a naturally fractured reservoir is used for the first time in this study. The logical combination of sub-diffusion, super-diffusion, and linear axial flow for evaluating the performance of a hydraulically-fractured horizontal well is another innovative approach in this research.

### 1.6 Organization of the Thesis

The thesis consists of six chapters and three appendices as follow

Chapter 1 is the introduction of the thesis that contains the problem statement, key idea of the research, objectives, procedure of the study and the contribution of this research.

Chapter 2 reviews the memory concept which is the fundamental idea of anomalous diffusion. This chapter investigates the definitions of memory, makes the comparison of the non-Darcy flow and anomalous diffusion, and shows the application of the memory concept in the petroleum reservoir.

Chapter 3 presents the literature review on the fluid flow models for the fractured reservoir, classification of the models, physical structures and the limitations of different approaches.

Chapter 4 develops a simplified model using the anomalous diffusion approach and multi-continuum approach and compares the responses to determine the characteristic limitations of the approaches.

Chapter 5 is devoted for the development of a linear mathematical model for the fractured reservoir using both the anomalous diffusion and the multi-continuum approach. The derived solution is validated by comparing them with the existing models and with the field data. The responses of the model are analyzed to determine the effect of the different parameters on the bottomhole pressure depletion.

Chapter 6 contains the conclusions and the recommendations of the study

Appendix A includes the derivation of the continuity equation for the anomalous diffusion and the derivation of the multi-continuum anomalous diffusion model.
Appendix B presents the derivation of the flow solution for a rectangular matrix block
Appendix C shows the derivation of the pressure solution for a two-dimensional linear flow in the hydraulic fracture.

**References**

Abdassah, D., & Ershaghi, I. (1986). Triple-porosity systems for representing naturally fractured reservoirs. SPE Formation Evaluation, 1(02), 113-127.

Alahmadi, H. A. H. (2010). A Triple-porosity model for fractured horizontal wells (Doctoral dissertation, Texas A & M University).

Albinali, A. (2016a). Analytical solution for anomalous diffusion in fractured nanoporous reservoirs. Colorado School of Mines.

Brown, M., Ozkan, E., Raghavan, R., & Kazemi, H. (2011). Practical solutions for pressure-transient responses of fractured horizontal wells in unconventional shale reservoirs. SPE Reservoir Evaluation & Engineering, 14(06), 663-676.

Caputo, M. (1969). Elasticitá e dissipazione (Elasticity and anelastic dissipation). Zanichelli Publisher, Bologna). Michele Caputo, M. (1997): Rigorous time domain responses of polarizable media. I, Ann. Geofis, 40(2), 423-434.

El-Banbi, A. H., & Wattenbarger, R. A. (1998, January). Analysis of linear flow in gas well production. In SPE Gas Technology Symposium. Society of Petroleum Engineers.

Fomin, S. E. R. G. E. I., Chugunov, V., & Hashida, T. O. S. H. I. Y. U. K. I. (2011). Mathematical modeling of anomalous diffusion in porous media. Fract. Differ. Calc, 1(1), 1-28.

Haubold, H. J., Mathai, A. M., & Saxena, R. K. (2011). Mittag-Leffler functions and their applications. Journal of Applied Mathematics, 2011.

Ozcan, O. (2014). Fractional diffusion in naturally fractured unconventional reservoirs. Colorado School of Mines.

Raghavan, R. (2011). Fractional derivatives: application to transient flow. Journal of Petroleum Science and Engineering, 80(1), 7-13.

Stehfest, H. (1970). Algorithm 368: Numerical inversion of Laplace transforms [D5]. Communications of the ACM, 13(1), 47-49.

Warren, J. E., & Root, P. J. (1963). The behavior of naturally fractured reservoirs. Society of Petroleum Engineers Journal, 3(03), 245-255.

Raghavan, R. "Fractional derivatives: application to transient flow." Journal of Petroleum Science and Engineering 80.1 (2011): 7-13.

Fulger, D., Scalas, E., & Germano, G. (2008). Monte Carlo simulation of uncoupled continuous-time random walks yielding a stochastic solution of the space-time fractional diffusion equation. Physical Review E, 77(2), 021122.

Montroll, E. W., & Weiss, G. H. (1965). Random walks on lattices. II. Journal of Mathematical Physics, 6(2), 167-181.

Caputo, M. (1999). Diffusion of fluids in porous media with memory. Geothermics, 28(1), 113-130.

# Chapter 2 A Critical Review on Memory Concept: Anomalous Diffusion and Non-Darcy Flow

**Preface**

Memory is the fundamental concept for understanding the behavior of the anomalous diffusion. The concept of memory is one of the most expanding ideas in fluid flow modeling. The recent advancement and the continuing research, moreover, makes it more promising in its potential application in the petroleum field. In the existing literature, there are a variety of perspectives about the definition of memory. This chapter discusses the current concept of memory in different fields and critically analyzes the representative mathematical tools for each corresponding model. This will conveniently facilitate the conceptualization of the memory. A discussion on the fractional derivative will clarify its relationship with memory. In practice, the integro-differential tool is widely used for escalating the memory formalisms and its impact on modeling complex reservoirs. A general definition of memory as a time-dependent phenomenon or as a deviation of Darcy flow in porous media, make it tumultuous with the term like the non-Darcy flow and the transient flow. Considering this fact, this study emphasizes the distinction between memory and the non-Darcy and the transient flow. There are diverse perspectives in the application of memory in petroleum reservoir engineering. This paper investigates these perspectives and comprehensively analyzes their formulations and limitations. Reviewing the difficulties in the implementation of the memory in the petroleum reservoir flow gives direction for the future research.

## 2.1 Introduction

Memory is the phenomenon which occurs if the medium itself and fluid that flows through the medium have a continuous interaction and the system traces the previous track at the present performance. The variations of the rock and fluid properties are usually included to modify the governing equations. Memory modifies the basic flow model by incorporating the effects of time which are created by the flow history from the alteration of rock and fluid properties.

The Memory has different definitions and formulations depending on the fields. In physics, memory is the psychological arrow of time that not only records the events of a system but also interacts with that system. It correlates with the system and moves forward or backward along the same direction of thermodynamic changes of that system, i.e., entropy change (Mlodinow *et*

*al.* 2014). In Geotechnics, memory is the criteria that causes and controls the propagation of fracture within a solid formation which is under the conditions of stress (Christensen *et al.* 2004). In earth science, memory is the time-dependent pore pressure diffusion due to fluid flow (Raileigh *et al.* 1976, Bell and Nur, 1978). In fluid flow modeling, memory is an approach to evaluate fluid flow under a frame of reference of internal observation by considering the matter and molecules within the flow (Hossain *et al.* 2006). Some studies represent memory with time-dependent correlations, by using a non-equilibrium expression within the equation or as the deviation part from the constitutional equations. In fluid flow through porous media, the effect of memory is represented with the integro-differential operator (Caputo, 1999; Iaffaldano *et al*. 2006; Hossain *et al.*, 2006; 2009; and Giueppe *et al.*,2009).

Memory concept creates a new era in reservoir engineering because the conventional approaches deal with the variation of fluid, solid, and semi-solid structure of the fluid medium properties. However, memory includes the effect of compositional and structural alteration of the fluid and medium over the flow time. There are three trends in characterizing memory in petroleum engineering. For the conventional reservoirs (permeability is ranged from Darcy to millidarcy), the impact of memory appears in the modification of the constitutive equations, and the corresponding fluid and rock properties which is directly related to time (Hussain *et al.*, 2006; 2007; 2008; 2009; and 2013). For unconventional reservoirs (permeability of Nano Darcy), an anomalous diffusion is assumed to be existent in the reservoir. This anomalous diffusion is characterized with the aid of the fractal parameters or by the modification of the flux law with the fractional time and space derivative (Chang and Yortos, 1990; Raghavan 2011; Chen and Raghavan 2015; Holy and Ozkan, 2016; Alibini *et al.*, 2016). In other approach, the impact of memory is evaluated in the homogenizing process of the flow between different subdomain and is related to the kernel of the integro-differential operator (Panfilov *et al.*, 2013; and Rasoulzadeh *et al.*, 2014).

This paper analyzes the definitions of memory in different fields and evaluates their mathematical expressions in a critical manner. There is a brief discussion on the non-Darcy flow in porous media. This intensive investigation clarifies the difference between memory and non-Darcy flow. The study also contrasts the time-dependent behavior of transient flow and the impact of memory on reservoir flow. Investigation on the application of memory in the

petroleum field updates the recent advancement in this new field. The discussion on challenges will make way for future research in this area.

area.

## 2.2 Memory Concept

Memory can be conceptualized as an anomalous behavior in the fluid flow, the time-dependent variation of the system properties or as the trace of the interaction of essential components of a system. Table 2.1 highlights the defining criteria of memory in different fields and tries to find out the mathematical roots of each approaches. The following section discusses the concepts in detail.

### 2.2.1 Geo Mechanics

In 1976, Raileigh *et al.* conducted an experiment at an oil field in Rangely, Colorado to correlate field pressure and earthquake frequency in an active zone. By measuring fluid pressure, they could predict the beginning of the earthquake. When the pressure diffusion within the formation was modelled, they faced some problems in utilizing the classical Darcy law, because the model was not able to solve their challenges. Later, in 1978, Bell and Nur encountered the same limitations in their interpretation of the relationship between hydrostatic pore pressure and seismicity in a fracture zone. Their investigation yields a time-dependent pore pressure diffusion due to fluid flow which is treated as memory in Geo Mechanics (Raileigh *et al.* 1976; and Bell and Nur, 1978). Roeloffs *et al.* (1988) investigated the stability of faults for the variations in water level. The study found that pore pressure diffusion depends on the compressibility of the rock and fluids. Depending on the stress condition, the impact of the periodic variation of the water level on the pore pressure is a time-dependent criterion. They validated their observation by using coupled and uncoupled stress equation and with field data.

### 2.2.2 Turbulent Fluid Flow

Shin *et al.* (2003) found a non-equilibrium effect on the segregation velocity of particle. The effect goes in the direction of the turbulence level in fluid flow which is generally decreasing. The flow contains an impact of previous mean and fluctuating velocities. This creates a non-equilibrium effect on particle deposition inside the turbulent boundary layer during the transportation of the inertia dominated particles. The effect of earlier motion on current flow is

termed as memory and modeled based on the intermediate diffusion time scale and mechanism of flow. Shin *et al.* (2003) modeled the turbophoretic velocity as

$$v_t^+ = \frac{24\,\tau_P}{R_{ep} C_D}\frac{d}{dy}\left(\zeta - D_{yy}\frac{dv_y}{dy}\right)\frac{1}{u^*} + \frac{24\,\tau_P}{R_{ep}\,C_D}\frac{d}{dy}\left(\tau_B\frac{d\zeta_{yy}}{dy}\right)\frac{1}{u^*} \qquad (2.1)$$

The last part of the equation represents the non-equilibrium effect due to memory.

### 2.2.3 Fluid Flow with Yield Stress

Chen *et al.* (2005) studied the mobilization and subsequent flow of the fluid with a yield stress, i.e., Bingham plastic, in a porous medium. With a yield stress, during the two-phase fluid flow in porous media, a minimum threshold for displacing fluid from the pore throat is always required (Rossen and Gauglitz, 1990). When an individual pore throat influences the capillary expression of fluid flow, there is a relationship between pore geometry and pressure gradient (Rossen, 1990; and Copx *et al.*, 2004). To evaluate this relationship, the concept of minimum threshold path (MTP) was proposed based on the simple percolation model (Rossen and Mamun, 1993), and percolation cluster within porous media (Feder, 1988). Identification of MTP is always challenging because of the complex formation geometry, i.e.; tortuosity. Therefore, a new concept is proposed to overcome this challenge, the invasion percolation with memory (IPM) (Kharabaf, 1996; Kharabaf and Yortsos 1997, 1998). In the absence of the flow effect, the static problem of single phase (Kharabaf and Yortsos 1997) and two phase (Kharabaf and Yortsos 1998) fluid flow with yield stress are discussed along with the properties of MTP. The static condition and formation microstructure also impose a dynamic effect on the flow rate and pressure gradient relationship at the mobilization of fluid flow, similar to the viscous effect (Falls *et al.* 1989, Sahimi 1993, Shah and Yortos 1995, Tian and Yao 1999, Shah *et al.* 1998, Xu and Rossen, 2003). Chen *et al.* (2005) worked with two types of cases, the static case and the dynamic case of which the viscous effect is important. Based on the algorithm of IPM, they proposed a pore network model with a distributed yield stress threshold. Memory appears in their model as the microstructure influence of pore network on fluid flow. The minimum threshold path between the two neighboring boundaries along which the sum of the threshold is minimized, controls the initial mobilization of fluid within the pore network. They modeled the mobilization and fluid flow in pore throat by the single capillary expression. In the model, the relationship between applied pressure gradient and flow rate for single phase flow is a function

of the microstructure. In conventional porous media, the relationship depends on the variable conductance of the pore throat. For example, against an applied pressure gradient, the increment rate of the fraction of the pore that belongs to the open path is lower in the dynamic case than in the static case.

### 2.2.4 Fluid Flow in Porous Media

Caputo (1999) modified Darcy's law with a fractional derivative to model the diffusion process in porous media. He started by using Rice and Cleasly (1976) formulation for the core equation of stress-induced fluid flow. This is the combined form of Biot's (1941) stress-strain relationship equation and the continuity equation, which satisfies the stress equilibrium and compatibility conditions. The study replaced the constant of consolidation (c) by pseudodiffusivity (A) and used Darcy's modified equation for the expression of mass flux rate. To illustrate the memory effect, he worked with the following uncoupled equation:

$$A\left(\frac{\partial^{\alpha}}{\partial t^{\alpha}}\right)\left(\frac{\partial^{2} p}{\partial x^{2}}\right) = \left(\frac{\partial p}{\partial t}\right) \tag{2.2}$$

Using Caputo's (1969) definition of fractional derivative, Caputo (1999) analytically solved the equation and found the solution as a form of a green function as follow:

$$P(x,t) = P(0) + \left(\frac{C_1}{\pi}\right)\int_0^{\infty} [\exp(-rt)]\left[\exp(-r^{\frac{z}{2}} A^{\frac{-1}{2}}\, x\, \cos\frac{z\pi}{2}))\right] \sin\left(r^{\frac{z}{2}} A^{\frac{-1}{2}}\, \sin\left(\frac{z\pi}{2}\right)\right) dr \tag{2.3}$$

Where z = 1 – α

To model the pressure distribution, he considered four types of boundary conditions: (i) delta pressure fluctuation, (ii) zero pressure, (iii) sinusoidal pressure, and (iv) constant pressure at the boundary. Zero or constant pressure was assumed at the half space of the medium. These boundary conditions are convolved with the Green function (Eq. 2.3), and a numerical investigation is made to evaluate the impact of memory. Caputo observed that in the case of step pressure, the variation of pressure with distance and time depends on memory parameter (z). When there is a zero pressure at the boundary, constant pressure at half space of the medium, and an increasing value of memory (α), pressure transforms more slowly from the half space and the time required to gain the maximum pressure gradient at a particular distance is delayed. When there is a sinusoidal pressure at the boundary, both the phase differences increase, and a growth of phase lag is also observed along the medium because of the impact of memory. Finally, when there is a constant pressure at the boundary, the effect of memory slows pressure response, which

travels more gradually through the medium. The amplitude of the pressure is decreasing at a certain distance from the medium. Based on these observations, the researcher recommended that the permeability of the medium is changing with time. This change impacts the current pressure diffusion within the medium at present. This scenario resembles the recollection of previous events. According to Caputo (1999), the deviation of permeability is caused for two reasons: (i) the effect of previous pressure gradient, and (ii) phenomena that are related to fluid flow, i.e. chemical reaction, mineral precipitation, temperature variations and fluid, solid interactions. However, Caputo's (1999) approach did not provide a complete numerical solution of the governing equation with fractional derivative, however it did numerical investigation of the Green function. It did not provide any physical basis for the value of α and assumed value for the pseudodiffusivity without experimental validation. Caputo's (1999) study is a comparative investigation based on mathematical findings, but as it does not consider experimental or field data, it is weakly connected to the actual scenario of flow in the porous medium.

Caputo (2000) extended his previous work and modeled fluid flux diffusion with memory. He modified the Darcy equation by a convolution of the integrodifferential operator at both sides, i.e. fluid flux and pressure gradient. In the same way, he changed the equation of state and considered time-dependent fluid rheology. The modified equations are presented in Eq. 2.4 and Eq. 2.5 as:

$$\left(a + b\,\frac{\partial^{m_2}}{\partial t^{m_2}}\right)P = \left(\alpha + \beta\,\frac{\partial^{m_1}}{\partial t^{m_1}}\right)m \tag{2.4}$$

$$\left(\gamma + \varepsilon\,\frac{\partial^{n_1}}{\partial t^{n_1}}\right)\bar{q} = \left(c + d\,\frac{\partial^{n_2}}{\partial t^{n_2}}\right)\frac{\partial p}{\partial x} \tag{2.5}$$

where a, b, c, d, α, β, ε, γ, and n are the parameters which scale up the memory impact in the flow modeling. This approach gives flexibility to model fluid flow with more time dependent rock and fluid properties and adaptability to match with experimental data in the evaluation process. The study examined two models. Model I was simplified by considering time independent fluid properties, and Model II modified the equation of state. Following the same solution procedure of previous work (Caputo, 1999), Caputo showed the Green function for the first model is:

$$q\,(x,t) = \left[\frac{2a}{\alpha A^{\frac{1}{2}}(1-n)\pi\left(xA^{\frac{-1}{2}}\right)^{\frac{(3+n)}{(1-n)}}}\right].\int_0^{\infty} u^{\frac{2(1+n)}{(1-n)}}\left[\exp(-\frac{u^{\frac{2}{(1-n)}}}{y})\right].\left\{\exp\left[-u\,\sin\frac{n\pi}{2}\right]\right\}.\cos\left[\left(\frac{n\pi}{2}\right)\right.$$
$$\left.-u\,\cos\frac{n\pi}{2}\right)]\,du \qquad (2.6)$$

$$A = \frac{\alpha d}{\gamma a} \qquad r = \frac{uA^{\frac{1}{2}\frac{2}{(1-n)}}}{x} \qquad y = \left(\frac{x}{A^{\frac{1}{2}}}\right)^{\frac{2}{(1-n)}}_{t}$$

Here the dimensionless pseudo-diffusivity (A) and boundary variable (y) are the combinations of memory parameters. This approach tried to explain the flux diffusion with memory instead of pressure diffusion by convolving this green function with different boundary conditions. It is found that flux diffusion slows down with effects of memory i.e. with the increasing order of differentiation. Although the amplitude of the maximum flux increases with memory, the average velocity decreases. Memory acts as a low pass filter in fluid diffusion. However, it is less sensitive to low frequency content of flow (e.g. phase lag, velocity), in contrast to pressure diffusion. All the analyses in these studies are based on the mathematical formulations and tried to understand the influence of memory related parameter on the response of the overall equation in different conditions. So, for the deficiency in the experimental validation and numerical analysis, the study is not able to model the overall flow performance with memory in real applications.

Iaffaldano *et al.* (2006) investigated fluid diffusion with memory in a porous medium. They measured the diffusion in a sand sample and observed that flux decreases with time, indicating that the permeability of the medium varies. They slightly modified the Caputo's model (Caputo, 2000) for one-dimensional flow and determined the memory parameters of the model by fitting the experimental finding with it. Although this study offered an experimental basis of the Caputo model, it worked with a sand column. Stress-induced consolidation and hence permeability reduction is a common observation in such settings (Schutjens, 1991). Therefore lack of, a clear distinction between the effect of memory and the compaction, as well as a short flow history (i.e. 10 hours) are the limitations of this study.

Giuseppe *et al.* (2010) used a similar mathematical model as Caputo (2000) and experimentally validated the model. In comparison to Iaffaldano *et al.* (2006) they worked on six types of porous media. The media was both homogeneous and non-homogeneous and used a vertical cylinder as

the sample chamber. They adapted their experimental data to the model and determined the memory parameters. Medium with high porosity have a high memory effect because of the high compaction. Large grain size increases the impact because of the higher probability what will change the formation shape. They found higher memory accumulation in the heterogeneous formation, and medium density increases the effect. However, this study has done an intensive experimental work, but it has the same limitations as Iaffaldano *et al.* (2006).

### 2.3 Memory and Non-Darcy Flow

For fluid flow modeling in a porous medium, the Darcy model is to date the most widely used and accepted equation formulated by an experimental investigation of the flow of water through a sand pack (Darcy, 1856). The model is valid for homogeneous viscous fluid flow in isotropic porous media. Darcy related the volumetric flux to the pressure gradient with a proportionality constant. Later, this constant is evaluated as permeability (Hazen 1892, Wenzel 1942, Jacob 1946, Rose, 1949). For the validity of Darcy's model, the original conditions are the proportional relationship of volumetric flux, pressure gradient, and the independent nature of permeability to fluid type. A non-Darcy flow is expected for violation of any of those conditions.

Many approaches have been attempted to evaluate the behavior of non-Darcy flow, its amplitude, mechanism, reasons that initiate this deviated flow from ideal nature. Generally, four distinct types of approach are found in literature. These are: (i) setting the criteria up that can predict the deviation point of Darcy flow to non-Darcy, i.e. Reynolds number, Forchheimer number, (ii) emphasizing the empirical relationship like Forchheimer equation and develop the expression for the non-Darcy coefficient, (iii) investigating the non-Darcy flow based on the physical structure of porous medium and derive the expression from fundamental conservation law, and (iv) determining the impact and causes of non-Darcy flow near the wellbore region by considering the production scenario. Table 2.2 summarizes some of the non-Darcy models and lists key reasons for their non-Darcy character, including the associated assumptions of the models.

**Table 2.1: Critical Analysis of Different Memory Concepts**

| Reference | Application area | Defining Criteria of Memory | Root for mathematical formulation with memory |
|---|---|---|---|
| Roeloff (1988) | Geo Mechanics | That causes and controls the propagation of fracture within a solid formation which is under stress conditions. | -Biot equation with compressible rock and fluid.<br><br>-Coupled and Uncoupled solution<br><br>-Specified Material properties. |
| Chang and Yortos (1990) | Fractal reservoir | Deviated or delayed pressure response within a fracture reservoir due to the fractal geometry in fracture network, that has disordered spatial distribution and different scale of conduit fracture. | -Anomalous diffusion in fractals<br>-The Modified dual porosity system for a fractal geometry<br>-Pressure transient test analysis of the Pressure response by using the solution of the modified diffusivity equation. |
| Caputo (1999) | Fluid flow in porous media | Filter that acts upon the spectral properties of fluid flow is working in time domain and increase the low-frequency content of flow (phase lag, velocity) whether decreases the high-frequency content (pressure amplitude) | -Fractional time derivative of pressure gradient<br><br>-Pseudo diffusivity (A) and Pseudo diffusivity ratio (η).<br><br>-Convolution of boundary condition with Green function. |
| Caputo (2000) | Flux diffusion in porous media | Characteristics of the medium that diminishes the permeability and interrupt the pressure response and fluid flux rate following the flow history. | -Modified Darcy's law and continuity equations with integrodifferential operators.<br><br>-Green function for flux diffusion |

| | | | |
|---|---|---|---|
| Shin *et al.* (2003) | Turbulent fluid flow | A non-equilibrium effect acting on the turbulent boundary layer where inertia force dominates the fluid flow | -The intermediate diffusion time scale<br><br>- Anomalous non-equilibrium part of the turbophoretic velocity. |
| Lynch *et al.* (2003) | Plasma Physics | Long range correlation in the dynamic behavior of the particle both in space and time event due to the unusual displacement, accelerated velocity or trapping of the particle. | -Fractional kinetics<br>-Continuous time random work (CTRW) for particle distribution<br>-Fractional space derivative. |
| Chen *et al.* (2005) | Fluid flow with yield stress in porous media | The local microstructure effect influences the relationship between applied pressure gradient and flow rate at the microscopic level regarding the minimum threshold path (MTP) of fluid flow with a yield | -Algorithm of invasion percolation with memory (IPM)<br><br>-A pore network model with a distributed yield stress threshold.<br><br>-Modeled the mobilization and fluid flow in the pore throat by single capillary expression. |
| Iaffaldano *et al.* (2006) | Water flow in porous media | As the impacts of previous pressure gradient and fluid flux conditions, on recent flow. | -Basic memory relation<br><br>-Laplace transformation and appropriate boundary conditions.<br><br>-Matching the experimental data and theoretical solution |

| | | | |
|---|---|---|---|
| Hossain *et al.* (2006, 2007, 2008) | Petroleum reservoir | Evaluation of reservoir flow under a frame of references of internal observation by considering the matters and molecules related to flow, instead of external observation | -Modification of constitutive equations with memory formalism.<br><br>-Time dependent rock and fluid properties.<br><br>-Fractional derivative for memory impact |
| Giuseppe *et al.* (2009) | Fluid flux in porous media | The effects of local pressure gradient, related fluid flux and pressure-density variation effects on current flow and reductions in permeability and fluid flux by mechanical compaction. | -Fractional order derivatives.<br><br>-Memory parameters for every local or non-local variance. |
| R. Raghavan (2011) | Petroleum reservoir | "Strange diffusion" across the disordered structures of geometrically complex porous medium due to the impact of the history of flow process. | -Continuous time random walk (CTRW) model<br>-Fractal dimentions<br>-Fractional diffusion<br>-Mittag-Leffler function |
| Rasoulzadeh *et al.* (2014) | Three scale fracture porous media | Delay in fluid flow between different sub domain of the formation. | -Microscopic model by proper parameterization<br><br>-Integrodifferential operators<br><br>-Two scale homogenizations |
| Chen and Raghavan (2015) | Petroleum Reservoir | The long range spatial effect and the trapping effect in temporal scale on the local character of the flow. | -Fractional time and space derivative<br>- Mittag-Leffler function<br>-Laplace transformation<br>-Fox function. |

**Table 2.2: Mathematical Model for Non-Darcy Flow.**

| Reference | Mathematical model | Application criteria | Key reason for non-Darcy flow |
|---|---|---|---|
| Forchheimer 1914 | $-\frac{dp}{dX} = \frac{\mu v}{k} + \beta\rho v^2$ | -High velocity isothermal flow of a macroscopically inviscid fluid<br>-Uniform isotropic elastic porous medium. | -Increased inertial force in high velocity flow at pore scale |
| Klinkenberg 1941 | $k_g = \alpha\frac{1}{\bar{P}} + k_L$ | -Steady state gas flow at high velocity<br>-Determination of effective permeability for Darcy equation. | -Slippage between fluid and pore wall at high velocity gas flow. |
| Brinkman 1947 | $-\frac{dp}{dX} = \frac{\mu v}{k} - \mu(\frac{\partial^2 v}{\partial Y^2} + \frac{\partial^2 v}{\partial Z^2})$ | -Flow through porous medium with the enough large pore throat, allowing the velocity change at the throat. | -Shear forces between the fluid and the pore structure during the high velocity flow at microscopic level |
| Polubarinova_Kochina 1957 | $-\frac{\Delta p}{\Delta x} = av + bv^2 + d\frac{dv}{dt}$ | -Unsteady state fluid flow | -Effects of fluid and rock properties like grain size and distribution, porosity, viscosity at pore level.<br><br>-Unsteady state condition |
| Irmay 1958 | $-\frac{dp}{dx} = \frac{a_i(1-\emptyset)^2\mu}{\emptyset^3 D^2} u + \beta\rho v^2 + \frac{b_i(1-\emptyset)\rho}{\emptyset^3 D^2} u^2 + \frac{1}{\varphi}\frac{\partial u}{\partial t}$ | -One dimensional viscous flow<br>-Isotropic porous media consist of sphere of equal diameter. | -Grain size distribution and porosity<br>-Effects of temperature, viscosity, and density on high velocity flow. |

| | | | |
|---|---|---|---|
| Geertsma 1974 | $\beta = 0.005\ \frac{1}{\emptyset^{5.5}\ k^{0.5}}\ .(\frac{1}{(1-s_w)^{5.5}k_{rel}^{o.5}})$ | -Gas flow in porous media with a water saturation | -Non-uniform medium either consolidated or unconsolidated with complex pore structure.<br><br>-Dominance of inertia force over viscous force due to high velocity. |
| Barak and Bear 979 | $g\mathbf{J} = \left(\boldsymbol{v}\boldsymbol{w}^{(2)} + \boldsymbol{B}^{(4)}{:}\frac{\mathbf{qq}}{\mathrm{q}} + \boldsymbol{C}^{(3)}\ .\mathbf{q}\right).\mathbf{q}$<br>**q** = Specific velocity (cm/sce) | -Saturated Steady state flow of high velocity.<br>-Homogeneous anisotropic medium | -Rock properties, formation structure, and the complexity of the porous medium. |
| Avila 1985 | $\beta\emptyset\ (1 - s_w)\ \sqrt{k} = c\ [\frac{\sqrt{k\rho\sigma}}{\mu}]^m$ | -Multiphase high velocity flow under high temperature and variable overburden pressure. | -Effects of permeability, porosity, residual fluid saturation, and effective stress on fluid flow |
| Blick et.al. 1987 | $-\frac{dp}{dX} = \frac{\mu v}{k} + \beta\rho v^2 + \frac{\rho}{\varphi^2}\ v\ \frac{\partial v}{\partial x} + \frac{\rho}{\varphi}\ \frac{\partial v}{\partial t}$ | -One dimensional single phase unsteady state fluid flow with high velocity. | -Along with inertial force the combined contribution of momentum flux and fluid acceleration in high velocity flow |
| Hassanizadeh *et al.* 1987 | $-\phi\left(P_{,k} - \rho g_k\right) = (a' + b'\left\|v_k^d\right\| + c'\left\|v_k^{d\,2}\right\|)\ v_k^d$<br>With temperature gradient: | -High velocity flow<br>-Uniform isotropic elastic medium<br>-Isothermal flow<br>-macroscopically inviscid fluid | -Microscopic inertial and viscous force.<br><br>-Viscous drag force have higher contribution to onset the nonlinear flow than inertial force and viscous drag force. |

| | | | |
|---|---|---|---|
| | $-\phi(P_{,k} - \rho g_k) = (a_1 + b_1\lvert v_k^d\rvert + c_{1\lvert\theta,k\rvert)}\, v_k^d + (a_2 + b_2\lvert v_k^d\rvert + c_{2\lvert\theta,k\rvert)}\, \theta_{,k}$ | | |
| X.Wang et. al 1998 | $-\mathbf{k}\ \nabla p = \mu\mathbf{v} + 10^{-3.25}\rho\boldsymbol{\tau}^{\mathbf{2}}\,\mathbf{v}\lvert\mathbf{v}\rvert$ | -Single phase flow<br>-Only pore scale anisotropy considers in a pore scale network model | -Extra pressure loss due to inertial effects in pore contraction, expansion, and bends in an anisotropic medium |
| Prada *et al.* 1999 | $u = \frac{q}{A} = \frac{k}{\mu}\left[\frac{\Delta p}{\Delta L} - \left(\frac{\Delta p}{\Delta L}\right)_{cr}\right]$ $for\ \frac{\Delta p}{\Delta L} > \left(\frac{\Delta p}{\Delta L}\right)_{cr}$ | -Low velocity liquid flow in low permeability formation with a threshold pressure gradient | -At low mobility ratio ($\frac{k}{\mu}$) fluid must overcome a threshold pressure gradient rather than the actual one. |
| Zeng *et al.* 2005 | $\frac{MA\,(p_1^2 - p_2^2)}{2zRT\mu l\rho_p Q_p} = \frac{1}{k} + \beta(\frac{\rho_p Q_p}{\mu A})$ $E = \frac{F_o}{1 + F_o}, F_o = \frac{k\beta\rho v}{\mu}$ | -Determination of critical Forchheimer number that responsible for the initialization of non-Darcy flow. | -Liquid-solid interactions and viscous resistance in high velocity gas flow. |
| Friedel *et al.* 2006 | $-grad\,\Phi = (\frac{\mu}{k} + \beta_t\rho\lvert\vec{u}\rvert)\vec{u}$ $\beta_r = 4.1\,.\,10^{11}\,k_{res}^{-1.5}$, $\beta_f = 1.\,10^{11}\,k_f^{-1.11}$ | -High velocity flow in the fracture and the reservoir<br>-Non-Darcy coefficient depends on stress condition. | -Inertial flow in the reservoir as well as in the fracture at the near wellbore region. |

| | | | |
|---|---|---|---|
| Cai 2014 | $V_s = a\left(\frac{\Delta p}{L_o} - J\right)$<br>$a = \frac{1}{32\,\mu_d\,L_o^{D_T-1}}\,\frac{2-D_f}{3+D_T-D_F}\,\frac{\emptyset\,\lambda_{max}^{1-D_T}}{1-\emptyset}$<br>$J = \frac{16\tau_o}{3}\,\frac{3+D_T-D_f}{3-D_f}\,L_o^{(\frac{D_T-1}{1+D_T})} \times (\frac{1}{32}\,\frac{\emptyset}{1-\emptyset}\,\frac{2-D_f}{3+D_T-D_F})^{\frac{D_T}{(1+D_T)}} \times K^{-\frac{D_T}{(1+D_T)}}$ | -Low velocity flow in a low permeability porous media | -Threshold pressure gradient (TPG) that related to porosity fractal dimension, maximum pore size, and fluid property. |
| Wang *et al.* 2016 | $v = \frac{k}{\mu}\,\nabla p\,(\frac{1}{1+e^{-b\lvert\nabla p\rvert}})$<br>$a = -0.6095\left(\frac{k}{\mu}\right)^3 + 2.5821\left(\frac{k}{\mu}\right)^2 - 3.4594\left(\frac{k}{\mu}\right) + 1.5836$<br>$b = 0.3603\,(\frac{k}{\mu})^2 - 0.1049\left(\frac{k}{\mu}\right) + 1.0935$ | -Low velocity flow in shale and tight oil reservoir | -In the rock liquid interaction, there exist a boundary layer that creates nonlinear effect. |

### 2.3.1 Onset of Non-Darcy flow

In the existing literature, there are two types of numbers to identify the Darcy flow to non-Darcy flow deviation point- i) Reynolds number ii) Forchheimer number. In the past, non-Darcy flow was treated as turbulent flow, and some researchers termed the non-Darcy coefficient as turbulence factor (Cornell and Katz,1953, Tek *et al.*, 1962). For that reason, it was a common practice to use the Reynolds number for identifying the beginning of this flow (e.g. pipe flow). There exist a variety of values of the Reynold number because different parameters were used to define this dimensionless number. Table 2.3 summarizes some available mathematical expressions for the Reynolds number and their critical value at the onset of the non-Darcy flow.

**Table 2.3: Reynolds and the Forchheimer number at the onset of non-Darcy flow**

| Mathematical Expression | Reference | Critical Value at Onset |
|---|---|---|
| $R_e = \frac{\rho D_p v}{\mu}$ | Chiton and Colburn (1931) | 40-80 |
| | Fracher and Lewis (1933) | 10-1000 |
| | Blick, and Eivan (1988) | 100 |
| $R_e = \frac{\rho D_p v_o}{\mu}$ | Tek (1957) | 1 |
| | Wright (1968) | 2 |
| | Dybbas and Edwards (1989) | 1-10 |
| | Hassanizadeh and Gray (1987) | 1 |
| $R_e = \frac{\rho D_p v^o}{\mu} \frac{1}{1-\emptyset}$ | Ergun (1952) | 3-10 |
| $R_e = \frac{\rho d_t v}{\mu}$ | Ma and Ruth (1993) | 3-10 |
| | Couland et.al. (1986) | 3-13 |
| $F_o = \frac{k_{o\beta}\rho v}{\mu}$ | Green and Duwez (1952) | 0.005-0.02 |
| | Ma and Ruth (1993) | 0.005-0.02 |
| | Zeng *et al.* (2005) | 0.11 |

Chiton and Colburn (1931) adapted the Reynold's number for investigating the porous medium and replaced the length by the diameter of particle and velocity by superficial velocity. They found that the non-Darcy flow occurs between the value 40 – 80. Using the same definition,

Fracher and Lewis (1933) evaluated it as 10-1000 for the unconsolidated porous medium. Blick and Eivan (1988) found it as 100. To make the definition more appropriate for the porous media Tek (1957) found the responsible Reynolds number for the non-Darcy flow was 1. He defined the inertia term by order of magnitude of flow velocity ($v_o$), density and microscopic characteristic length as one. Wright (1968) used the same definition and assessed the value as 2 and Dybbas and Edwards (1989) as 1-10. Hassanizadeh and Gray (1987) used the Tek (1957) definition and evaluated the Reynolds number as ten at the onset of the deviated flow.

Ergun (1952) added the porosity in the definition and replaced the velocity term by actual velocity ($v_0$) of the fluid. Based on his definition the Reynolds value of 3-10 creates the non-Darcy flow. Numerical simulation of the solution of Navier-stokes equation also gives the critical points for nonlinear flow behavior. Ma and Ruth (1993) showed the critical Reynolds number as 3-10, and Couland et.al. (1986) gave the range as 3-13.

All the above definitions have a pore diameter or characteristic length. Both can be determined for a packed column of sample particle. However, it is very inconvenient to determine the exact characteristic length of a porous structure. Researchers tried to find another dimensionless number that would contain the closely related parameters of the porous medium. The Forchheimer number was proposed to solve the problem (Li and Engler, 2001, Gidley, 1991). Green and Duwez (1952) considered the liquid and solid interactions. They introduced the permeability and a non-Darcy coefficient into the definition. For gas flow, they determined 0.1-0.2 as the critical value for the non-Darcy flow. With the same trend, Ma and Ruth (1993) defined the Forchheimer number and they determined the critical value in the range of 0.005-0.02. For determining $\beta$ from different types of formations, Zeng *et al.* (2005) followed the same procedure of Cornell and Hatz (1953). They have done extensive work on the Forchheimer number and defined the number as the ratio of liquid, solid interaction, and viscous resistance. A non-Darcy effect (E) calculates the magnitude of deviation of the non-Darcy flow from the Darcy flow. In addition, they gave a theoretical basis and experimental procedure to calculate the Forchheimer number for the gas flow. According to the study, the non-Darcy effect is more severe in low permeability rocks, and the critical number is 0.11 which is in good agreement with the previous studies.

### 2.3.2 Determination of non-Darcy coefficient

Several researchers tried to evaluate the non-Darcy coefficient as a rock and fluid property. Considering the experimental data of Cornell and Kartz (1953), a porosity and permeability dependent correlation for non-Darcy coefficient was established by Janicek and Katz (1969). For an hetarogeneous formation, a similar type of work has been done by Gewers and Nichol (1969). They incorporated the effects of residual liquid saturation in the relationship of permeability to β. Cooke (1973) worked with particle size distribution of the porous medium to represent β. By an empirical correlation, Geerstma (1979) linked β with porosity and permeability in the case of high-velocity gas flow with a water saturation. Their investigation is based on dimensional analysis of Forchheimer equation and experimental findings.

Avila (1985) established an expression for the non-Darcy coefficient through an experimental work. He considered the effects of permeability, porosity, residual fluid saturation, and effective stress on fluid flow. Tiss *et al.* (1989) used Avila's correlation and investigated the dependence of β on those parameters in more details. In addition, they examined the effect of higher temperature and higher pressure both on β and permeability, and the mutual relationship between low permeability and β. Finally, they validated Avila's correlation by experimental findings.

### 2.3.3 Non-Darcy flow model based on constitutive equations and physical model

Apart from empirical correlation, many studies focused on the physical structure of the porous medium and flow geometry to analyze the reasons beyond the nonlinear character of the Darcy equation (Ergun and Orning, 1949, Barak and Bear, 1979, Wang *et al.* 1998,). Using the fundamental governing equation of flow, researchers developed the model and tried to find out the source of nonlinearity from the model (Forchheimer, 1914, Irmay, 1958, Blick and Civan, 1987, Hassanizadeh, 1987).

The Darcy model deals with the linear relationship between flow velocity and driving force (pressure gradient). Forchheimer (1914) introduced the non-linear effect for high velocity in the equation of motion with an empirical constant. Irmay (1958) worked with Navier-stokes equation of viscous flow. He investigated the validity of the Darcy and Forchheimer models in the case of an isotropic porous model consisting of the sphere of equal diameter. He revealed that the Darcy's model is valid only at low flow rate with minimum kinetic energy within the homogeneous thermodynamic system. In contrast, the Forchheimer model is valid for the high

Reynolds number but the coefficient contains the effects of formation porosity and grain size distribution. Irmay (1958) considered the viscosity and temperature effects and proposed a new model with an extra factor.

Blick and Civan (1987) added additional terms in the Forchheimer equation to estimate the contribution from momentum and mass conservation. Using the capillary-orifice model, they derived a general equation from momentum and mass conservation law. In the case of gas flow, they showed that the flow behaves differently from Forchheimer and Darcy's equation at the early time due to high acceleration. They validated their findings with experimental data.

Hassanizadeh (1987) proposed a model for high-velocity flow based on the continuum approach and investigated the impact of microscopic drag force on the global flow character. He initiated the development of the general equation from the macroscopic equation of momentum conservation where the inertial term appeared as a deviated term in stress field and drag force added as a surface force (Hassanizadeh and Gray 1979). Taking the thermodynamic process in consideration Hassanizadeh and Gray (1980) derived the equation for those force terms. Hassanizadeh (1987) worked on their previous expression by employing dimensional analysis. He showed that microscopic viscous drag force has higher order contribution in the constitutive equation than macroscopic inertial force. Therefore, drag force causes the initialization of the non-Darcy flow. Like the Forchheimer equation, he proposed a three-dimensional equation for high-velocity isothermal flow for isotropic elastic media.

Researchers also developed a general equation by imposing the governing law on an idealized physical model and solved the equation for this model with certain assumptions (Barakand Bear, 1979; Wang *et al.*, 1998). Barak and Bear (1979) worked to develop an approximate expression for the relationship between volumetric flow rate, pressure gradient, and formation properties for the steady-state saturated, and high-velocity flow. This flow is uniform at the microscopic scale. Three tensors were added to measure the impact of tensorial rock properties on the flow equation. They considered five types of models (Figure 2.1) to formulate the expression and compared the theoretical and experimental results in each case. In four of those physical models, they assumed the structure of the porous medium as the different arrangements of pipe and junctions, where the fifth model was a fissured porous media. The study demonstrated the influence of physical structure on the flow performance and recommended that the form of mathematical expression should be reformed according to the complexity of the flow medium.

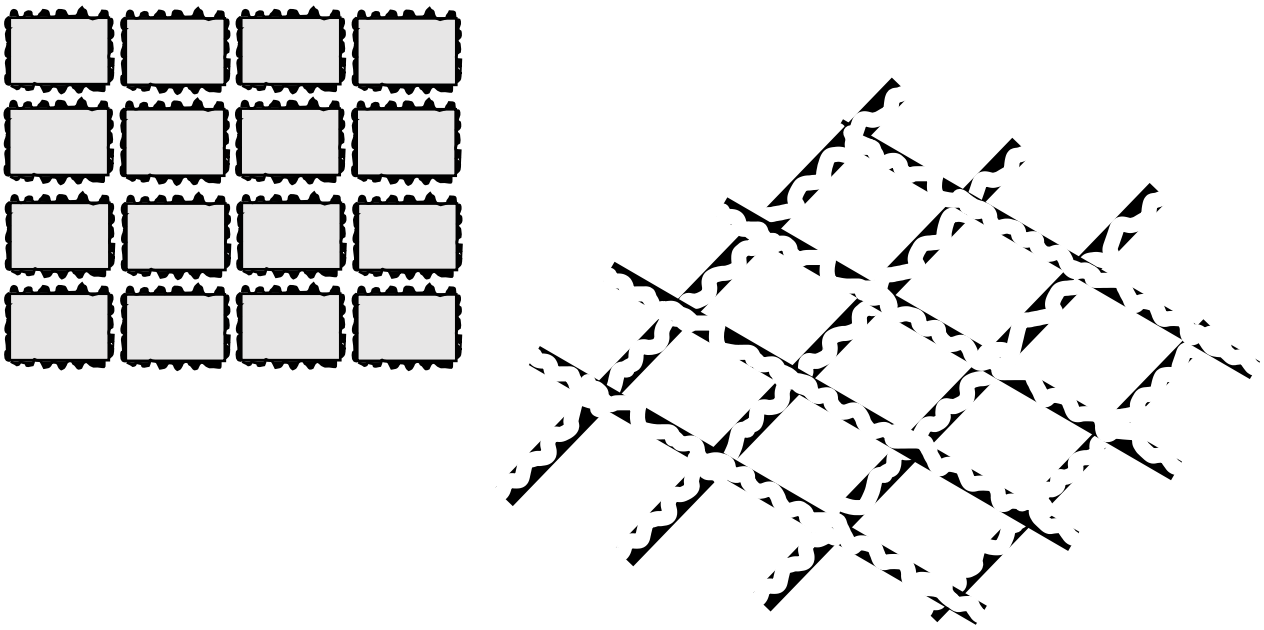

**Figure 2.1: Two-dimensional physical model of Barak and Bear (1979).**

One of the functional physical models to characterize the porous media is the pore network model that can illustrate the transport phenomenon at the microscopic level in an anisotropic media with complex geometry. This model is working on a distributed network of pore body and connected throat (Ionnidis and Chatzis, 1993, Friedman and Seaton, 1996, Mani and Mohanty, 1997). Wang *et al.* (1998) proposed a tensorial form of the Forchheimer model for the single-phase flow in an anisotropic medium. They induced the anisotropy into three different ways; termed as, size influenced (i.e. different throat size), connectivity induced (i.e. different throat connectivity), and spatial correlation induced (i.e. different body size). In their simulation process within the network model, they determined the permeability tensor from the tensorial form of the Darcy law and measured only the viscous pressure loss. At high-velocity flow, they calculated the non-Darcy coefficient tensor from the tensorial form of the Forchheimer equation. They included pressure loss due to bending, expansion, and contraction, which was proportional to the square of superficial velocity. In their observation, the non-Darcy flow primarily occurs because of inertia effect, and there exists a correlation between the morphological parameters of the medium and the microscopic flow properties.

### 2.3.4 Non-Darcy flow related to production

For inspecting the non-Darcy flow related to production, most of the studies focused on the tight-gas reservoir and at the fracture near well bore region. Many the investigations tried to evaluate the non-Darcy flow coefficient by considering inertia dominated flow within the fracture (Millheim and Cichowicz, 1968, Holditch and Morse, 1976, Guppy *et al.* 1982, Smith *et al.* 2004). The non-Darcy flow can affect the results of well-test analysis and the inherent error in the test results may lead to the overestimation of the future production performance of the well (Umnuay *et al.* 2000, Alvarez *et al.* 2002). Therefore, some researchers proposed the modified type curve that accounts the contribution of the non-Darcy flow (Shiqing *et al.* 1996, Liu *et al.* 2004). During the hydraulic fracture operation, the propped fracture and proppant concentration causes a non-Darcy flow (Jin and Penny, 1998, Barree *et al.* 2007, Shah *et al.* 2010). Koh (1977) considered gas flow in this region and scaled up the non-Darcy flow coefficient and related it to the stress condition within the fracture zone and proppant concentration.

Friedel and Voigt (2006) investigated the well performance when the non-Darcy flow exists in the reservoir, and the well fractures. They corrected the non-Darcy coefficient by including the inertial effects and the effects of stress induced variable permeability. Based on a detailed simulation, they figured out the impact of the non-Darcy flow on the production performance with constant non-Darcy coefficient and permeability dependent coefficient. The non-Darcy flow significantly reduces the production rate of the well significantly while the reservoir non-Darcy flow affects the production rate less severely than the fracture non-Darcy flow. However, the non-Darcy flow at the reservoir is prominent as the drainage area increases at a longer time performance. This study proposed a new type-curve for including a new dimensionless parameter for the reservoir non-Darcy flow. The non-Darcy impact and model was validated by well test data.

Threshold pressure gradient (TPG) is an impotent aspect for the non-Darcy flow in a low permeability reservoir. For low permeability formation, the relationship between velocity and pressure gradient is linear at a high-pressure gradient, and it becomes non-linear at low gradient. The idea of TPG comes from the extrapolation of the non-linear part to zero velocity. The minimum pressure gradient is required to initiate the fluid flow. TPG mainly exists due to the interaction between solid molecules and liquid molecules and decreases with increasing value of mobility ratio. Many studies concentrate on this phenomenon and developed correlation for the

non-Darcy flow (Miller and Low, 1963; Prada and Civan, 1999). Many studies tried to establish a correlation for determining the TPG through core flooding experiments. Yang *et al.*, (2004) used brine and oil, Yan *et al.*, (2006) worked with water. Li *et al.*, (2008) and Hao *et al.*, (2008) with oil to formulate the expression that correlates TPG with permeability and viscosity.

Tight or shale reservoir has low permeability, and TPG controls the non-linear flow in this reservoir that changes the production performance of the reservoir (Zeng *et al.*, 2010). Previous studies have recommended that for shale and tight oil reservoir the low-velocity non-Darcy flow does not depend on TPG rather it depends on the thickness of boundary layer along the pore body (Liu *et al.*, 2005, Sen *et al.*, 2015). These researchers emphasized more on the rock-fluid interactions and the thickness of the boundary layer that depends on mobility ratio. By the molecular dynamics simulation, it was shown that high viscous flow at low permeability rock creates the larger thickness of boundary layer and that initiates the nonlinear behavior of the flow. Wang *et al*, (2016) investigated the well production performance in the shale and tight oil reservoirs. They proposed a model for low-velocity non-Darcy flow and suggested that the non-Darcy flow starts from the zero-pressure gradient. By using the curve fitting technique, they evaluated the coefficient of the model based on the experimental data of Wang *et al.*, (2011). They evaluated the performance of a vertical well and a horizontal well with multi-fracture after solving the modified diffusivity equation. The observation of massive ultimate recovery reduction in a vertical well and the less affected response of the non-Darcy flow at the horizontal well states the importance of the horizontal well in the production of a low permeable reservoir.

### 2.3.5 Remarks of the discussion on memory and non-Darcy flow

The above detailed discussion on the non-Darcy flow reveals that this flow occurs at a distorted linear relationship between the flow flux and the pressure gradient. In other word, nonlinear behavior is observed in the velocity and pressure gradient curve. The key causes of the flow can be summarized as variable rock properties i.e. porosity, permeability, grain size and distribution of the formation and complexity of the porous medium. Another cause is the associated impact of the high velocity flow, for example, a high inertial force, a slippage between fluid and pore wall, a shear forces between the fluid and the pore structure, the effects of the temperature, the fluid viscosity and density, the momentum of the flux and the fluid acceleration and the additional pressure loss due to the inertial effects in pore contraction, expansion, and bends. Additionally some of the local and global effects on fluid flow, such as, residual fluid saturation

and effective stress, microscopic inertial and viscous drag force, threshold pressure gradient (TPG) and liquid-solid interactions also cause this flow. The Researchers try to include these effects into the Darcy equation in a variety of ways so that they can explain the nonlinearity in an appropriate approach. The non–Darcy flow existed because of the current characteristics of the medium, fluid and the overall flow and deviated from the ideal conditions. On the contrary, the memory effects illustrate the time dependent nature of the formation and flow. Memory takes the flow-history into account and considers the variation of the formation and fluid properties with time. After determining the magnitude of influence from previous events on present flow, the memory formulation can predict the future flow performance in an accurate manner. However, both idea of the memory and the non-Darcy flow deal with the modification of the Darcy equation but after comparing the mathematical models of the non-Darcy flow (Table 2.3) and the concept of memory, it is obvious that both of those do the model of the fluid flow in different ways. When it is considered as the deviation from the classical diffusion process, every memory-based flow model has a non-Darcy character. However, every non-Darcy flow model does not include the impact of memory.

## 2.4 Applications of Memory Concepts in Petroleum Reservoir Flow

The concepts of memory in petroleum reservoirs have three major trends (Figure 2.2). The concept of memory is incorporated in the fluid flow model as an anomalous diffusion. The anomalous behavior of the complex reservoir is characterized though the inclusion of fractal exponent or the fractional time and space derivatives. In second approach researchers tried to modify the constitutive equation with the addition of time dependent rock and fluid properties. In this practice, the fractional order of differentiation reflects the memory impact, and time dependent correlation modifies the properties. In the other approach, memory accumulation evaluated at multiscale flow dominantly occurs in a fractured reservoir. Integro-differential operator expresses the delay in different subdomain in this concept. Table 4.4 summarizes the available model with memory and their characteristics.

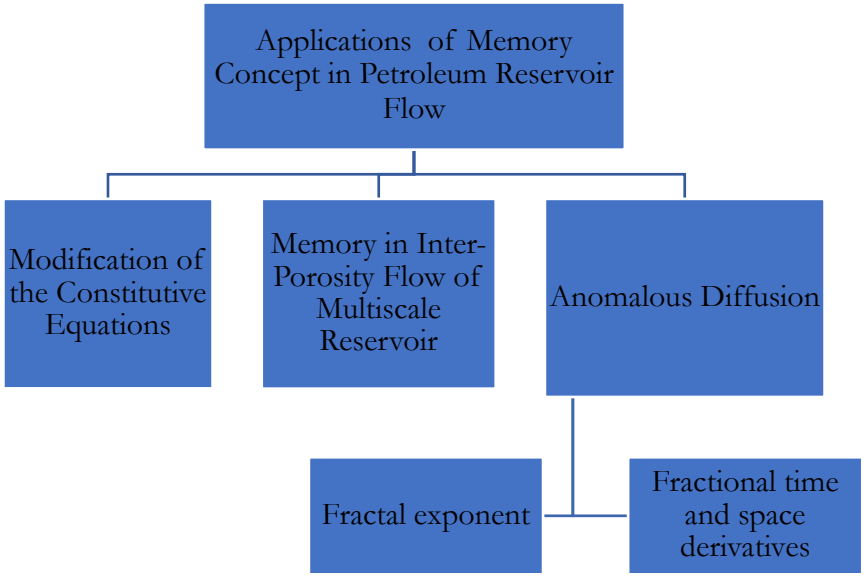


**Figure 2.2: Application of memory concept in petroleum reservoir**

### 2.4.1 Anomalous Diffusion

The anomalous diffusion is a characteristics diffusion process that occurs in the medium with a complex structure. To model the anomalous diffusion the flux law is modified in such a way that the value of the pressure gradient is not instantaneous or local. Rather, it has global character and contains the effects of the long distance and the larger time events. The complexity of the flow path restricts or accelerates the flow. The internal mechanism of the anomalous flow can be explained the Continuous Time Random Walk (CTRW) model (Montroll and Weiss, 1965; Fulger *et al.*, 2008). According to this model the particle distribution of the flow does not follow the Gaussian distribution unlike the classical diffusion. As a random walker, the particle has variable waiting time between two consecutives movement. More interestingly the mean square displacement of the particle follows a power law, instead of a proportional relationship with time (Gefen *et al.*, 1983; Chang and Yortos, 1990; Caputo, 1998; Fomin *et al.*, 2011; Raghavan, 2011; Chen and Raghavan, 2015).

Chang and Yortsos (1990) have done an extensive investigation of the pressure transient response of fractal reservoir which is based on the concept of the anomalous diffusion in fractals

(O'Shaughnessy and Procaccia (1985). They developed a modified diffusivity equation for a physical model consisting of a fracture network and a Euclidean matrix. Chang and Yortsos (1990) reformed the porosity () and the permeability formulation for the fractal. They added the matrix contribution on the overall flow by using the Warren and Root's dual porosity approximation, where the inter-porosity parameter and the exchange rate is escalated for the fractal geometry. A slower response at the early time and a faster changing at a larger time are predicted in the dimensionless pressure and the dimensionless pressure derivative plot of the model. Raghavan (2011) analyzed the application of anomalous diffusion in the transient flow of a fractal system. The study referred to the work of the Camacho-Velazquez et al. (2008) which investigated two different models for the anomalous diffusion. The first model is the Chang and Yortos's (1990) model for the fractal geometry and consists of some exponents to represent the fractal dimensions. The other one is the Metzler et al. (1994) model, is pertaining a fractional derivative and the fractal exponents. Raghavan (2011) modified the model by using a material balance equation (Le M Haut (1984)) for the fractal media and overcome the limitations in the explicit expression of the diffusivity term. The impact of memory yields a flatter slope in the pressure transient analysis of the diffusion process in the fractal system. In the extended work of Chen and Raghavan (2013;2015) showed a general solution for the transient diffusion equation with a fractional time and space derivative. They solved the equation by using the Laplace transformation and the Mittag-Leffler function according to the algorithm of the Stehfest (1970) and the Gorenflo et al. (2002). The analysis of the pressure response at the well-bore for different boundary conditions shows that early the model behaves as a stretched exponential and at the late time it obeys the power law. The behavior of the trilinear model of Ozkan et al. (2011) is analyzed by the outcome of the findings. The slope of the derivative plot signifies the contribution of the different regions at the different time.

### 2.4.2 Modification of the Constitutive Equations

The stress-strain relationship is an important criterion for predicting the production performance of the reservoir as the viscosity do the change in the mobility ratio of the flow and hence changes the production. Hossain *et al.* (2008b) developed a new stress-strain relationship for the crude oil with the inclusion of memory. Conventional approaches do not include the influences of the surface tension and interfacial tension on the viscosity. In the flow of reservoir, fluid velocity depends on the pressure distribution and on the temperature variation. Therefore, in the response

to the fluctuation of pressure and temperature, the velocity shows deviated value. This approach (Hossain *et al.* (2008b)) incorporated effects of the temperature on the viscosity by the Arrhenius model and the effect of surface tension by the Margoni number into the Newtons law of viscosity. Modification of the velocity term by the formalism of memory gives the time variant character to the model. Apart from the simple strain rate and viscosity relationship, this study shows that the shear stress rate related to the impact of surface tension, effects of memory, pressure, pseudo-permeability and temperature. Nevertheless, the study has a limitation in the solution procedure of the model and do not evaluate the piecewise impact of memory.

Diffusivity equation is the basic equation to model the fluid flow in the reservoir. Hossain *et al.* (2008) developed a basic diffusivity equation with the memory for any axial flow of a single-phase fluid in a porous medium. Using the Ahmehaideb (2003) correlation for the viscosity and the permeability correlation (Beal *et al.* 2006, Civan, 2000) they quantified the memory parameter (η). They developed the flow equation by combining continuity equation, modified rate equation and modified equation of state. With the memory parameters, the study changed the rate equation and followed the memory formalism and the definition of the fractional order derivative of Caputo (2000), and by assuming time variable porosity, it modified the equation of state. Finally, they gave the numerical solution with finite difference discretization. They found that along with production life of a reservoir the memory parameter varies in a significant manner that indicates the diminish of permeability. As the pressure depleted with time, reservoir permeability also decreases. They concluded that the variation of porosity and permeability with time is a substantial evidence of memory effect. However, the study developed the governing equation by assuming invariant properties of fluid. In the solution procedure, the parameter with memory impact appears as a constant value in the numerical discretization. It determined the pseudo diffusivity (η) value from correlation and no real correlation between the order of differentiation (α) the medium, so the time dependency is not measured correctly in this model.

Material balance equation is the most used tool to estimate the field production and evaluate the flow performance of a reservoir. Hossain *et al.* (2009) developed a general material balance equation with memory concept by considering the time-dependent rock and fluid property. Comparing with the conventional MBE (Craft and Hawkins, 1959, Dake, 1983, Ahmed, 2006), this approach handles the expansion drive mechanism with more accuracy. It included "associated volume" (Fetkovich, 1998) in the volume expansion term of the equation. To

incorporate the time-dependent properties, it used the memory-based stress-strain relationship (Hossain *et al.* 2007) and replaced the pressure difference term in the expression of the dimensionless parameter ($C_{epm}$) from the simplified equation of Hossain *et al.* (2008). Later, this study made a numerical investigation of the proposed model without memory and the conventional MBE and made a detailed comparison between them. The formulated memory-based MBE has highly non-linear character, and due to the lack of solution, the study could not be able to illustrate the memory impact.

**Table 2.4: Reservoir Flow Modeling with Memory**

| Reference | Mathematical Model | Representing criteria | Special Character | Limitations |
|---|---|---|---|---|
| Chang and Yortsos (1990) | $c_f\left(\frac{\partial p}{\partial t}\right) = [(\frac{m}{\mu})(\frac{1}{r^{D-1}})\frac{\partial}{\partial r}(r^{\beta}\frac{\partial p}{\partial r})]$ | Anomalous diffuson in fractal | -Expression for the permeability of fractal and for the flow rate by using the fractal exponent of a fractal geometry.<br>-Dual porosity model for fractal and matrix.<br>-Analysis of the pressure transient response. | -The matrix is not interconnected<br>-Single phase flow<br>-Evaluation of fractal exponent |
| Hossain *et al.* 2006 | $\tau_T = (-1)^{0.5} \times \left(\frac{\partial\sigma}{\partial T}\frac{\Delta T}{\alpha_D M_a}\right) \times \left[\frac{\int_0^t (t-\zeta)^{-\alpha}\left(\frac{\delta^2 p}{\delta\zeta^2}\right)d\zeta}{\Gamma(1-\alpha)}\right]^{0.5} \times \frac{k^2 \Delta p A_{xz}\Gamma(1-\alpha)}{\mu_o \eta \rho_o \varphi y c \int_0^t (t-\zeta)^{-\alpha}\left(\frac{\delta^2 p}{\delta\zeta^2}\right)d\zeta} \times \left(\frac{\delta\sigma}{\delta T}\frac{6K\mu_0\eta}{\frac{\partial p}{\partial x}}\right)^{0.5} \times e^{\left(\frac{E}{RT}\right)}\frac{du_x}{dy}$ | Stress-strain model | -Yields accurate reservoir simulation result<br>-Enable exact rheological study<br>-Make the optimum surfactant and foam selection for EOR process | -Illustrates the influence of memory formulism on the overall response of equation.<br>-Inadequate solution of the governing equation. |

| | | | | |
|---|---|---|---|---|
| Hossain *et al.* 2008 | $\frac{1}{\eta}\frac{\partial \eta}{\partial x}\left[\frac{\int_0^t((t-\zeta)^{-\propto})\left(\frac{\partial^2 p}{\partial \zeta \partial x}\right)\partial\zeta}{\Gamma(1-\alpha)}\right] + c_f\frac{\partial p}{\partial x}\left[\frac{\int_0^t((t-\zeta)^{-\propto})\left(\frac{\partial^2 p}{\partial \zeta \partial x}\right)\partial\zeta}{\Gamma(1-\alpha)}\right] + \frac{\partial}{\partial x}\left[\frac{\int_0^t((t-\zeta)^{-\propto})\left(\frac{\partial^2 p}{\partial \zeta \partial x}\right)\partial\zeta}{\Gamma(1-\alpha)}\right] = \frac{\phi c_t}{\eta}\frac{\partial p}{\partial x}$ | Diffusivity Equation | -Considered time dependent rock properties.<br><br>-Model the fluid flow in case of enhanced oil recovery process related to non-Newtonian fluid flow | -Only for single phase fluid at axial flow condition<br><br>-Invariant physical properties of fluid.<br><br>-Inadequate evaluation of memory parameters. |
| Hossain *et al.* 2009 | $\gamma_{pm} = \frac{\alpha_{SF}}{\sqrt{k\varphi}}\frac{\eta}{(1-)}\int_0^t (t-\zeta)^{-\alpha}\frac{\delta^2 p}{\delta\zeta\delta x}d\zeta$<br>$\mu_{eff} = \mu_\infty + \frac{\mu_0-\mu_\infty}{\left[1+\left(\frac{\alpha_{SF}}{\sqrt{k\varphi}}\frac{\lambda\eta}{(1-)}\int_0^t (t-\zeta)^{-\alpha}\frac{\delta^2 p}{\delta\zeta\delta x}d\zeta\right)^a\right]^{\frac{n}{a}}}$ | Apparent shear rate | -Time dependent relation between viscosity and permeability in shear thinning fluid.<br><br>- Applicable for heterogenous formation. | -Consider one dimensional flow of Newtonian fluid.<br><br>-Assume isentropic process |
| Hossain *et al.* 2009 | $N_p - (W_e - W_p B_w) = N(B_o - B_{oi} + B_{oi}C'_{epm})$ | Material Balance Equation | -Addition of associated volume in the expansion drive mechanism<br><br>-Model with time dependent rock and fluid properties.<br><br>-Better evaluation of water | -Highly non-linear equation.<br><br>-Inadequate numerical solution of the memory base model |

| | | | | |
|---|---|---|---|---|
| | $C'_{epm} = \left[S_{oi}C_o + S_{wi}C_w + S_{gi}C_g \left(\frac{R_{soi}}{B_{oi}} + \frac{R_{swi}}{B_{wi}}\right)B_{gi} + C_s + M\,(C_w + C_s)\right] \times [\{6\,K\mu_o\eta\,(L - x)\left(\frac{\partial\sigma}{\partial T}\frac{\Delta T}{\alpha_D M_a}\right)^2 \left[\int_0^t ((t - \zeta)^{-\infty})\left(\frac{\partial^2 p}{\partial\zeta\partial x}\right)\partial\zeta\right] e^{2\left(\frac{E}{RT_T}\right)}\left(\frac{du_x}{dy}\right)^2 \times u_x\,\Delta t \times \frac{1}{\tau_T^2\{\Gamma(1-\alpha)\}}\} \times \frac{1}{/1 - S_{wi}}]$ | | saturation | |
| Raghavan (2011) | $\frac{1}{r^{n-1}}\frac{\partial}{\partial r}\left[r^{n-1}\lambda(r)\frac{\partial p(r,t)}{\partial r}\right] = \phi c\frac{\partial^{\Upsilon} p(r,t)}{\partial t^{\Upsilon}}$ | Transient reservoir flow | -Modification of the Darcy law with a fractional time derivative<br>-Incorporation of the fractal parameters in the differential equation.<br>-Analytical solution for instantaneous line source condition in Cartesian and Cylindrical coordinates. | -Inadequate evaluation of the pressure response<br>-Proper expression for the fractal exponent. |
| Rasoulzadeh *et al.* 2014 | $\hat{B}^{(2)}\frac{\partial P^2}{\partial t} = div\left(\hat{A}^{(2)}\,grad\,P^{(2)}\right) - \gamma\lambda\hat{B}^{(1)} \times \frac{\partial}{\partial t}\left(\int_0^t \sqrt{t-\tau}\,\frac{\partial P^{(2)}}{\partial\tau}\,\partial\tau\right)$ | Three scale fracture flow | -Parameterization of permeability and fracture thickness<br><br>-Asymptotic two scale | -Consider the source flow only at the boundary of the matrix. |

| | | | | |
|---|---|---|---|---|
| | | | Homogenization of diffusivity equations.<br><br>-Integrodifferential operators. | |
| Chen and Raghavan (2015) | $\frac{\partial}{\partial x}\left\{\lambda_{\alpha,\beta}\frac{\partial^{\beta}}{\partial x^{\beta}}p(x,t)\right\} = \phi c\frac{\partial^{\alpha}}{\partial t^{\alpha}}p(x,t)$ | Transient diffusion equation | -Combined effect of fractional time and Space derivative on the flow equation<br>-A general solution by Laplace transformation and Mittag-Leffler function.<br>-Analysis of the early and the late time pressure responses of production well and making contrast. | -Lack of field application<br>-Computational complexity<br>-Practical aspect of memory parameters. |

### 2.4.3 Memory in Inter-Porosity Flow of Multiscale Reservoir

In the case of the multiscale porous media there exist a different type of memory. The actual natural porous medium system consists of a different arrangement of fracture and matrix block, and each media have unique properties. A multiporosity and multipermeability system are defined by Aifantis (1977) as a medium that has a finite discontinuity in porosity field. The existing double porosity models (Warren and Root, 1963, Kazemi, 1969, Raghavan *et al.* 1981, Spivey *et al.* 2000) and triple porosity models (Abdassah and Ershaghi, 1986, Liu *et al.* 2003, Ozkan *et al.* 2009, Ahamadi *et al.* 2010) worked with different combinations of matrix and fracture arrangement and with different flow and boundary conditions within each medium. The memory for the multiscale reservoir is the delay in the flow of macroscopic model that occurs due to the delay in the flow between the different subdomain at the boundary at the macroscopic level. Memory accumulation is multiscale reservoir depends on three basic parameters, the distance between the various unit, permeability ratio of adjacent units and the relative pore space in the fractures. Arbogast *et al.* (1990) analyzed the memory in double porosity model by an integrodifferential equation that represents the flow between the matrix and the fracture at the boundary. These effects added to the macroscopic equation along the homogenization of diffusivity equation of two media. Amaaziane *et al.* (2007) evaluated the memory for triple porosity model by two integrodifferential operators at the homogenization process of three media. They worked with self-similar types of medium that have the same order of distance and same permeability ratio.

Rasoulzadeh *et al.* (2014) investigated the memory accumulation at three scale media with the non-self-similar medium. In their parameterization process, they ensure the contribution of each medium. They applied asymptotic two-scale homogenization techniques for two times, firstly for the flow between the matrix and thin fracture and secondly the thick fracture and the first unit with fracture and matrix. They consider the flow only occur at the thin boundary layer of the matrix block so the exchange kernel itself equivalent to the memory of the average flow.

## 2.5 Challenges in Application

Parameterization is a complicated step during the evaluation of memory in the multiscale reservoir (Rasoulzadeh *et al.*, 2014). The contributions of all subdomain must include in the single parameter. In highly heterogenous reservoir representation of the permeability and thickness of the medium is relatively difficult. For conventional reservoir, the proper definition of the memory parameter is problematic for the specification of the model. The review of the available memory model for fluid flow shows that all the model has the limitations with the determination the magnitude of memory implications in a medium (Caputo, 1999,2000; Raghavan, 2011). Most of the study assumed the value, but a proper proceeding should be existed. Determination of the order of the fractional derivative for the targeted formation remains unsolved. Memory formalism makes the governing equation to be highly non-linear (Hossain, 2008; Hossain and Islam, 2009). Moreover, the definition of the fractional derivative shows that the discretization process for the numerical solution of the memory model is an immense limitation to implement this concept (Podlubny, 1998). An appropriate discretization algorithm is the prospective area of development. Table 5 reveals that every mathematical model with memory has a great difficulty with the computational costs. Although memory inclusion gives more accuracy at reservoir simulation, the advantage of exactness should not be suppressed by massive computational expenses (Oldham and Spanier, 1974; Chen and Raghavan, 2015). The determination of the computational cost and its comparative study is a promising area for future.

## 2.6 Conclusions

Although memory concept has the different defining approach but in general, it is the impact of the history of a system. In fluid flow, memory causes the delay in pressure diffusion. Fractional order of differentiation is the standard mathematical tools to deal with the fluid flow memory. Non-Darcy flow considers the impact of the deviated local or global behavior of the flow from ideal one. For this reason, the way non-Darcy flow modify the equation is entirely different than that from memory. Mathematical formulation and the fundamental difference in definition make the clear distinction between the memory impact and the transient flow. Although recently the memory

concept has explored in the petroleum engineering aspect, different approaches are applied to determine the memory impact in the reservoir fluid flow. The appropriate parameterization, conceptualization of memory impact, high non-linearity in the governing equation and numerical solution in an efficient way, are the unsolved difficulties for the proper establishment of this idea in the petroleum field.

**Nomenclature**

| | | |
|---|---|---|
| c | = | regression constant |
| a,b,d | = | empirical constant |
| $a', b', c'$ | = | Coefficient of Hassanizadeh's model and f(ρ,θ,ϕ) |
| $w^{(2)}, B^{(4)}$ $C^{(3)}$ | = | Tensor related to rock properties |
| $c_f$ | = | Total fluid compressibility of the system($c_o$+$c_w$), 1/pa |
| $c_t$ | = | Total compressibility of the system (=$c_f$+$c_s$), 1/pa |
| $c_s$ | = | Formation rock compressibility of the system, 1/pa |
| $c_w$ | = | Formation water compressibility of the system, 1/pa |
| $dt$ | = | Time step, s |
| ξ | = | A dummy variable for time i.e., real part in the plane of the integral, *s* |
| dξ | = | Dummy time step, s |
| $k_g$ | = | effective gas permeability (Darcy) |
| $k_{rel}$ | = | relative permeability |
| $k_g$ | = | Liquid permeability (Darcy) |
| L | = | Length (cm; m) |
| $L_o$ | = | straight line length of the porous sample (in,cm,m) |
| l | = | Microscopic characteristic length |
| m | = | Avila's regression constant |
| $\frac{\Delta p}{\Delta L}$ | = | applied pressure gradient |
| $\left(\frac{\Delta p}{\Delta L}\right)_{cr}$ | = | threshold pressure gradient (TPG) |
| $\bar{P}$ | = | average pressure |
| Q,q | = | flow rate |
| $q^o$ | = | Order of magnitude of flow velocity |

$S_w$ = water saturation

$v$ = fluid velocity (ft $sec^{-1}$, $ms^{-1}$)

$V_k$ = macroscopic fluid velocity vector

Greek Symbols

$\rho$ = density (lbm $ft^{-3}$; g $cm^{-3}$)

$\phi$ = porosity (fraction)

$\sigma$ = effective stress (psi; KPa)

$\mu$ = viscosity (cP, mPa s)

$\alpha$ = Klinkenberg constant

**References**


Abdassah, D., & Ershaghi, I. (1986). Triple-porosity systems for representing naturally fractured reservoirs. SPE Formation Evaluation, 1(02), 113-127.

Ahmed, T. (2006). Reservoir engineering handbook. Gulf Professional Publishing.

Aifantis, E.C., 1977, On the Problem of Diffusion in Solids, Acta Mech., 9, 209-2011, 1977

Al Ahmadi, H. A., Almarzooq, A. M., & Wattenbarger, R. A. (2010, January). Application of linear flow analysis to shale gas wells-field cases. In SPE Unconventional Gas Conference. Society of Petroleum Engineers.

Almehaideb, R. A. (2003). Improved correlations for fluid properties of UAE crude oils. Petroleum science and technology, 21(11-12), 1811-1831.

Alvarez, C. H., Holditch, S. A., & McVay, D. A. (2002, January). Effects of Non-Darcy Flow on Pressure Transient Analysis of Hydraulically Fractured Gas Wells. In SPE Annual Technical Conference and Exhibition. Society of Petroleum Engineers.

Amaziane, B., Pankratov, L., & Piatnitski, A. (2007). Homogenization of a single phase flow through a porous medium in a thin layer. Mathematical Models and Methods in Applied Sciences, 17(09), 1317-1349.

Arbogast, T., Douglas, Jr, J., & Hornung, U. (1990). Derivation of the double porosity model of single phase flow via homogenization theory. SIAM Journal on Mathematical Analysis, 21(4), 823-836.

Avila, Carlos Eduardo. 1985. The effects of temperature and overburden pressure on the non-Darcy flow coefficient in porous media.

Baoquan, Z., Linsong, C., & Fei, H. (2010, January). Experiment and Mechanism Analysis on Threshold Pressure Gradient with Different Fluids. In Nigeria Annual International Conference and Exhibition. Society of Petroleum Engineers.

Barak, A. Z., & Bear, J. (1981). Flow at high Reynolds numbers through anisotropic porous media. Advances in Water Resources, 4(2), 54-66.

Barree, R. D., & Conway, M. (2007, January). Multiphase non-Darcy flow in proppant packs. In SPE Annual Technical Conference and Exhibition. Society of Petroleum Engineers.

Beal, C. (1946). The viscosity of air, water, natural gas, crude oil and its associated gases at oil field temperatures and pressures. Transactions of the AIME, 165(01), 94-115.

Bell, M. L., & Nur, A. (1978). Strength changes due to reservoir-induced pore pressure and stresses and application to Lake Oroville. Journal of Geophysical Research: Solid Earth, 83(B9), 4469-4483.

Biot, M. A. (1941). General theory of three-dimensional consolidation. Journal of applied physics, 12(2), 155-164.

Blick, E. F., & Civan, F. (1987, January). Porous media momentum equation for highly accelerated flow. In SPE Production Operations Symposium. Society of Petroleum Engineers.

Caponetto, R. (2010). Fractional order systems: modeling and control applications (Vol. 72). World Scientific.

Caputo, M. (1969). Elasticitá e dissipazione (Elasticity and anelastic dissipation). Zanichelli Publisher, Bologna). Michele Caputo, M. (1997): Rigorous time domain responses of polarizable media. I, Ann. Geofis, 40(2), 423-434.

Caputo, M. (1999). Diffusion of fluids in porous media with memory. Geothermics, 28(1), 113-130.

Caputo, M. (2000). Models of flux in porous media with memory. Water resources research, 36(3), 693-705.

Chang, J., & Yortsos, Y. C. (1990). Pressure transient analysis of fractal reservoirs. SPE Formation Evaluation, 5(01), 31-38.

Chilton, Thomas H., and Allan P. Colburn, 1931. II—Pressure Drop in Packed Tubes1. Industrial & Engineering Chemistry 23.8 (1931): 913-919.

Civan, F. (2015). Reservoir formation damage. Gulf Professional Publishing.

Cooke Jr, C. E. 1973. Conductivity of fracture proppants in multiple layers. Journal of Petroleum Technology 25.09: 1-101.

Cornell, David, and Donald L. Katz, 1953. Flow of gases through consolidated porous media. University Microfilms.

Coulaud, O., Morel, P., & Caltagirone, J. P. (1986). Effets non linéaires dans les écoulements en milieu poreux. Comptes rendus de l'Académie des sciences. Série 2, Mécanique, Physique, Chimie, Sciences de l'univers, Sciences de la Terre, 302(6), 263-266.

Cox, S.J., Neethling, S., Rossen, W.R., Schleifenbaum, W., Schmidt- Wellenburg, P., Cilliers, J.J., 2004. A theory of the effective yield stress of foam in porous media: the motion of a soap film traversing a three-dimensional pore. Colloids and Surfaces A: Physicochemical and Engineering Aspects 245, 143–151.

Craft, B. C., & Hawkins, M. F. (1959). Applied Petroleum Reservoir Engineering Chap. 2 Prentice-Hall. Englewood Cliffs, NJ.

Dake, L. P. (1983). Fundamentals of Reservoir Engineering., 1978.

Darcy, H. (1856). Les fontaines publiques de la ville de Dijon: exposition et application... Victor Dalmont.

Davison, M., & Essex, C. (1998). Fractional differential equations and initial value problems. Mathematical Scientist, 23(2), 108-116.

Di Giuseppe, E., Moroni, M. and Caputo, M., 2010. Flux in porous media with memory: models and experiments. Transport in Porous Media, 83(3), pp.479-500.

Dybbs, A., & Edwards, R. V. (1984). A new look at porous media fluid mechanics—Darcy to turbulent. In Fundamentals of transport phenomena in porous media (pp. 199-256). Springer Netherlands.

Ergun, S. (1952). Fluid flow through packed columns. Chem. Eng. Prog., 48, 89-94.

Ergun, S., & Orning, A. A. (1949). Fluid flow through randomly packed columns and fluidized beds. Industrial & Engineering Chemistry, 41(6), 1179-1184.

Falls, A.H., Musters, J.J., Ratulowski, J., 1989. The apparent viscosity of foams in homogeneous bead packs. SPERE, 155–164.

Fancher, G. H., & Lewis, J. A. (1933). Flow of simple fluids through porous materials. Industrial & Engineering Chemistry, 25(10), 1139-1147.

Feder, J. (1988). Fractals Plenum. New York, 9.

Fetkovich, M. J., Reese, D. E., & Whitson, C. H. (1998). Application of a General Material Balance for High-Pressure Gas Reservoirs (includes associated paper 51360). SPE journal, 3(01), 3-13.

Friedel, T., & Voigt, H. D. (2006). Investigation of non-Darcy flow in tight-gas reservoirs with fractured wells. Journal of Petroleum Science and Engineering, 54(3), 112-128.

Friedman, S. P., & Seaton, N. A. (1996). On the transport properties of anisotropic networks of capillaries. Water Resources Research, 32(2), 339-347.

Fulger, D., Scalas, E., & Germano, G. (2008). Monte Carlo simulation of uncoupled continuous-time random walks yielding a stochastic solution of the space-time fractional diffusion equation. Physical Review E, 77(2), 021122.

Geertsma, J. 1974. Estimating the coefficient of inertial resistance in fluid flow through porous media. Society of Petroleum Engineers Journal 14.05: 445-450.

Gewers, C. W. W., and L. R. Nichol. 1969. Gas turbulence factor in a microvugular carbonate. Journal of Canadian Petroleum Technology 8.02: 51-36.

Gidley, J. L. (1991). A method for correcting dimensionless fracture conductivity for non-Darcy flow effects. SPE production engineering, 6(04), 391-394.

Green Jr, L., & Duwez, P. (1951). Fluid flow through porous metals. J. Applied Mech., 18.

Guppy, K. H., Cinco-Ley, H., & Ramey Jr, H. J. (1982). Non-Darcy flow in wells with finite-conductivity vertical fractures. Society of Petroleum Engineers Journal, 22(05), 681-698.

Hao, F., Cheng, L. S., Hassan, O., Hou, J., Liu, C. Z., & Feng, J. D. (2008). Threshold pressure gradient in ultra-low permeability reservoirs. Petroleum Science and Technology, 26(9), 1024-1035.

Hassanizadeh, M., & Gray, W. G. (1979). General conservation equations for multi-phase systems: 1. Averaging procedure. Advances in water resources, 2, 131-144.

Hassanizadeh, M., & Gray, W. G. (1980). General conservation equations for multi-phase systems: 3. Constitutive theory for porous media flow. Advances in Water Resources, 3(1), 25-40.

Hassanizadeh, S. M., & Gray, W. G. (1987). High velocity flow in porous media. Transport in porous media, 2(6), 521-531.

Hazen A. 1892. Some physical properties of sand and gravels. Rep. Massachusetts State Board of Health, P. 541

Holditch, S. A., & Morse, R. A. (1976). The effects of non-Darcy flow on the behavior of hydraulically fractured gas wells (includes associated paper 6417). Journal of Petroleum Technology, 28(10), 1-169.

Hossain, M. E. (2008). An experimental and numerical investigation of memory-based complex rheology and rock/fluid interactions (Vol. 69, No. 11).

Hossain, M. E., & Islam, M. R. (2009). A comprehensive material balance equation with the inclusion of memory during rock-fluid deformation. Advances in Sustainable Petroleum Engineering Science, 1(2), 141-162.

Hossain, M. E., Mousavizadegan, S. H., & Islam, M. R. (2008a). A new porous media diffusivity equation with the inclusion of rock and fluid memories.

Hossain, M. E., Mousavizadegan, S. H., Ketata, C., & Islam, M. R. (2008b). A NOVEL MEMORY-BASED STRESS-STRAIN MODEL FOR RESERVOIR CHARACTERIZATION. Nature Science and Sustainable Technology Research Progress, 297.

Iaffaldano, G., Caputo, M., & Martino, S. (2005). Experimental and theoretical memory diffusion of water in sand. Hydrology and Earth System Sciences Discussions, 2(4), 1329-1357.

Ioannidis, M. A., & Chatzis, I. (1993). Network modelling of pore structure and transport properties of porous media. Chemical Engineering Science, 48(5), 951-972.

Irmay, S. (1958). On the theoretical derivation of Darcy and Forchheimer formulas. Eos, Transactions American Geophysical Union, 39(4), 702-707.

Jacob C. E. 1946. Notes on Darcy's law and permeability. Trans. American Geophysical Union, Vol. 27, No. 2, P. 265.

Janicek, John Daniel, and Donald La Verne Katz. 1955. "Applications of unsteady state gas flow calculations.

Kazemi, H. (1969). Pressure transient analysis of naturally fractured reservoirs with uniform fracture distribution. Society of petroleum engineers Journal, 9(04), 451-462.

Kharabaf, H., 1996. Ph.D. Dissertation, University of Southern California.

Kharabaf, H., Yortsos, Y.C., 1997. Invasion percolation with memory. Physical Review E 55, 7177–7191.

Kharabaf, H.,Yortsos,Y.C., 1998. Pore-network model for foam formation and propagation in porous media. SPEJ 42–53.

Klinkenberg, L. J. (1941, January 1). The Permeability of Porous Media To Liquids And Gases. American Petroleum Institute

Koh, W.I.,1977. Non-Darcy flow of a gas in propped fractures. PH.D. dissertation, Texas A&M University College Station, Tex.

LI, A. F., ZHANG, S. H., LIU, M., WANG, W. G., & ZHANG, L. (2008). A new method of measuring starting pressure for low permeability reservoir [J]. Journal of China University of Petroleum (Edition of Natural Science), 1, 019.

Li, D., & Engler, T. W. (2001, January). Literature review on correlations of the non-Darcy coefficient. In SPE Permian Basin Oil and Gas Recovery Conference. Society of Petroleum Engineers.

LI, S. Q., CHENG, L. S., LI, X. S., & Fei, H. A. O. (2008). Nonlinear seepage flow of ultralow permeability reservoirs. Petroleum Exploration and Development, 35(5), 606-612.

Liu, D.X., Yue, X.A., Yan, S. (2005). The effects of adsorbed water layer on flow mechanism in low permeability reservoir. Petroleum Geology and Recovery Efficiency. Volume 6, Pages 40-42

Liu, J., Bodvarsson, G. S., & Wu, Y. S. (2003). Analysis of flow behavior in fractured lithophysal reservoirs. Journal of contaminant hydrology, 62, 189-211.

Liu, Q. G., YANG, X. M., & LI, Y. (2004). Study of well-test model of low permeability's dual-pore media with flowing boundary in oil and gas. JOURNAL-SOUTHWEST PETROLEUM INSTITUTE, 26, 30-33.

Lynch, Vickie E., et al. "Numerical methods for the solution of partial differential equations of fractional order." Journal of Computational Physics192.2 (2003): 406-421.

Ma, H., & Ruth, D. W. (1993). The microscopic analysis of high Forchheimer number flow in porous media. Transport in Porous Media, 13(2), 139-160.

Mani, V., & Mohanty, K. K. (1997). Effect of the spreading coefficient on three-phase flow in porous media. Journal of Colloid and Interface Science, 187(1), 45-56.

Miller, K. S., & Ross, B. (1993). An introduction to the fractional calculus and fractional differential equations.

Miller, R. J., & Low, P. F. (1963). Threshold gradient for water flow in clay systems. Soil Science Society of America Journal, 27(6), 605-609.

Millheim, K. K. (1968). Testing and analyzing low-permeability fractured gas wells. Journal of Petroleum Technology, 20(02), 193-198.

Mlodinow, L. and Brun, T.A., Relation between the psychological and thermodynamic arrows of time, (89) 052102 (2014)

Mlodinow, L., & Brun, T. A. (2014). Relation between the psychological and thermodynamic arrows of time. Physical Review E, 89(5), 052102.

Montroll, E. W., & Weiss, G. H. (1965). Random walks on lattices. II. Journal of Mathematical Physics, 6(2), 167-181.

Oldham, K., & Spanier, J. (1974). The fractional calculus theory and applications of differentiation and integration to arbitrary order (Vol. 111). Elsevier.

Ozkan, E., Brown, M. L., Raghavan, R. S., & Kazemi, H. (2009, January). Comparison of fractured horizontal-well performance in conventional and unconventional reservoirs. In SPE Western Regional Meeting. Society of Petroleum Engineers.

Podlubny, I. (1998). Fractional differential equations: an introduction to fractional derivatives, fractional differential equations, to methods of their solution and some of their applications (Vol. 198). Academic press.

Prada, A., & Civan, F. (1999). Modification of Darcy's law for the threshold pressure gradient. Journal of Petroleum Science and Engineering, 22(4), 237-240.

Raghavan, R. "Fractional derivatives: application to transient flow." Journal of Petroleum Science and Engineering 80.1 (2011): 7-13.

Raghavan, R., & Ohaeri, C. U. (1981, January). Unsteady flow to a well-produced at constant pressure in a fractured reservoir. In SPE California Regional Meeting. Society of Petroleum Engineers.

Raleigh, C. B., Healy, J. H., & Bredehoeft, J. D. (1976). An experiment in earthquake control at Rangely, Colorado. Science, 191(4233), 1230-1237.

Rasoulzadeh, M., Panfilov, M., & Kuchuk, F. (2014). Effect of memory accumulation in three-scale fractured-porous media. International Journal of Heat and Mass Transfer, 76, 171-183.

Rice, J. R., & Cleary, M. P. (1976). Some basic stress diffusion solutions for fluid-saturated elastic porous media with compressible constituents. Reviews of Geophysics, 14(2), 227-241.

Robinson, T. W. (1939). Earth-tides shown by fluctuations of water-levels in wells in New Mexico and Iowa. Eos, Transactions American Geophysical Union, 20(4), 656-666.

Rose W. 1949. Theoretical generalizations leading of the evaluation of relative permeability. Petroleum Transportation, American Institute of Mining Engineering, Technical Paper 2563, P. 111

Rossen, W.R., 1990. Theory of mobilization pressure gradient of flowing of foams in porous media. I. Incompressible foam. II. Effect of compressibility. III. Asymmetric lamella shapes. Journal of Colloid and Interface Science 136, 1–53.

Rossen, W.R., Gauglitz, P.A., 1990. Percolation theory of creation and mobilization of foam in porous media. A.I.Ch.E. Journal 36, 1176–1188.

Rossen,W.R., Mamun, C.K., 1993. Minimal path for transport in networks. Physical Review B 47, 11815–11825.

Sahimi, M., 1993. Non-linear transport processes in disordered media. A.I.Ch.E. Journal 39 (3), 369–385.

SCHUTJENS, P. M. (1991). Experimental compaction of quartz sand at low effective stress and temperature conditions. Journal of the Geological Society, 148(3), 527-539.

Sen, W. A. N. G., Qihong, F. E. N. G., Ming, Z. H. A., Shuangfang, L. U., Yong, Q. I. N., Tian, X. I. A., & ZHANG, C. (2015). Molecular dynamics simulation of liquid alkane occurrence state in pores and slits of shale organic matter. Petroleum Exploration and Development, 42(6), 844-851.

Shah, C., Kharabaf, H., Yortsos, Y.C., 1998. Immiscible displacements involving power-law fluids in porous media. In: Proceedings of the Seventh UNITAR International Conference on Heavy Crude and Tar Sands, Beijing, China.

Shah, C., Yortsos, Y.C., 1995. Aspects of flow of power-law fluids in porous media. A.I.Ch.E. Journal 41 (5), 1099–1122.

Shah, S. N., Vincent, M. C., Rodriquez, R. X., & Palisch, T. T. (2010, January). Fracture orientation and proppant selection for optimizing production in horizontal wells. In SPE Oil and Gas India Conference and Exhibition. Society of Petroleum Engineers.

Shin, M.; Kim, D.S.; Lee, J.W.: Deposition of inertia-dominated particles inside a turbulent boundary layer. Int. J. Multiph. Flow **29**, 893–926 (2003)

Shiqing, C., Lunxun, X., & Dechao, Z. (1996). Type curve matching of well test data for non-darcy flow at low velocity [J]. Petroleum Exploration and Development, 4.

Smith, M. B., Bale, A., Britt, L. K., Cunningham, L. E., Jones, J. R., Klein, H. H., & Wiley, R. P. (2004, January). An investigation of non-Darcy flow effects on hydraulic fractured oil and gas well performance. In SPE Annual Technical Conference and Exhibition. Society of Petroleum Engineers.

Spivey, J. P., & Lee, W. J. (2000, January). Pressure transient response for a naturally fractured reservoir with a distribution of block sizes. In SPE Rocky Mountain Regional/Low-Permeability Reservoirs Symposium and Exhibition. Society of Petroleum Engineers.

Tek, M. R. (1957). Development of a generalized Darcy equation. Journal of Petroleum Technology, 9(06), 45-47.

Tek, M. R., K. H. Coats, and D. L. Katz. 1962. The effect of turbulence on flow of natural gas through porous reservoirs. Journal of Petroleum Technology 14.07: 799-806.

Tian, J.-P., Yao, K.-L., 1999. Immiscible displacements of two-phase non- Newtonian fluids in porous media. Physics Letters A 261, 174–178.

Tiss, M., and R. D. Evans, 1989. Measurement and correlation of non-Darcy flow coefficient in consolidated porous media. Journal of Petroleum Science and Engineering 3.1-2: 19-33.

Umnuay ponwiwat, S., Ozkan, E., Pearson, C. M., & Vincent, M. (2000, January). Effect of non-Darcy flow on the interpretation of transient pressure responses of hydraulically fractured wells. In SPE Annual Technical Conference and Exhibition. Society of Petroleum Engineers.

Wang, X., & Sheng, J. J. (2017). Effect of low-velocity non-Darcy flow on well production performance in shale and tight oil reservoirs. Fuel, 190, 41-46.

Wang, X., Thauvin, F., & Mohanty, K. K. (1999). Non-Darcy flow through anisotropic porous media. Chemical Engineering Science, 54(12), 1859-1869.

Warren, J. E., & Root, P. J. (1963). The behavior of naturally fractured reservoirs. Society of Petroleum Engineers Journal, 3(03), 245-255.

Wenzel L. K. 1942. Method of determining permeability of water bearing materials. United States Geological Survey, Water Supply Paper No. 887

Wright, D. E. (1968). Nonlinear flow through granular media. Journal of the Hydraulics Division, 94(4), 851-872.

Xu, Q., & Rossen, W. R. (2003). Effective viscosity of foam in periodically constricted tubes. Colloids and Surfaces A: Physicochemical and Engineering Aspects, 216(1), 175-194.

Xue-wu, W., Zheng-ming, Y., Yu-ping, S., & Xue-wei, L. (2011). Experimental and theoretical investigation of nonlinear flow in low permeability reservoir. Procedia Environmental Sciences, 11, 1392-1399.

YAN, M., WU, C. H., & WANG, Y. J. (2006). Tendency of Starting Pressure Gradient Changes in Heterogeneous Reservoirs [J]. Journal of Oil and Gas Technology, 3, 040.

Yang, Q., Nie, M. X., & Song, F. Q. (2004). Threshold pressure gradient of low permeability sandstone. J Tsinghua Univ (Sci Tech), 44, 1650-1652.

Zeng, B. Q., Cheng, L. S., & Hao, F. (2010). Experiment and mechanism analysis on threshold pressure gradient with different fluids. SPE, 140678, 859-863.

Zeng, Z., & Grigg, R. (2006). A criterion for non-Darcy flow in porous media. Transport in porous media, 63(1), 57-69.

# Chapter 3 A Review on Fluid Flow Models for Fractured Reservoir

## Preface

This chapter is a review of the fluid flow models for the fractured reservoir, a complex structure of alternative matrix and fracture. An accurate analysis of the characteristic behavior of such a reservoir becomes more challenging due to the complex reservoir formation and the irregular flow patterns in discrete domains. Current literature covers various methods which predict the flow behavior in a fractured reservoir; however, a wide variation in physical models and inherent assumptions make it difficult to select an accurate-representative scheme. This study investigates different approaches, inspects the physical arrangements, analyzes the contrasts, and examines the mathematical formulations and their limitations. The analysis shows that the continuum-based approaches differ for the different fracture network, inter-flow condition, continuum-number, and the interface transfer function. The linear flow approach assumes simplified flow condition in a complex network and gives the computational advantage whereas the anomalous diffusion approach captures the heterogeneity of the reservoir by the fractional time or space derivative. The evidence from this study suggests that increasing the number of the continuum in the physical structure raises the precision. Nevertheless, the required-additional number of intrinsic properties is the critical challenge in the continuum approach. Although the anomalous diffusion minimizes the number of properties, the determination of the memory parameters is ambiguous in this method. A combination of the continuum approach and the anomalous diffusion is recommended as an alternative approach for the modeling of fluid flow in a fractured reservoir.

### 3.1 Introduction

The fractured reservoir has a complex structure, which is comprised of a network of repeating fractures and matrices. The challenges in the modeling of the fluid flow for such a reservoir are determination of the influences of the constituents, identification of the heterogeneity of the fractures and the matrix, the analysis of pressure response that is being observed at the pressure transient test of the reservoir. Since the fluid transfer in a fractured reservoir depends on its physical structure, the details of the reservoir formation are mandatory for an accurate fluid flow model.

Dual porosity models consider two sets of homogeneous components: fractures and matrix, instead of a single continuous medium, and adds a degree of detail about formation (Warren and Root, 1963; Kazemi, 1969; de Swaan, 1976). Two additional parameters terms the inter-porosity flow parameter and the fluid capacitance co-efficient, are being used to characterize the deviated behavior of the fractured reservoir from the conventional homogeneous reservoir. However, double porosity models were proved to be insufficient to explain the abrupt slope change in the pressure response of a tight gas or an unconventional reservoir. Triple porosity models attempt to solve this problem by considering one additional continuum, either a fracture or a matrix. The inter-porosity flow conditions between two adjacent domains, the unsteady state or the semi-steady state condition, the arrangement of continuum, and the direction of fluid flow make the variations in different models (Abdassah and Ershaghi, 1986; Jalali and Ershaghi, 1987; Liu et al., 2003; Wu et al., 2011). Regardless, Multi-porosity and multi-permeability models consider more distinctive continuum in the formation structure so that the model could make an accurate representation of the highly fractured reservoir (Khulman et al.; 2015).

Apart from these multi-continuum approaches, El-banbi (1998) introduced the concept of linear flow for a hydraulically fractured reservoir. Brown et al. (2009) extended this idea to the Tri-linear model (TLM), which divided the flow region into three segments: outer reservoir, inner reservoir and the hydraulic fracture, and assumed linear flow for every region. Although all the continuum-based models make a better representation of the actual reservoir structure, it requires many reservoir parameters to be determined. The

Anomalous diffusion approach, which incorporates a fractional order of differentiation or the fractal exponents into the constitutive flow equations to capture the heterogeneity of the reservoir, eliminates the intrinsic properties of the formation from the fluid flow model (Raghavan, 2011; Chen and Raghavan, 2015, Alibini, 2016; Holy and Ozkan, 2016).

This study is an overview of all the available models for the fractured reservoir. It takes a new look at the formulations of different models and analyzes the limitations. A recommendation is made at the end of this study on the appropriate flow model for the naturally fractured reservoir based on a comparative analysis.

### 3.2 Dual Porosity Model

Warren and Root (1963) have introduced the dual porosity model in the petroleum reservoir. They modified Barenblalt et al.'s (1960) work, and their model demonstrates a new approach to analyze the pressure test data. The deviated behavior of the homogeneous reservoir is explained by a sugar-cube structure (Figure 3.1) where the matrix block is assumed as a source medium of fluid, and the fracture is considered the primary conduit for the fluid transfer. Although the model only studies the semi-steady state behavior of the reservoir, it can characterize the deviation of response by two additional parameters; one denotes the relative fluid capacitance, and the other signifies the comparable transfer rate of the respective media. The study also estimates the parameters from the pressure build-up data of a reservoir. This research is considered a reference for the fluid flow modeling of a heterogeneous reservoir; however, it is valid for late time response of a reservoir, and there is still considerable ambiguity about the analysis of a stratified reservoir and shape factor determination of the interface condition. Kazemi (1969) has tried to eliminate that limitation by considering transient flow condition through a slab porosity model (Figure 3.1). His work makes an accurate prediction of the flow behavior at the early time, but the model cannot be applied in a complex reservoir and is not valid for the late time response.

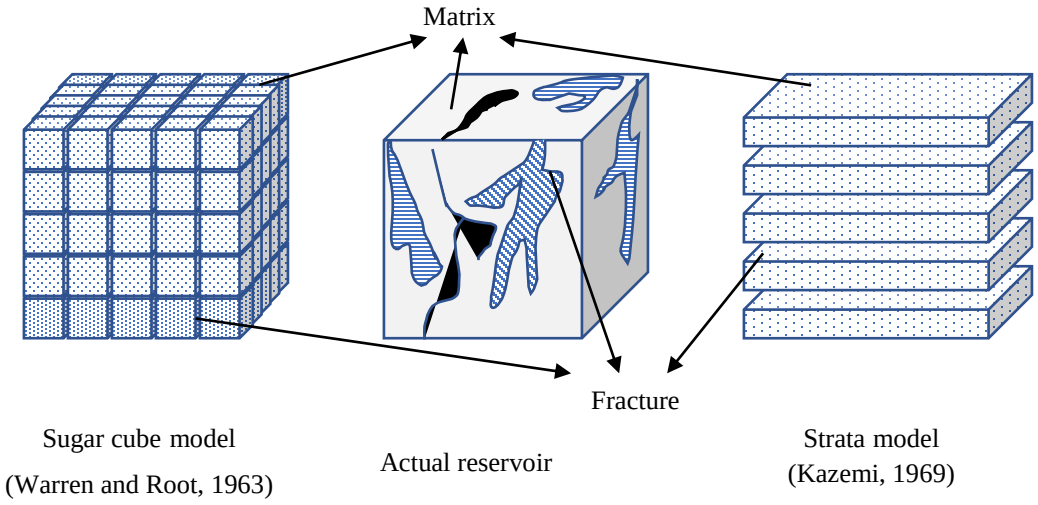


**Figure 3.1: Physical structure of the dual porosity model (Redrawn from Warren and Root, 1963; Kazemi, 1969)**

### 3.3 Triple Porosity Model

Abdassah and Ershaghi (1986) have investigated the reason for the anomalous slope change during the transition period in a pressure response curve of the fractured reservoir. Based on their observation, they have proposed a triple porosity model, which is comprised of two separate sets of matrix blocks and a set of fracture (Figure 3.2). Their study considers both the strata model and the sugar cube model under the transient flow condition. For mathematical formulation, they follow Lai et al.'s (1983) approach and find the expression of the dimensionless pressure. The pressure drawdown and the pressure build-up behavior of both models, however, show the deviated slope change that is being related to a ratio of the inter-porosity flow co-efficient and a ratio of fluid capacitance co-efficient. Moreover, a correlation is established for estimating the ratio of the inter-porosity co-efficient. The research has tended to focus on the transient behavior of the reservoir but in case of an unconventional reservoir with high matrix permeability semi-steady state flow may begin at an early flow time.

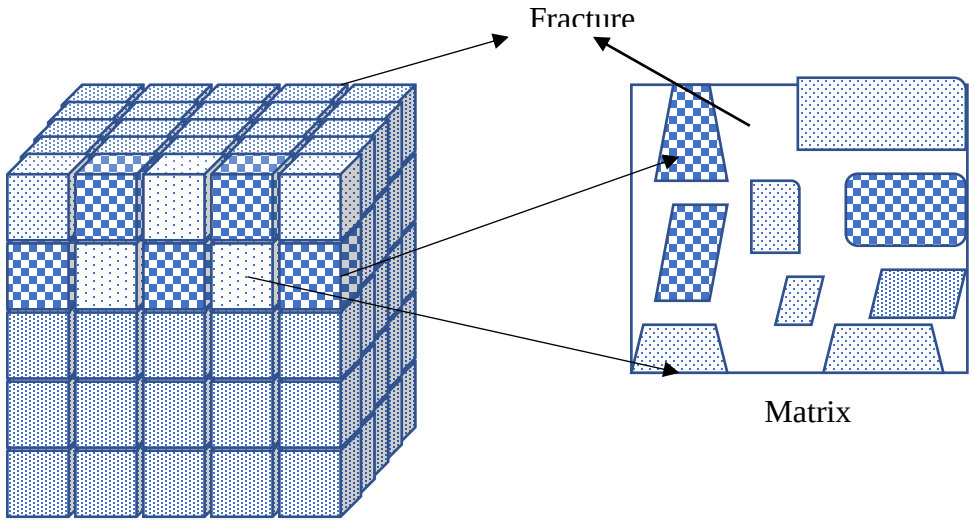


**Figure 3.2: Triple porosity sugar-cube model (Redrawn from Abdassah and Ershaghi, 1986)**

### 3.4 Anomalous Diffusion

Chang and Yortsos (1990) have conducted an extensive investigation on the pressure transient response of a fractal reservoir which is based on the concept of the anomalous diffusion in fractals (O'Shaughnessy and Procaccia, 1985). They have developed a modified diffusivity equation for a physical model consisting of a fracture network and a Euclidean matrix. The fracture network is characterized by the fractal geometry (Fractal dimension, D). Therefore, the flow equation for the fracture network contains a number of fractal exponents (a, D, θ). Chang and Yortsos (1990) reform the porosity ($\phi_f$) and the permeability formulation for the fractal. They add the matrix contribution on the overall flow by using Warren and Root's (1963) dual porosity approximation where the inter-porosity parameter and the exchange rate is escalated for the fractal geometry. The pressure drawdown and the pressure buildup analysis demonstrate the deviated response of the fractal and shows the procedure to evaluate the related reservoir fractal-exponent. A slower response at the early time and a faster changing at late time are predicted in the dimensionless pressure and the dimensionless pressure derivative plot of the model. The

main weakness in their study is that they do not propose any procedure for the determination of the fractal exponent; therefore, the model has a difficulty in the practical perspective. Moreover, in the early time pressure response, the impact of fractal exponent is not evaluated.

Raghavan (2011) has made an analysis of the application of anomalous diffusion in the transient flow of a fractal system. The study is referred to in the work of the Camacho-Velazquez et al. (2006) which investigates two different models for the anomalous diffusion. The first one is Chang and Yortos's (1990) model for the fractal geometry and consists of a number of exponents to represent the fractal dimensions. The other is the Metzler et al. (1994) model which pertains a fractional derivative and the fractal exponents. Raghavan (2011) has modified the model by using a material balance equation (Le M, 1984)) for the fractal media and overcame the limitations in the explicit expression of the diffusivity term. A key problem with the approach is that it does not provide a practical basis for signifying the fractal structure. The study also develops a fractional continuity equation for Cartesian and radial systems. The mobility expression in the equation is defined in terms of a fractal exponent that imposes a slower growth in the mobility of the medium. The solution of the diffusivity equation for the production at a constant rate and for the production at a constant pressure shows that the response follows a power law rather than an exponential decay. The impact of memory yields a flatter slope in the pressure transient analysis of the diffusion process in the fractal system. The study shows the effects of fractional order derivative; however, the model shows less consistency with the reservoir physical model.

Chen and Raghavan (2015) have shown a general solution for the transient diffusion equation with a fractional time and space derivative. They have solved the equation by using the Laplace transformation and the Mittag-Leffler function according to the algorithm of the Stehfest (1970) and the Gorenflo *et al.* (2002). The analysis of the pressure response at the well-bore for different boundary conditions shows that at the early time the model behaves as a stretched exponential and at late time it obeys the power law. The functional behavior of the Mittag-Leffler has the same shape. A key problem with this approach is the asymptotic expression of the Mittag-leffler function in

the solution process that yields an approximate result. Chen and Raghavan (2015) also analyze the contributions of the sub-diffusion and the super-diffusion on the transient pressure response and find an opposite impact of the space derivative and the time derivative in the response. The slope of the response curve is flattened with an increasing order space derivative. Due to the influence of the fractional derivative, the predicted pressure distribution in the reservoir is different from the classical diffusion's response. The behavior of the trilinear model of Ozkan et al. (2011) is analyzed by the outcome of the findings. The slope of the derivative plot signifies the contribution of the different regions at the different times. One of the main limitations of the study, however, is the anticipated value of the memory parameter that should be related to the particular reservoir.

### 3.5 Linear Model

Linear modes consider linear flow in the individual continuum and show a convenient approach for characterizing the tight gas or shale gas reservoir. According to Wattenbarger (2007), the linear flow assumption is more applicable for the fractured shale gas reservoir because highly pervious fracture drains the fluid from a low permeable matrix. Because of perpendicular linear flow in the adjacent medium, in a dual porosity arrangement the flow is bi-linear. Similarly, it is tri-linear in a triple-porous reservoir. El-banbi (1998) establish a solution technique for the linear reservoir flow in a dual porosity arrangement. Alahmadi (2010) has developed a linear triple porosity model for shale gas reservoirs. The study considers two sets of orthogonal fractures and matrix (Figure 3.3) that follows the solution technique of El-banbi (1998). This paper has conducted an intensive investigation of the reservoir behavior by considering four different types of flow model. Each model considers a distinctive combination of inter-porosity flow conditions termed transient flow condition and pseudosteady state condition. To find out the appropriate combination of flow conditions, he compares the response of the models with the establish model and simulation results. The fully transient model has the best match with the both. Finally, Alahmadi (2010) shows a field application of the transient model in case of shale gas reservoir. The study shows a simplified mathematical approach for analyzing the reservoir data; however, it has same limitations of triple continuum

approaches. Moreover, this paper does not consider the long-range effects and irregularities of the time and space event in the flow performance.

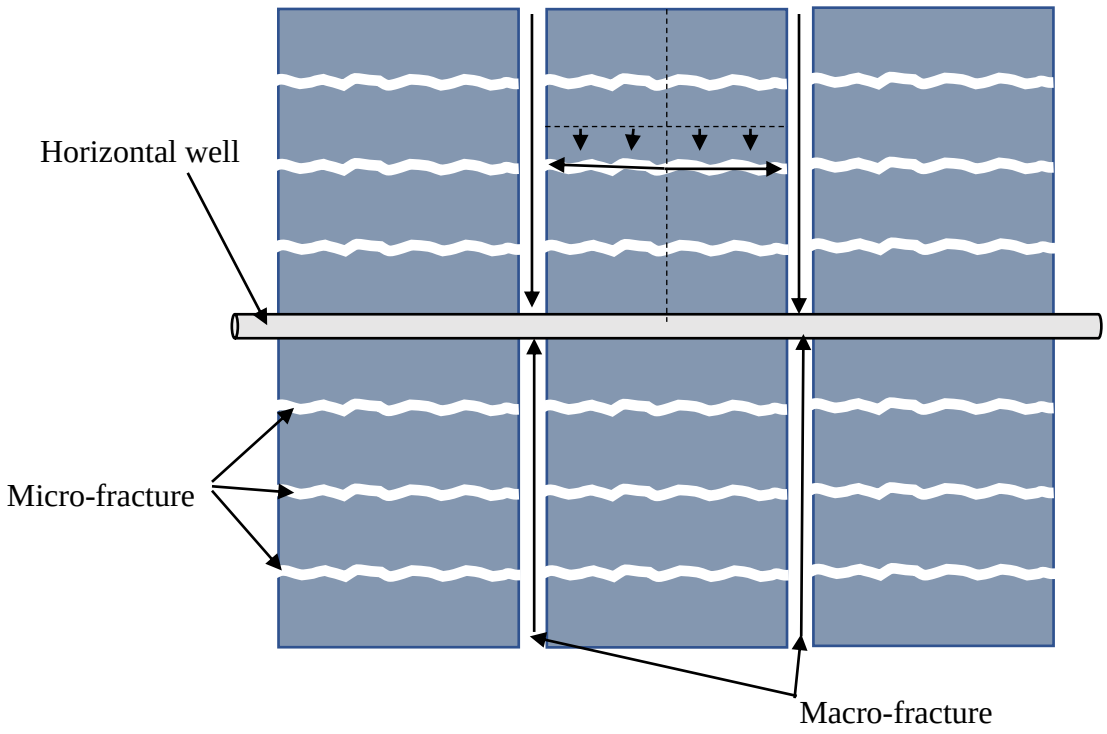


**Figure 3.3: Linear triple porosity model (Redrawn from Alahmadi, 2010)**

Tri-linear models (Brawn et al., 2009, Ozkan *et al.*, 2011, Apaydin, 2011, Ozcan, 2014, Albinali, 2016) Work on well-defined physical structure that divides the whole reservoir into three regions, termed inner reservoir, outer reservoir and hydraulic fracture (Figure 3.4). To evaluate the horizontal well performance in a hydraulically fractured tight reservoir the tri-linear models consider linear flow in each segment of the reservoir. The structure of the inner reservoir and the type of flow in the individual region make the variation in the tri-linear model related studies. Table 3.1 shows an analysis on the tri-linear models.

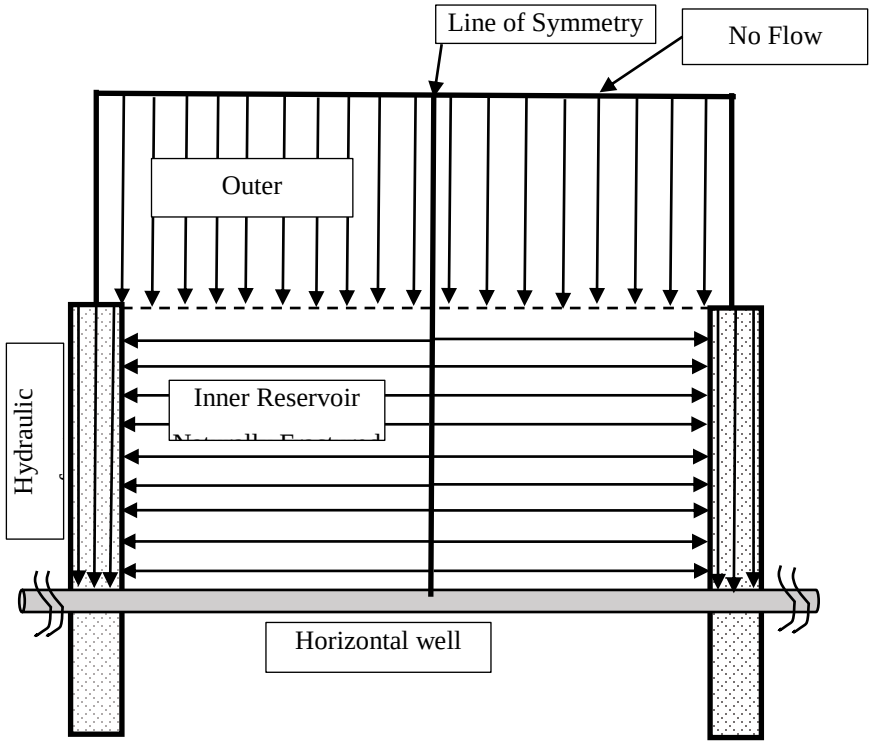


**Figure 3.4: General structure of the tri-linear model (Redrawn from Brawn et al., 2009)**

Ozkan *et al.* (2011) have discussed about the horizontal well performance that follows the Brawn's tri-linear model (2009) and they compare the performance of a conventional tight gas reservoir to an unconventional shale gas reservoir. They determine the effects of the outer reservoir, matrix permeability, natural fracture permeability and density, and the hydraulic fracture permeability and spacing in the production performance of a fractured well. The orientation of the natural fracture network and the density of the fractures control the performance of an unconventional reservoir. A high matrix permeability and an elevated hydraulic-fracture conductivity cannot be able to increase the productivity in an unconventional reservoir. According to their observation the inner reservoir or the stimulated area between two hydraulic fracture is the limiting drainage area in a shale gas reservoir. However, induced fracture and the optimization of the hydraulic fracture conductivity can make a productivity improvement.

**Table 3.1: Analysis of the Tri-linear models**

| Criteria | Brown, 2009 | Apaydin, 2011 | Ozcan, 2014 | Albinali, 2016a | Albinali, 2016b |
|---|---|---|---|---|---|
| Outer Reservoir | | | | | |
| Physical Structure | Unstimulated zone | Unstimulated zone | Unstimulated zone | Unstimulated zone | Unstimulated zone |
| Flow Condition | Transient | Transient | Transient | Transient | Transient |
| Flow Type | Conventional | Conventional | Conventional | Anomalous | Anomalous |
| Inner Reservoir | | | | | |
| Physical Structure | Dual porosity | Dual porosity | Dual porosity | Dual porosity | Fractal Structure |
| Matrix Flow Condition | Transient and semi-steady state | Transient | Transient | Transient | Transient |
| Matrix Flow Type | Bi-linear axial flow | Radial flow in special arrangement of micro-fracture at the surface layer | Bi-linear anomalous flow | Radial anomalous flow with fractional time derivative | Radial anomalous flow with fractal exponents |
| Fracture Flow Condition | Transient and semi-steady state | Transient | Transient | Transient | Transient |
| Fracture Flow Type | Bi-linear axial flow | Axial flow | Bi-linear anomalous flow | Linear anomalous flow with fractional time derivative | Linear anomalous flow with fractal exponents |
| Hydraulic Fracture | | | | | |

| Criteria | Brown, 2009 | Apaydin, 2011 | Ozcan, 2014 | Albinali, 2016a | Albinali, 2016b |
|---|---|---|---|---|---|
| Physical Structure | Rectangular | Rectangular | Rectangular | Rectangular | Rectangular |
| Flow Condition | Bi-linear axial flow | Bi-linear axial flow | Bi-linear axial flow | Bi-linear axial flow | Bi-linear axial flow |
| Flow Type | Transient | Transient | Transient | Transient | Transient |

### 3.6 Conclusion

The Chapter has investigated some of the approaches for modeling the fluid flow through a naturally fractured reservoir. The analysis from this study suggests that the continuum-based models consider the physical structure of the reservoir and increase the accuracy in the prediction of the reservoir behavior; however, the required reservoir parameters for the new continuum are difficult to be determined. Alternatively, anomalous diffusion concept requires less parameter compare to the continuum approaches, but a high uncertainty exists in the precise determination of the order of the differentiation or the fractal exponent. Future studies on the current topic therefore require a logical combination of continuum approach and anomalous diffusion. It will not only reduce the complication but also increase the accuracy in the fractured-reservoir characterization.

**References**


Abdassah, D., & Ershaghi, I. (1986). Triple-porosity systems for representing naturally fractured reservoirs. SPE Formation Evaluation, 1(02), 113-127.

Alahmadi, H. A. H. (2010). A Triple-porosity model for fractured horizontal wells (Doctoral dissertation, Texas A & M University).

Albinali, A. (2016). Analytical solution for anomalous diffusion in fractured nanoporous reservoirs. Colorado School of Mines.

Brown, M., Ozkan, E., Raghavan, R., & Kazemi, H. (2011). Practical solutions for pressure-transient responses of fractured horizontal wells in unconventional shale reservoirs. SPE Reservoir Evaluation & Engineering, 14(06), 663-676.

Camacho Velazquez, R., Fuentes-Cruz, G., & Vasquez-Cruz, M. A. (2006, January). Decline curve analysis of fractured reservoirs with fractal geometry. In International Oil Conference and Exhibition in Mexico. Society of Petroleum Engineers.

Chang, J., & Yortsos, Y. C. (1990). Pressure transient analysis of fractal reservoirs. SPE Formation Evaluation, 5(01), 31-38.

Chen, C., & Raghavan, R. (2015). Transient flow in a linear reservoir for space–time fractional diffusion. Journal of Petroleum Science and Engineering, 128, 194-202.

de Swaan O, A. (1976). Analytic solutions for determining naturally fractured reservoir properties by well testing. Society of Petroleum Engineers Journal, 16(03), 117-122.

El-Banbi, A. H., & Wattenbarger, R. A. (1998, January). Analysis of linear flow in gas well production. In SPE Gas Technology Symposium. Society of Petroleum Engineers.

Gorenflo, R., Mainardi, F., Moretti, D., & Paradisi, P. (2002). Time fractional diffusion: a discrete random walk approach. Nonlinear Dynamics, 29(1), 129-143.

Holy, R. W., & Ozkan, E. (2016, May). A Practical and Rigorous Approach for Production Data Analysis in Unconventional Wells. In SPE Low Perm Symposium. Society of Petroleum Engineers.

Jalali, Y., & Ershaghi, I. (1987, January). Pressure transient analysis of heterogeneous naturally fractured reservoirs. In SPE California Regional Meeting. Society of Petroleum Engineers.

Kazemi, H. (1969). Pressure transient analysis of naturally fractured reservoirs with uniform fracture distribution. Society of petroleum engineers Journal, 9(04), 451-462.

Kuhlman, K. L., Malama, B., & Heath, J. E. (2015). Multiporosity flow in fractured low-permeability rocks. Water Resources Research, 51(2), 848-860.

Le Mehaute, A. (1984). Transfer processes in fractal media. Journal of Statistical Physics, 36(5), 665-676.

Liu, G. R., & Liu, M. B. (2003). Smoothed particle hydrodynamics: a mesh free particle method. World Scientific.

Metzler, R., Glöckle, W. G., & Nonnenmacher, T. F. (1994). Fractional model equation for anomalous diffusion. Physica A: Statistical Mechanics and its Applications, 211(1), 13-24.

O'Shaughnessy, B., & Procaccia, I. (1985). Analytical solutions for diffusion on fractal objects. Physical review letters, 54(5), 455.

Ozkan, E., Brown, M. L., Raghavan, R., & Kazemi, H. (2011). Comparison of fractured-horizontal-well performance in tight sand and shale reservoirs. SPE Reservoir Evaluation & Engineering, 14(02), 248-259.

Raghavan, R. (2011). Fractional derivatives: application to transient flow. Journal of Petroleum Science and Engineering, 80(1), 7-13.

Warren, J. E., & Root, P. J. (1963). The behavior of naturally fractured reservoirs. Society of Petroleum Engineers Journal, 3(03), 245-255.

Wu, Y. S., Di, Y., Kang, Z., & Fakcharoenphol, P. (2011). A multiple-continuum model for simulating single-phase and multiphase flow in naturally fractured vuggy reservoirs. Journal of Petroleum Science and Engineering, 78(1), 13-22.

# Chapter 4 A Comparative Study of Mathematical Models for Fractured Reservoirs: Anomalous Diffusion and Continuum Approach

## Preface

This study aims to determine an appropriate representative flow-model of a fractured reservoir after comparing two existing approaches: the anomalous diffusion and the continuum approach. The comparison of these two current approaches is the first time effort to capture the relative impact of the assumptions those are made in the development of the approaches. A fractured reservoir is assumed in this paper that drains the fluid in transient condition, to a hydraulically fractured horizontal well. To investigate the comparison, dimensional consistency is maintained for both the anomalous diffusion and the continuum approach. Chen and Raghavan's (2015) model is considered as the anomalous diffusion model with modified boundary conditions. Continuum approach model considers the linear flow in a triple continuum structure that consists of matrix slab, micro-fracture, and hydraulic fracture. An analysis of the pressure response curves and the field data evaluates the proper approach for the analysis of the flow behavior. The solution of the wellbore pressure is derived in Laplace domain and is inverted by the Stehfest algorithm. Slope of the pressure response curve depends on the order of differentiation at the anomalous diffusion model. Conversely, the permeability of the hydraulic fracture controls the transient behavior at the continuum approach. The first set of analyses states that the continuum-based model considers the physical structure of the reservoir and increases the accuracy in the prediction of the reservoir behavior; however, more reservoir parameters are required for new continuum, those are difficult to determine. Alternatively, anomalous diffusion approach requires less parameter compared to the continuum approaches, but a high uncertainty exists in the precise determination of the order of the differentiation or the fractal exponent. The anomalous diffusion shows a good agreement with the synthesized field data at the early stage whereas the continuum approach matches better at late stage of the response.

## 4.1 Introduction

An accurate analysis of the characteristic behavior of a fractured reservoir is challenging since the complex reservoir formation, and the irregular flow patterns in the discrete domain brings computational challenges. Instead of a single homogeneous model, dual porosity models consider two sets of homogeneous components, which are recognized as fractures and matrix (Warren and Root, 1963; Kazemi, 1969; de Swaan, 1976). The fluid flow in such a reservoir is controlled by two parameters termed the inter-porosity flow parameter and the fluid capacitance co-efficient. However, double porosity models were proved to be insufficient to explain the abrupt slope change in the pressure profile of a tight gas or an unconventional reservoir. Triple porosity models attempt to solve this problem by considering one additional continuum, either a fracture or a matrix. The inter-porosity flow conditions between two adjacent domains, the unsteady state or the semi-steady state condition, the arrangement of continuum, and the direction of fluid flow are the major variations in different models (Abdassah and Ershaghi, 1986; Jalali and Ershaghi, 1987; Liu et al., 2003; Wu et al., 2011).

Chen and Raghavan (2015) have shown a general solution for the transient diffusion equation with a fractional time and space derivative. They solved the equation by using the Laplace transformation and the Mittag-Leffler function according to the algorithm of the Stehfest (1970) and the Gorenflo *et al.* (2002). The analysis of the pressure response at the well-bore for different boundary conditions shows that at the early stage the model behaves as a stretched exponential function and at a late stage, it obeys the power law. The functional behavior of the Mittag-Leffler has the same shape. A fundamental problem with this approach is the asymptotic expression of the Mittag-leffler function in the solution process that yields an approximate result. Chen and Raghavan (2015) also analyze the contributions of the sub-diffusion and the super-diffusion on the transient pressure response and found an opposite impact of the space derivative and the time derivative in the response. The slope of the response curve is flattened with an increasing order space derivative. Due to the influence of the fractional derivative, the predicted pressure distribution in the reservoir is different from the classical diffusion response. The behavior of the trilinear model of Ozkan et al. (2011) is also analyzed in the study. The

slope of derivative plot signifies the contribution of the different regions at the different stages. One of the main limitations of the study, however, is the uncertainty with the anticipated value of the memory parameter. Apart from these diffusion approaches, El-banbi (1998) introduced the concept of linear flow for a hydraulically fractured reservoir. Alahmadi (2010) proposed a triple porosity model for a horizontal well production and follows the solution procedure of the El-Banbi (1998). The study assumes linear flow in the three domains of the reservoir; matrix, macro-fracture, and the micro-fracture. All the possible conditions of fluid flow are assumed as an inter-porosity transfer condition and the shape factor are defined according to the definition of Kazemi (1969). In the pressure response curve, Alahmadi (2010) found five different slopes that reflect the domination of the different regions of the reservoir at different stages of time.

Both the anomalous diffusion approach and the continuum-based approach are recognized as the most updated tools for the characterizing of the fractured reservoir. The comparison, therefore, provides a basis for the application of the correct approach. The validation of the models with the field data shows their comparative applicability at different flow times.

## 4.2 Anomalous Diffusion Model

### 4.2.1 Physical Model

A rectangularly shaped reservoir is assumed as in figure 4.1.

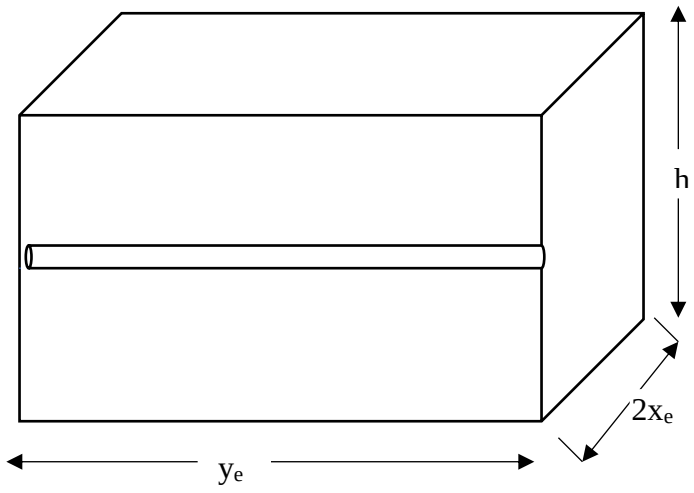


**Figure 4.1: The Physical Structure of the reservoir for the Anomalous Diffusion model (Model I)**

### 4.2.2 Model Development

The anomalous diffusion equation for a slightly compressible fluid for the reservoir (Figure 4.1) (Chen and Raghavan, 2015)

$$\frac{\partial}{\partial x}\left(\frac{k_{\alpha,\beta}}{\mu}\frac{\partial^{\beta}\Delta p(x,t)}{\partial x^{\beta}}\right)=\phi\, c_t\,\frac{\partial^{\alpha}\Delta p(x,t)}{\partial t^{\alpha}} \tag{4.1}$$

At the initial time, equilibrium condition is existed in the system. So,

$$p(x,o)=p_i \tag{4.2}$$

The inner boundary condition:

$$q=-\frac{k_{\alpha,\beta}}{\mu}\frac{\partial^{1-\alpha}}{\partial t^{1-\alpha}}\left(\frac{\partial^{\beta}\Delta p(x,t)}{\partial x^{\beta}}\right)_{x=0} \tag{4.3}$$

The outer boundary condition:

$$\left.\frac{\partial\Delta p(x,t)}{\partial x}\right|_{x=x_e}=0 \tag{4.4}$$

The dimensionless form of the Eq. 4.1:

$$\frac{\partial}{\partial x_D}\left(\frac{\partial^\beta p_D}{\partial {x_D}^\beta}\right) = \lambda_{\alpha,\beta}\ \frac{\partial^\alpha\ p_D}{\partial {t_D}^\alpha} \tag{4.5}$$

$\eta = \frac{k_{\alpha,\beta}}{\phi\ c_t \mu}$ and $\lambda_{\alpha,\beta} = \frac{x_e {x_e}^\beta}{\eta\left(\frac{x_e^2 \phi\ c_t \mu}{k_{\alpha,\beta}}\right)^\alpha}$ which is a dimensional parameter. If $\alpha = 1\ and\ \beta = 1$, this denotes the conventional diffusion and the parameter $\lambda_{\alpha,\beta}$ is a dimensionless diffusivity constant.

The solution of the Eq. 4.5 is derived in Laplace domain by performing the Laplace transformation for two times in the equation, the first transformation is done with respect to the time (t) and the second one with respect to the space (x). The analogous solution technique, however, is used in Fomin *et al.* (2011), Atangana and Kilicman (2013) and in Chen and Raghavan (2015), for a constant terminal rate boundary condition. The Laplace transformation of the Eq. 4.5 with respect to the time (t) is:

$$\frac{\partial}{\partial x_D}\left(\frac{\partial^\beta \overline{p_D}(x,s)}{\partial {x_D}^\beta}\right) = \lambda_{\alpha,\beta} s^\alpha\ \overline{p_D}(x,s) \tag{4.6}$$

Now applying the Laplace transformation on the Eq. 4.6 for space (x):

$$\tilde{s}\left[\tilde{s}^\beta \overline{\overline{p_D}}(s,\tilde{s}) - \tilde{s}^{\beta-1}\overline{p_D}(0,s)\right] - \left(\frac{\partial^\beta \overline{p_D}(x_D,s)}{\partial {x_D}^\beta}\right)_{x_D=0} - \lambda_{\alpha,\beta} s^\alpha \overline{\overline{p_D}}(s,\tilde{s}) = 0 \tag{4.7}$$

$$\overline{\overline{p_D}}(s,\tilde{s}) = \frac{\tilde{s}^\beta}{\tilde{s}^{\beta+1} - \lambda_{\alpha,\beta} s^\alpha}\bar{p}_D(0,s) + \frac{1}{\tilde{s}^{\beta+1} - \lambda_{\alpha,\beta} s^\alpha}\left(\frac{\partial^\beta \bar{p}_D(x_D,s)}{\partial {x_D}^\beta}\right)_{x_D=0} = 0 \tag{4.8}$$

Inverting Eq. 4.8 with the basic properties of the Mittag-Leffler function yields:

$$\bar{p}_D(x_D,s) = \bar{p}_D(0,s) E_{\beta+1}\left(\lambda_{\alpha,\beta} s^\alpha {x_D}^{\beta+1}\right) + \left(\frac{\partial \bar{p}_D(x_D,s)}{\partial {x_D}^\beta}\right)_{x_D=0} {x_D}^\beta E_{\beta+1,\beta+1}\left(\lambda_{\alpha,\beta} s^\alpha {x_D}^{\beta+1}\right) \tag{4.9}$$

The constant flow rate is $\frac{q}{4}$ as only one fourth of the total drainage area is considered for modelling in this context. The inner boundary condition (Eq. 4. 3) will be

$$\frac{q}{4} = -\frac{k_{\alpha,\beta} A_F}{\mu} \frac{\partial^{1-\alpha}}{\partial t^{1-\alpha}} \left( \frac{\partial^{\beta} \Delta p(x,t)}{\partial x^{\beta}} \right)_{x=0} \tag{4.10}$$

$$\frac{\partial^{1-\alpha}}{\partial {t_D}^{1-\alpha}} \left( \frac{\partial^{\beta} \Delta p_D}{\partial {x_D}^{\beta}} \right)_{x_D=0} = -\frac{\pi}{c_{AF}} \tag{4.11}$$

$$\left( \frac{\partial^{\beta} \overline{\Delta p}_D(x_D, s)}{\partial {x_D}^{\beta}} \right)_{x_D=0} = -\frac{\pi}{c_{AF} s^{2-\alpha}} \tag{4.12}$$

Using the value of the 4.13 in 4.9:

$$\bar{p}_D(x_D, s) = \bar{p}_D(0, s) E_{\beta+1}\left(\lambda_{\alpha,\beta} s^{\alpha} {x_D}^{\beta+1}\right) - \frac{\pi}{c_{AF} s^{2-\alpha}} {x_D}^{\beta} E_{\beta+1,\beta+1}(\lambda_{\alpha,\beta} s^{\alpha} {x_D}^{\beta+1}) \tag{4.13}$$

Using the derivative properties of the Mittag-Leffler function (Hombole *et. al.*, 2011; Fomin *et. al.*, 2010) in the outer boundary condition (Eq. 4.4)

$$\frac{d\bar{p}_D(x_D, s)}{dx_D} = \bar{p}_D(0, s) \lambda_{\alpha,\beta} s^{\alpha} {x_D}^{\beta} E_{\beta+1,\beta+1}\left(\lambda_{\alpha,\beta} s^{\alpha} {x_D}^{\beta+1}\right) - \frac{\pi}{c_{AF} s^{2-\alpha}} {x_D}^{\beta-1} E_{\beta+1,\beta}\left(\lambda_{\alpha,\beta} s^{\alpha} {x_D}^{\beta+1}\right) \tag{4.14}$$

$$\frac{\partial \bar{p}_D}{\partial {x_D}_{|x_D=1,s}} = \bar{p}_D(0, s) \lambda_{\alpha,\beta} s^{\alpha} E_{\beta+1,\beta+1}\left(\lambda_{\alpha,\beta} s^{\alpha}\right) - \frac{\pi}{c_{AF} s^{2-\alpha}} E_{\beta+1,\beta}\left(\lambda_{\alpha,\beta} s^{\alpha}\right) = 0 \tag{4.15}$$

$$\bar{p}_D(0, s) = \frac{\pi E_{\beta+1,\beta}\left(\lambda_{\alpha,\beta} s^{\alpha}\right)}{c_{AF} s^2 \lambda_{\alpha,\beta} E_{\beta+1,\beta+1}\left(\lambda_{\alpha,\beta} s^{\alpha}\right)} \tag{4.16}$$

Substitute the value of the Eq.4.16 in Eq. 4.14

$$\bar{p}_D(x_D, s) = \frac{\pi E_{\beta+1,\beta}\left(\lambda_{\alpha,\beta} s^{\alpha}\right)}{c_{AF} s^2 \lambda_{\alpha,\beta} E_{\beta+1,\beta+1}\left(\lambda_{\alpha,\beta} s^{\alpha}\right)} E_{\beta+1}\left(\lambda_{\alpha,\beta} s^{\alpha} {x_D}^{\beta+1}\right) - \frac{\pi}{c_{AF} s^{2-\alpha}} {x_D}^{\beta} E_{\beta+1,\beta+1}(\lambda_{\alpha,\beta} s^{\alpha} {x_D}^{\beta+1}) \tag{4.17}$$

This is the expression for the dimensionless pressure drop for the constant terminal rate flow in the wellbore.

At $x_D = 0$ the dimensionless pressure drop will be the bottom-hole pressure drop. The expression can be deduced from the Eq.4.17:

$$\bar{p}_D(x_D, s)|_{x_D=0} = \bar{p}_{wD}(x_D, s) = \frac{\pi E_{\beta+1,\beta}\left(\lambda_{\alpha,\beta} s^{\alpha}\right)}{c_{AF} s^2 \lambda_{\alpha,\beta} E_{\beta+1,\beta+1}\left(\lambda_{\alpha,\beta} s^{\alpha}\right)} \tag{4.18}$$

$$\left[E_{\beta+1}(0) \approx 1\right]$$

This is the expression for the dimensionless bottom-hole pressure for the constant terminal rate flow. For $\alpha = 1, \beta = 1$ the flow will be the classical flow equation and that yields $\lambda_{\alpha,\beta} = 1, c_{AF} = \frac{y_e B}{2x_e}$

$$\bar{p}_{wD}(x_D, s) = \frac{\pi}{c_{AF} s \lambda_{\alpha,\beta} s^{\alpha} \tanh(\sqrt{\lambda_{\alpha,\beta} s^{\alpha}})} \tag{4.19}$$

$$\bar{p}_{wD}(x_D, s) = \frac{\pi}{c_{AF} s} \tag{4.20}$$

### 4.3 Linear Triple Porosity Model

#### 4.3.1 Physical Model

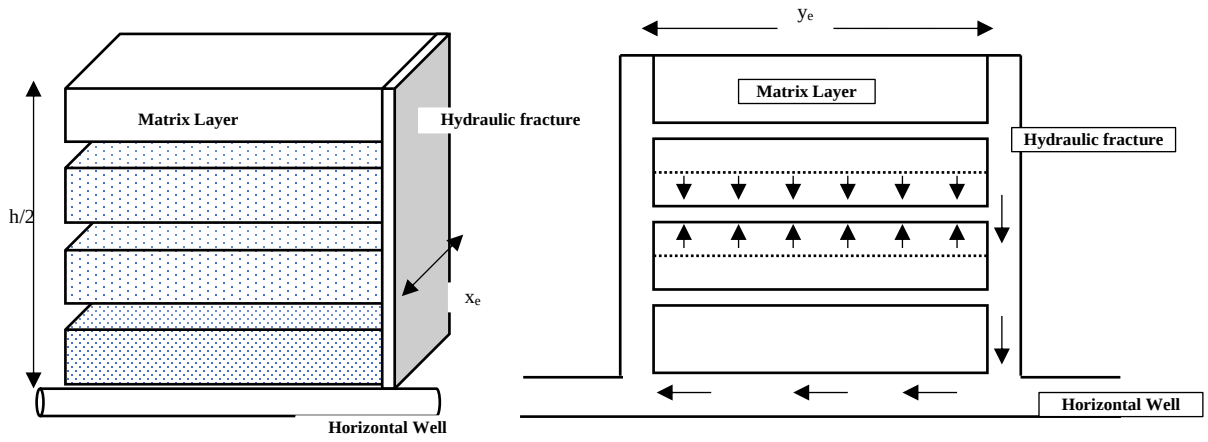


**Figure 4.2: The Physical Structure of the reservoir for the linear model (Model II)**

For the model II, strata duel porosity model (Kazemi, 1969) is assumed in the bounded region of two hydraulic fractures (Figure 4.2). Linear flow (El-Banbi, 1998; Ahmadi and Wattenbarger, 2011) is sustained in all the regions. Fluid is flowing from the reservoir to the horizontal wellbore through the hydraulic fracture only.

#### 4.3.2 Model Development

The governing flow equation in the matrix layer is:

$$\frac{\partial^2 \Delta p_m}{\partial z^2} = \frac{(\phi\, c_t)_m \mu}{k_m} \frac{\partial \Delta p_m}{\partial t} \tag{4.21}$$

The initial condition

$$\Delta p_{mD(z_D,0)} = 0 \tag{4.22}$$

The inner Boundary conditions

$$\frac{\partial \Delta p_m}{\partial z}_{|z=0} = 0 \tag{4.23}$$

The outer boundary conditions

$$\Delta p_m\Big|_{z=\frac{L_{nf}}{2}} = \Delta p_{nf}\Big|_{z=\frac{L_{nf}}{2}} \tag{4.24}$$

The dimensionless form of Eq. 4.21:

$$\frac{\partial^2 \Delta p_{mD}}{\partial {z_D}^2} - \frac{3\omega_m}{\lambda_m} \frac{\partial \Delta p_{mD}}{\partial t_D} = 0 \tag{4.25}$$

Taking the Laplace transformation:

$$\frac{\partial^2 \overline{\Delta p}_{mD}}{\partial {z_D}^2} - \frac{3\omega_m}{\lambda_m} \left\{ s\overline{\Delta p}_{mD}(z_D, s) - \Delta p_{mD}(z_D, 0) \right\} = 0 \tag{4.26}$$

The initial condition yields

$$\frac{\partial^2 \overline{\Delta p}_{mD}}{\partial {z_D}^2} - \frac{3\omega_m}{\lambda_m} s\overline{\Delta p}_{mD}(z_D, s) = 0 \tag{4.27}$$

$$[\alpha_m = \frac{3\omega_m s}{\lambda_m}]$$

The general solution of the Eq. 4.27:

$$\overline{\Delta p}_{mD} = A exp\left(-\sqrt{\alpha_m} z_D\right) + B exp(\sqrt{\alpha_m} z_D) \tag{4.28}$$

Now for the inner boundary condition (Eq. 4.23):

$$\overline{\Delta p}_{mD} = 2B cosh\left(\sqrt{\alpha_m} z_D\right) \tag{4.29}$$

For the outer boundary condition (Eq. 4.23):

$$\overline{\Delta p}_{mD} = \frac{\overline{\Delta p}_{nfD} cosh\left(\sqrt{\alpha_m} z_D\right)}{cosh\left(\sqrt{\alpha_m}\right)} \tag{4.30}$$

The fluid flow equation in the natural fracture:

The source term in the natural fractured flow model is evaluated by the definition of Kazemi (1969).

$$\frac{\partial^2 \Delta p_{nf}}{\partial y^2} = \frac{(\phi\, c_t)_{nf}\mu}{k_{nf}} \frac{\partial \Delta p_{nf}}{\partial t} + \frac{\mu}{k_{nf}} q_{Source,m} \tag{4.31}$$

$$\frac{\partial^2 \Delta p_{nf}}{\partial y^2} = \frac{(\phi\, c_t)_{nf}\mu}{k_{nf}} \frac{\partial \Delta p_{nf}}{\partial t} + \frac{k_m}{k_{nf}} \frac{2}{L_{nf}} \frac{\partial \Delta p_m}{\partial z}\Big|_{z=\frac{L_{nf}}{2}} \tag{4.32}$$

$$\frac{\partial^2 \Delta p_{mfD}}{\partial {y_D}^2} = \frac{y_{eD}^2}{4} \frac{\partial \Delta p_{nfD}}{\partial t_D} + \lambda_{mf} \frac{\partial \Delta p_{mD}}{\partial z_D}_{|z_D=1} \tag{4.33}$$

Initial condition for the natural fracture

$$\Delta p_{nfD}(y_D, o) = 0 \tag{4.34}$$

The inner and outer boundary conditions

$$\frac{\partial \overline{\Delta p}_{nfD}}{\partial y_D}_{|y_D=o,s} = 0 \tag{4.35}$$

$$\overline{\Delta p}_{nfD_{|y_D=1,s}} = \overline{\Delta p}_{HFD_{|y_D=1,s}} \tag{4.36}$$

From Eq. 4.30

$$\frac{\partial \Delta p_{mD}}{\partial z_D}_{|z_D=1} = \overline{\Delta p}_{nfD} \sqrt{\alpha_m} \tanh\left(\sqrt{\alpha_m}\right) \tag{4.37}$$

Laplace transformation of the Eq. 4.37

$$\frac{\partial^2 \overline{\Delta p}_{nfD}}{\partial y_D^2} = \frac{y_{eD}^2}{4} \left\{ s\overline{\Delta p}_{nfD}(y_D, s) - \Delta p_{nfD}(y_D, 0) \right\} + \lambda_{mf} \frac{\partial \overline{\Delta p}_{mD}}{\partial z_D}_{|y_D=1} = 0 \tag{4.38}$$

Using the Eq. 4.34 and Eq. 4.37

$$\frac{\partial^2 \overline{\Delta p}_{nfD}}{\partial {y_D}^2} = \frac{y_{eD}^2 s}{4} \overline{\Delta p}_{nfD} + \lambda_{mf} \sqrt{\alpha_m} \tanh\left(\sqrt{\alpha_m}\right) \overline{\Delta p}_{nfD_{|z_D=1}} = 0$$

$$\frac{\partial^2 \overline{\Delta p}_{nfD}}{\partial {y_D}^2} - \alpha_{nf} \overline{\Delta p}_{nfD} = 0 \tag{4.39}$$

$$[\alpha_{nf} = \frac{y_{eD}^2 s}{4} + \lambda_{mf} \sqrt{\alpha_m} \tanh\left(\sqrt{\alpha_m}\right)]$$

The general solution of the Eq. 4.39

$$\overline{\Delta p}_{nfD} = A exp\left(-\sqrt{\alpha_{nf}} y_D\right) + B exp\left(\sqrt{\alpha_{nf}} y_D\right) \tag{4.40}$$

Apply the inner boundary condition

$$\overline{\Delta p}_{nfD} = 2Bcosh\,(\sqrt{\alpha_{nf}}y_D) \tag{4.41}$$

At the outer boundary (Eq. 4.36)

$$B = \frac{\overline{\Delta p}_{HFD_{|y_D=1}}}{2cosh\,(\sqrt{\alpha_{nf}})} \tag{4.42}$$

From the Eq. 4.41

$$\overline{\Delta p}_{nfD} = \overline{\Delta p}_{HFD_{|y_D=1}} \frac{cosh\,(\sqrt{\alpha_{nf}}y_D)}{cosh\,(\sqrt{\alpha_{nf}})} \tag{4.43}$$

The flow equation in the hydraulic fracture

$$\frac{\partial^2 \Delta p_{HF}}{\partial x^2} = \frac{(\phi\, c_t)_{HF}\mu}{k_{HF}} \frac{\partial \Delta p_{HF}}{\partial t} + \frac{\mu}{k_{HF}} q_{Source,mf} \tag{4.44}$$

$$\frac{\partial^2 \Delta p_{HF}}{\partial x^2} = \frac{(\phi\, c_t)_{HF}\mu}{k_{HF}} \frac{\partial \Delta p_{HF}}{\partial t} + \frac{k_{nf}}{k_{HF}} \frac{2}{y_e} \frac{\partial \Delta p_m}{\partial y}_{|y=\frac{y_e}{2}} \tag{4.45}$$

$$\frac{\partial^2 \Delta p_{HFD}}{\partial {x_D}^2} = \frac{\omega_{HF}}{k_{MFD}} \frac{\Delta p_{HFD}}{\partial t_D} + \frac{\lambda_{HF}}{3} \frac{\partial \Delta p_{nfD}}{\partial y_D}_{|y_D=1} \tag{4.46}$$

Initial condition for the hydraulic fracture

$$\Delta p_{HFD}(y_D, o) = 0 \tag{4.47}$$

At the well bore the hydraulic fracture maintains a constant flow rate

$$q = -\frac{k_{HF}A}{\mu} \frac{\partial p_{HF}}{\partial x}\Big|_{x=0} \tag{4.48}$$

$$\left(\frac{\partial \bar{p}_{HFD}}{\partial x_D}\right)_{x_D=0,s} = -\frac{\pi}{c_{AD}s} \tag{4.49}$$

Now flow condition at outer boundary gives

$$\frac{\partial \Delta p_{HF}}{\partial x}_{|x=x_e,t} = 0 \tag{4.50}$$

The general flow equation for the hydraulic fracture, from Eq. 4.46, Eq. 4.47 and Eq.4.49

$$\frac{\partial^2 \bar{p}_{HFD}}{\partial {x_D}^2} - \alpha_{HF}\bar{p}_{HFD} = 0$$

Hydraulic fracture pressure solution

$$\bar{p}_{HFD} = \frac{\pi cosh\,(\sqrt{\alpha_{HF}}(1 - x_D)}{c_{AFD}s\sqrt{\alpha_{HF}}sinh\,(\sqrt{\alpha_{HF}})} \tag{4.51}$$

This is the expression for the dimensionless hydraulic fracture pressure for the constant terminal rate flow. At $x_D = 0$ the hydraulic fracture pressure will be the bottom-hole pressure.

$$\bar{p}_{wD} = \frac{\pi}{c_{AFD} s \sqrt{\alpha_{HF}} tanh(\sqrt{\alpha_{HF}})} \tag{4.52}$$

This is the expression for the dimensionless bottom-hole pressure for the constant terminal rate flow and has the same form of Eq. 4.19; although, it has a different non-Homogeneous function. If $\alpha_{HF} = 1$ then from the asymptotic expression of the $\tanh(1)$, it can be shown that the Eq. 4.52 becomes:

$$\bar{p}_{wD}(x_D, s) = \frac{\pi}{c_{AFD} s} \tag{4.53}$$

This is the general expression for the bottom-hole pressure at constant flow rate for the linear reservoir.

**4.4 Results and Analysis**

The dimensionless pressure response of the homogeneous reservoir is a single slope line. It is evident that the response curve has more than one slope in the dual or triple continuum reservoir (Warren and Root, 1968, Abdassah and Ershaghi, 1986). The response curve of tri-linear models also shows a slope change at the transition of the earlier and the intermediate to late time response (Brawn, 2009; Ozkan *et al.*, 2011,2012, Albinali *et al.*, 2016a, 2016b). Figure 4.3 shows the dimensionless pressure response of the anomalous diffusion model and the triple porosity model. The impact of space and time events create lower pressure drop during initial period in the anomalou diffusion model. On the contrary, the response of the triple porosity model has two distinct slopes. The initial slope holds the contributions of the hydraulic fracture whereas the second slope changes according to the late stage pressure response.,

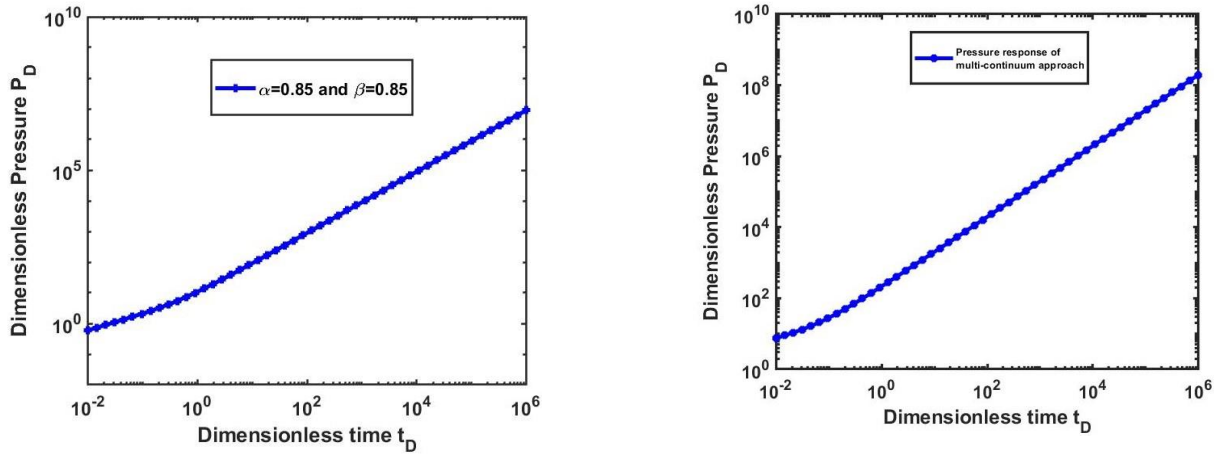


**Figure 4.3: Dimensionless wellbore pressure for the anomalous diffusion model and for the linear triple porosity model**

Figure 4.4 and 4.5 shows the impact of space and time derivative in the anomalous diffusion model. The effect of the super-diffusion is evaluated according to the order of the space derivative. As the value of $\beta$ decreases from the unity, the space event becomes more significant; hence, the flow will be accelerated at the same pressure gradient. The sub-diffusion has a negligible effect at the late time response of the reservoir. Figure 4.5 shows that the space events cause a lower pressure-drop to maintain the same production rate. The single most marked observation to emerge from the figure is the impact of the super-diffusion is prolonged from the very early time to the late time. This result has further strengthened the hypothesis that the space event in the hydraulic fracture can significantly alter the flow characteristics.

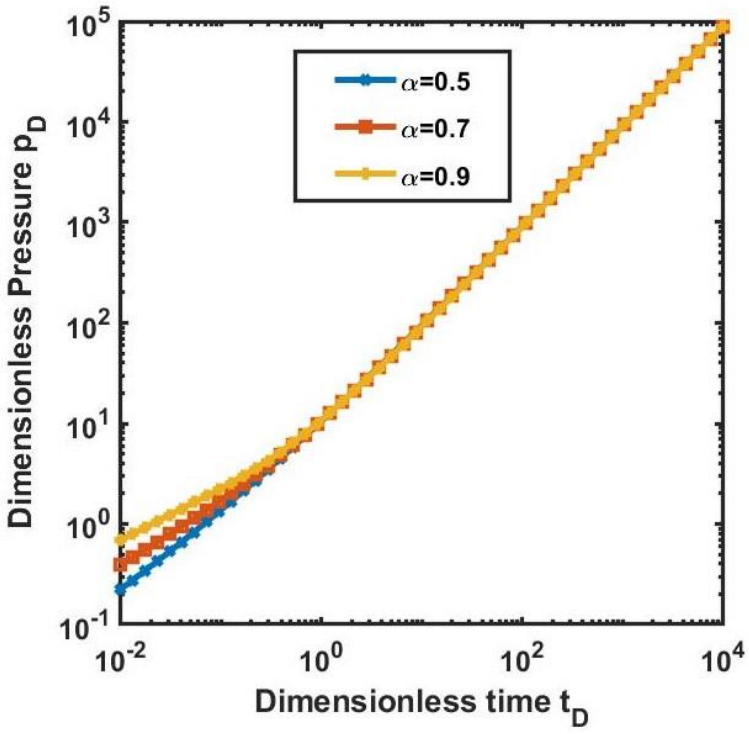


**Figure 4.4: Effect of fractional time order in the anomalous diffusion model**

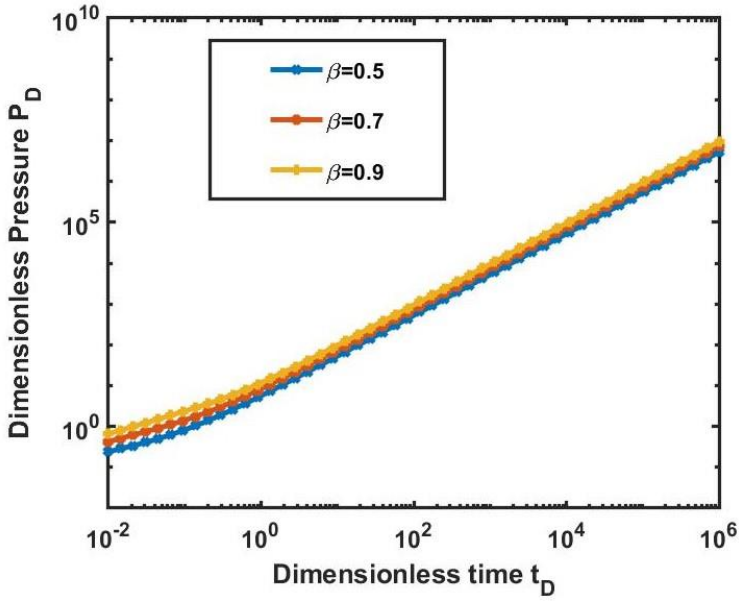


**Figure 4.5: Effect of fractional space order in the anomalous diffusion model**

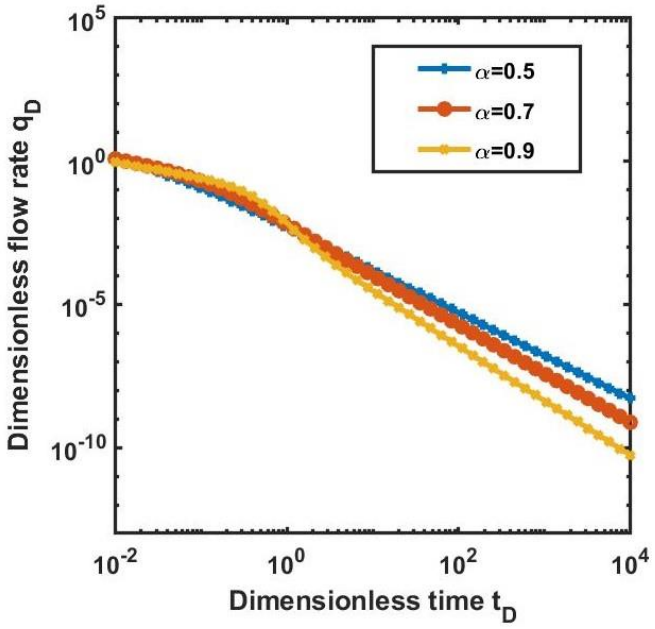


**Figure 4.6: Dimensionless flow rate at constant bottom hole pressure of the anomalous diffusion model**

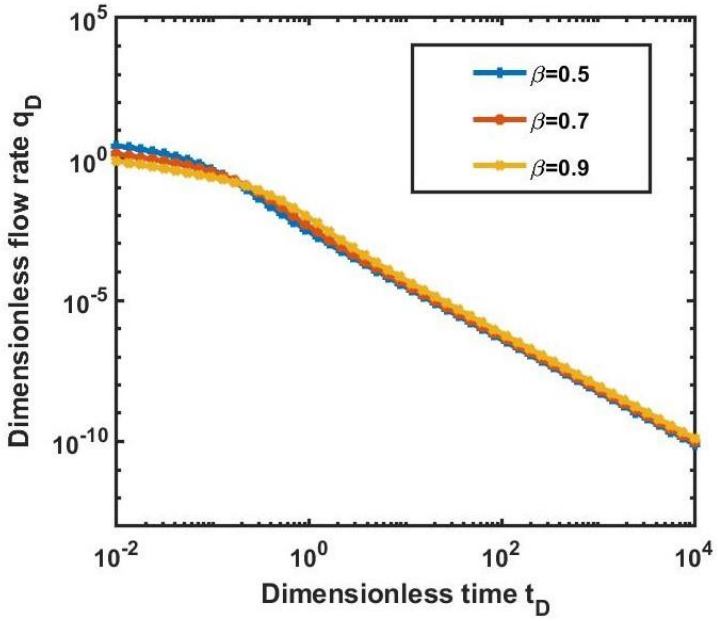


**Figure 4.7: Dimensionless flow rate at constant bottom hole pressure of the anomalous diffusion model**

Figure 4.6 and figure 4.7 shows the responses of the anomalous model for constant bottom hole pressure. The depletion trends of the production rate show the effects of sub-diffusion and super-diffusion on the production performance.

Figure 4.8 shows the effect of the hydraulic fracture permeability on the pressure response. Hydraulic fracture is the main conduit in the model as it is the only medium that transfer the fluids to the reservoir; thus, the permeability-alteration in the hydraulic fracture changes the pressure response from the earlier time to the late time of the production ($t_D = 10.6E4$). However, at the early to intermediate time, the hydraulic fracture permeability causes the most variation in the pressure response. At later time the flow capacitance of the macro-fracture reaches to the maximum and the flow is influenced by the boundary effect.

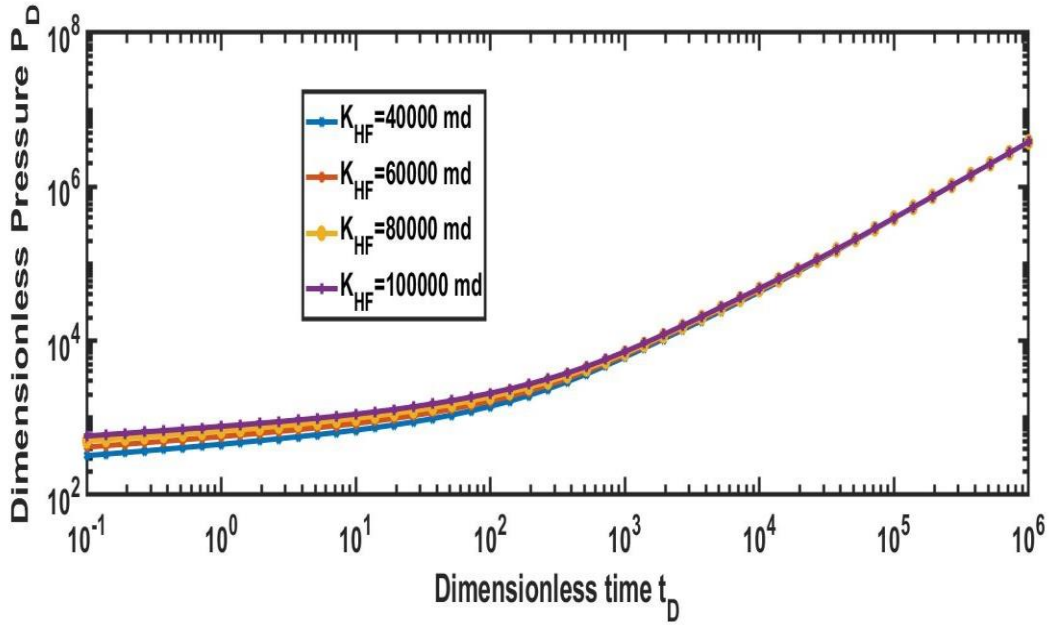


**Figure 4.8: Effect of Hydraulic fracture permeability in the multi-continuum model**

The comparison of the responses of the two models (Figure 4.9) reveals the consistency of the results. The reactions of the two models are to be similar to the order of the differentiation in the anomalous model is closing to a unit value. However, a lower pressure drop at the early time is the evidence of the super-diffusion in the hydraulic fracture that makes the difference between the two models.

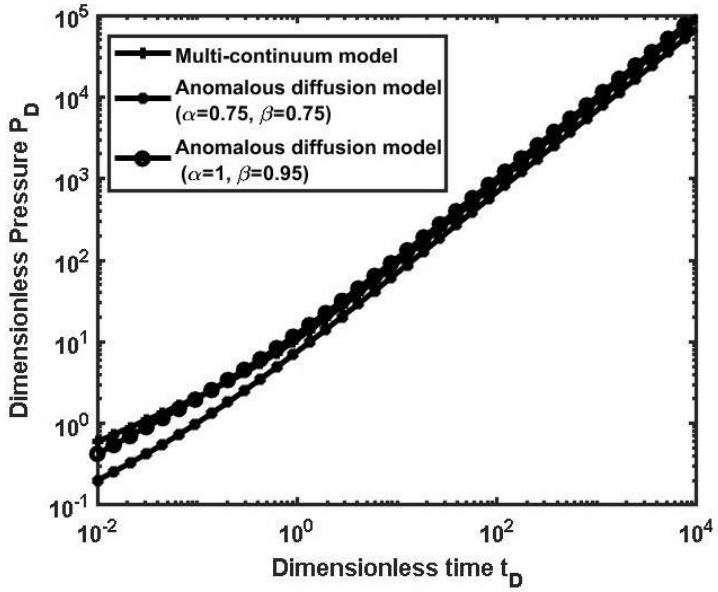


**Figure 4.9: Comparison of the multi-continuum approach and the Anomalous diffusion method**

### 4.5 Conclusions

The study has developed two models to analyze the performance of a hydraulically fractured reservoir. The analysis from this study suggests that the continuum-based models consider the physical structure of the reservoir; however, the required reservoir parameters for the new continuum are difficult to be determined. Alternatively, anomalous diffusion concept requires less parameter compare to the continuum approaches, but a high uncertainty exists in the precise determination of the order of the differentiation or the fractal exponent. The magnitudes of the effects of the time and space events are related to the order of the differentiation. The space events control both the early and late stage responses of the pressure curve. The time events have a negligible effect on the late stage performance. The permeability of the hydraulic fracture is the dominating parameter in the multi-continuum approach. A higher permeability in the hydraulic fracture can increase the flow rate of the reservoir. Future studies on the current topic, therefore, require a logical combination of continuum approach and anomalous diffusion. It will not only reduce the complication but also increase the accuracy in the fractured-reservoir characterization.

## Nomenclature

| | |
|---|---|
| h | Reservoir thickness, ft |
| $r_w$ | Wellbore radius, ft |
| $y_e$ | Horizontal well length, ft |
| $L_F$ | Spacing of natural fracture, ft |
| $x_e$ | Distance to boundary parallel to well, ft |
| μ | Viscosity, cp |
| q | Constant flow rate, Stb/day |
| ∅ | Porosity, fraction |
| $K_\beta$ | Phenomenological coefficient, md-hr$^{1-\alpha}$ |
| $c$ | Total compressibility, Psi$^{-1}$ |
| w | Hydraulic fracture width, ft |
| β | Memory Parameter (Space) |
| K | Permeability, md |
| $\alpha$ | Memory Parameter, |

## References


Abdassah, D., & Ershaghi, I. (1986). Triple-porosity systems for representing naturally fractured reservoirs. SPE Formation Evaluation, 1(02), 113-127.

Alahmadi, H. A. H. (2010). A Triple-porosity model for fractured horizontal wells (Doctoral dissertation, Texas A & M University).

Albinali, A. (2016). Analytical solution for anomalous diffusion in fractured nanoporous reservoirs. Colorado School of Mines.

Brown, M., Ozkan, E., Raghavan, R., & Kazemi, H. (2011). Practical solutions for pressure-transient responses of fractured horizontal wells in unconventional shale reservoirs. SPE Reservoir Evaluation & Engineering, 14(06), 663-676.

de Swaan O, A. (1976). Analytic solutions for determining naturally fractured reservoir properties by well testing. Society of Petroleum Engineers Journal, 16(03), 117-122.

El-Banbi, A. H., & Wattenbarger, R. A. (1998, January). Analysis of linear flow in gas well production. In SPE Gas Technology Symposium. Society of Petroleum Engineers.

Fomin, S. E. R. G. E. I., Chugunov, V., & Hashida, T. O. S. H. I. Y. U. K. I. (2011). Mathematical modeling of anomalous diffusion in porous media. Fract. Differ. Calc, 1(1), 1-28.

Haubold, H. J., Mathai, A. M., & Saxena, R. K. (2011). Mittag-Leffler functions and their applications. Journal of Applied Mathematics, 2011.

Kazemi, H. (1969). Pressure transient analysis of naturally fractured reservoirs with uniform fracture distribution. Society of petroleum engineers Journal, 9(04), 451-462.

Ozcan, O. (2014). Fractional diffusion in naturally fractured unconventional reservoirs. Colorado School of Mines.

Ozkan, E., Brown, M. L., Raghavan, R., & Kazemi, H. (2011). Comparison of fractured-horizontal-well performance in tight sand and shale reservoirs. SPE Reservoir Evaluation & Engineering, 14(02), 248-259.

Raghavan, R. "Fractional derivatives: application to transient flow." Journal of Petroleum Science and Engineering 80.1 (2011): 7-13.

Raghavan, R. (2011). Fractional derivatives: application to transient flow. Journal of Petroleum Science and Engineering, 80(1), 7-13.

Stehfest, H. (1970). Algorithm 368: Numerical inversion of Laplace transforms [D5]. Communications of the ACM, 13(1), 47-49.

Warren, J. E., & Root, P. J. (1963). The behavior of naturally fractured reservoirs. Society of Petroleum Engineers Journal, 3(03), 245-255.

# Chapter 5: Development of A Linear Fluid Flow Model for the Naturally Fractured Reservoir Based on the Memory and Multi-Continuum Approach

## Preface

Naturally fractured reservoir is a highly heterogeneous formation with an irregular arrangement of matrix and fracture in different scales. Hence, a proper approximation of the reservoir formation and the accurate assumption of the flow conditions are essential to capture the inherent heterogeneity of the fractured reservoir. This study aims to develop a linear mathematical model for a naturally fractured reservoir through an assumption of the multi-continuum approach and a combination of the conventional diffusion and the anomalous diffusion at the transient condition. The study introduces the triple porosity model in the inner reservoir. The logical combination of super-diffusion and sub-diffusion also innovatively utilizes in the model development process. The complex physical structure of the model reservoir can be able to capture the heterogeneity of the fractured reservoir in more details. The heterogeneity of separate formation, however, appears as a function of time in the final expression. Therefore, the heterogeneous behavior of an individual region can be captured and analyzed by this model. The pressure response curve comprises areas with distinguishing slopes; consequently, the value of the slope reflects the typical flow behavior of a flow domain. Moreover, the model is proved to be flexible for varying idealization of the physical arrangement in a flow region since the domain function can be altered and distinct physical structure of the area is related to the domain function. The model can be reduced to the expression of a homogeneous reservoir after imposing the proper condition, which states the validity of the model. The sensitivity analysis shows the effects of flow-parameters on the overall flow performance. The most remarkable observation to emerge from the study is the anomalous slope change in the pressure response curve. This finding reinforces the impact of the super-diffusion in the hydraulic fracture of the reservoir. Hence, this model can be used as a better alternative tool for the pressure transient data analysis of a naturally fractured reservoir.

## 5.1 Introduction

The fractured reservoir attributes an anomalous characteristic behavior since it has a complex structure of alternating matrices and fractures, and different flow-conditions exist in distinctive flow-domains. The first attempt to capture the heterogeneity of such type of reservoir is the dual continuum approach both for the transient condition (Kazemi, 1969, de Swaan-O, 1976) and the semi-steady state condition (Warren and Root, 1968). The two continua are termed matrix and fracture; additionally, the matrix is considered the primary source and the fracture as the principal conduit. A sudden slope change in the pressure-response curve of a fractured reservoir is related to the relative capacitance of the matrix and the fracture. Triple continuum approaches (Abdassah and Ershaghi, 1986) add an extra continuum either a matrix or a fracture in the physical structure of the reservoir. The additional continuum is related to the anomalous slope change in the pressure-response curve that is evident in some fractured reservoir case. El-Banbi (1998) has considered the linear flow in the fractured reservoir for the early time and develops a linear dual porosity model. Linear flow, a flow that is perpendicular to any flow surface, occurs when a high permeable continuum drains the fluid from a tight formation with very low permeability (Wattenbarger, 2007). Alahmadi (2010) has developed a linear model of triple continuum medium in the case of a fractured reservoir which produce through a horizontal well. He identifies five regions in the pressure response curve; moreover, the slope of each curve is related to the properties of the respective continuum. Brawn (2009) has introduced a tri-linear model for the horizontal well and considers the dual continuum approximation for the inner reservoir whereas linear axial flow is regarded as both for the outer reservoir and the hydraulic fracture. A continuum-function captures the inherent heterogeneity of each region and can be determined from the pressure response curve.

Ozcan (2011) has modified the tri-linear model by introducing a bi-linear anomalous diffusion in the inner reservoir. The natural and induced heterogeneity of the inner reservoir is related to the order of the fractional time derivative of the flow equation. Albinali (2016) has proposed another modified tri-linear model and assigns anomalous diffusion both in the outer reservoir and in the inner reservoir. The anomalous diffusion-

approaches utilize the fractional time or space derivative to scale up the heterogeneity of the reservoir; however, the determination of the proper order of the differentiation is the vital challenge in these approaches. Furthermore, no previous study considers the heterogeneous behavior of the hydraulic fracture zone. Alternatively, the continuum approaches need a number of intrinsic properties of the distinctive zone. The intrinsic properties of the outer reservoir and the hydraulic fracture are inconvenient to be determined. The aim of this study is to develop a linear mathematical model that considers both the continuum approach and the anomalous diffusion. In this study, the drainage area of a hydraulically fractured horizontal well is approximated by a modified Tri-linear model (TLM), which is comprised of three regions: outer reservoir, inner reservoir, and hydraulic fracture. The inner reservoir has a triple porosity arrangement with a characteristic spherical shale matrix. Though out the model development, the matrix is the main source of fluid and has the higher storability/fluid capacitance than the fracture. On the other hand, the fracture has a higher flow capacity than the matrix, so it behaves as a conduit. Flow is linear in all the regions under transient flow condition; however, the super-diffusion and the sub-diffusion are assigned respectively for the hydraulic fracture and the outer reservoir. A dimensionless pressure expression is derived in Laplace domain, and Stehfest algorithm inverses the solution to the real-time field. The expression of dimensionless hydraulic-fracture pressure contains Mittag-Leffler function due to the fractional derivative of space.

The adaptation of the triple porosity model in the inner reservoir region in a Tri-linear model to capture the heterogeneity is used for the first time in this model. The logical combination of sub-diffusion, super-diffusion, and linear axial flow for evaluating the performance of a hydraulically-fractured horizontal well is another innovative approach to this model.

**5.2 Model Reservoir**

The model reservoir follows the Tri-linear model (TLM) concept (Brawn, 2009; Ozcan, 2014; Alibini, 2016). According to the TLM, the reservoir has three main regions: outer reservoir, inner reservoir, and hydraulic fracture. Fluid-transfer occurs from the reservoir

to the well only through the hydraulic fracture. Fig. 5.1 shows the modeled reservoir, for the simplicity only two hydraulic fractures are shown in the figure.

### 5.2.1 Outer reservoir

Outer reservoir is extended beyond the tip of the hydraulic fracture. It consists of matrix and natural fracture; this region has no impact from the completion and the stimulation processes. Diffusion process in outer reservoir is controlled by the tight compressed-matrix and low permeability natural fracture. The complex network of the matrices and fractures distorts the fluid flow of the reservoir. This region, therefore, exhibits a sub-diffusion process. A fractional time derivative takes all the heterogeneity into accounts and the order of the differentiation is correlated to the degree of heterogeneity.

### 5.2.2 Inner Reservoir

Inner reservoir is defined as the confined area between two adjacent hydraulic fractures. A triple-continuum model approximates the fluid flow path in the inner reservoir. Three main continua are known as matrix, micro-fracture, and macro-fracture. The study considers two different shapes of the matrix; one is the spherical-shaped matrix, and another is the slab-sized matrix block. The spherical-shaped matrix represents highly-fractured tight-shale formation whereas the slab matrix block is applicable for the formation that has the higher matrix permeability. A general structure of the reservoir is shown in fig. 5.3 in a 2D view and the flow directions and boundaries conditions are also indicated. fig. 5.4 illustrated the details of the inner reservoir with spherical-shaped matrix while fig. 5.5 shows the slab matrix.

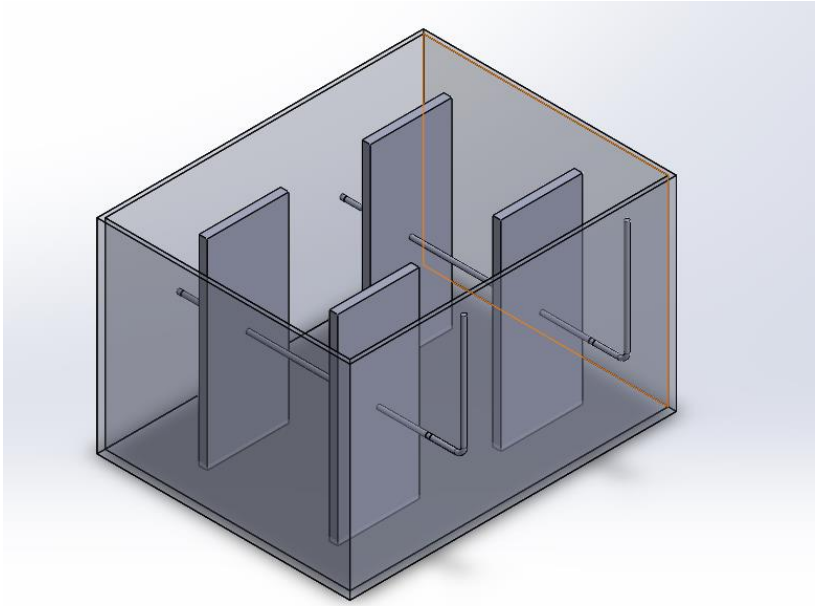

**Figure 5.1: Two Parallel horizontal well with hydraulic fracture.**

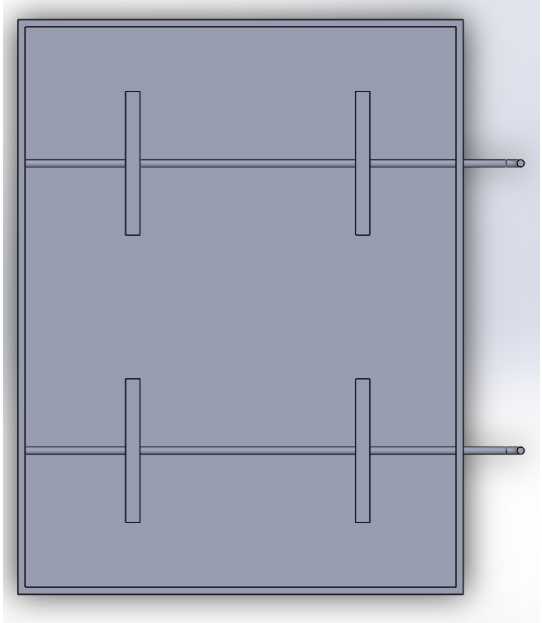

**Figure 5.2: Top view of the reservoir.**

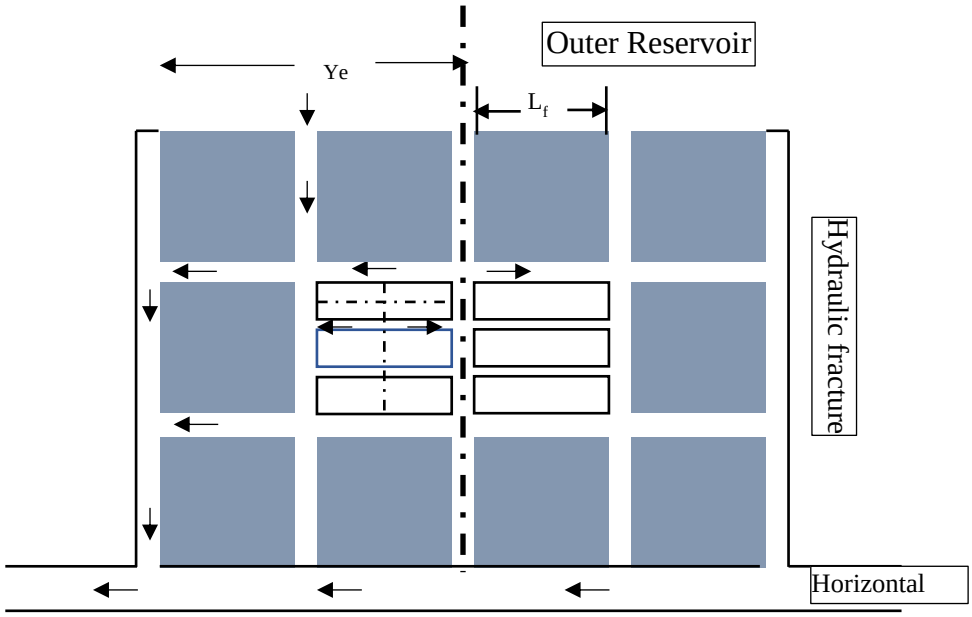


**Figure 5.3: Two-dimensional view of the reservoir and the flow direction for the model.**

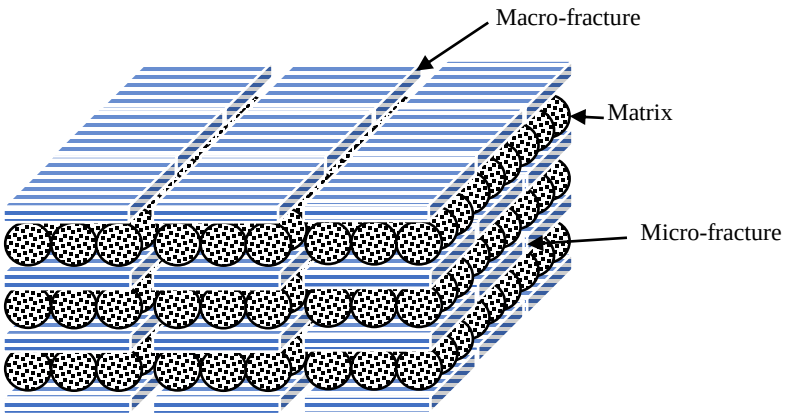


**Figure 5.4: Three-dimensional view of the inner reservoir (Spherical-shaped matrix).**

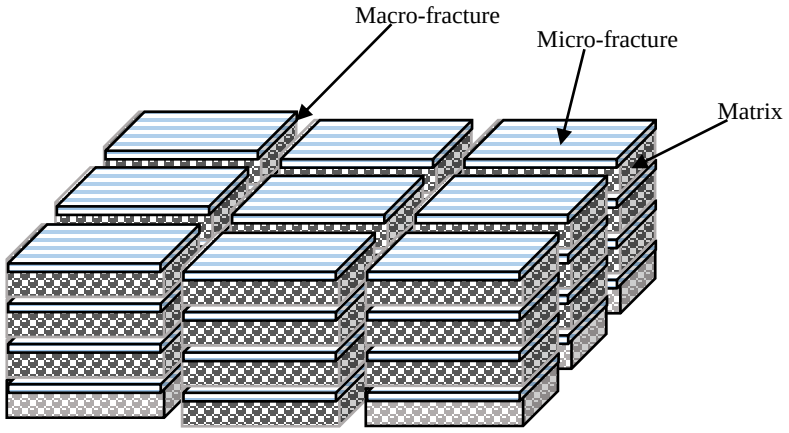


**Figure 5.5: Three-dimensional view of the inner reservoir (Matrix-Block)**

The matrix sphere has a fractured surface on its external area, is defined as matrix-cake and the physical structure is approximated according to the concept of Osman *et al.*, (2011). Fig. 5.6 demonstrates the structure of an individual matrix sphere which consists of three different continua, are named as core matrix, cake matrix, and cake fracture. The cake fracture is the only conduit that transfers fluid to the micro-fracture. Both the spherical-shaped core matrix and the cake matrix which is assumed as a sheet like structure, maintain a linear flow to the cake fracture. Fluid transfer from the matrix to the macro-fracture is assumed to be negligible. Not only the matrix slab but the micro-fracture also transfers a very slight amount of fluid to the hydraulic fracture. At the hydraulic fracture boundary, hence, macro-fracture conserves a pressure continuity and a flow continuity at this mutual boundary of inner reservoir and hydraulic fracture.

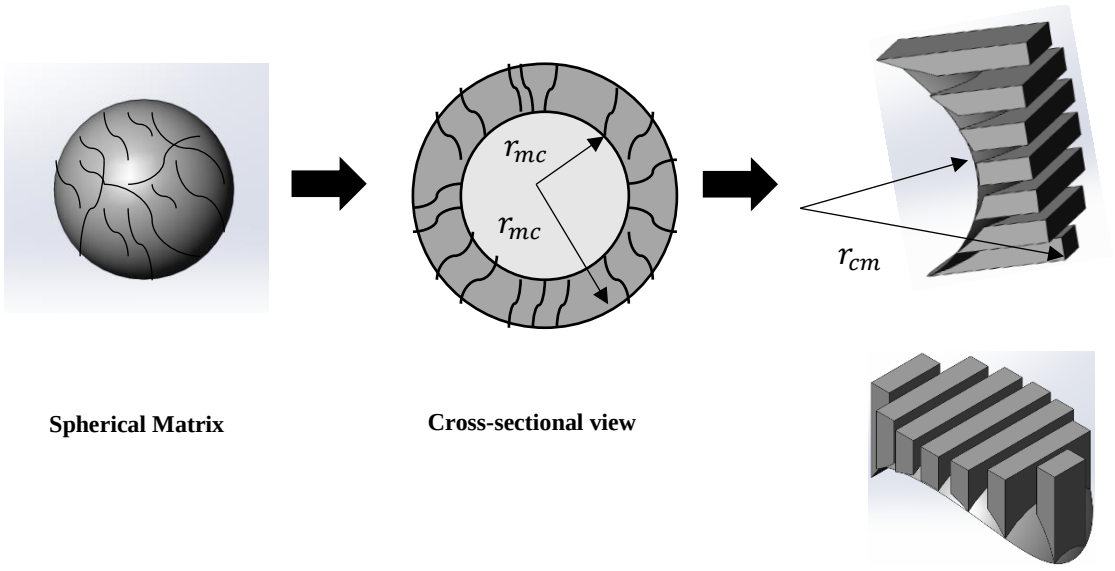


**Figure 5.6: Simplification of the matrix structure (Adapted from Osman *et al.;* 2011)**

### 5.2.3 Hydraulic Fracture

Hydraulic fracture is assumed to be rectangular shaped that is extended over the whole thickness ($h$) of the reservoir in the model. No fluid flow occurs at the tip of the hydraulic fracture; in the $x$ direction the tip denotes the outer-boundary location of the inner reservoir. Although the thickness of the hydraulic fracture is very thin compared to the inner reservoir width, the well inflow occurs only through this region. The total flow in the hydraulic fracture is the sum of the fluid fluxes that linearly comes in the $y$ direction from the inner reservoirs of the both sides.

## 5.3 Assumptions in the Model

- Single phase flow in a naturally fractured reservoir to a horizontal well.
- One dimensional linear flow of the slightly compressible fluid.
- A Flow symmetry at the midpoint of the two-lateral horizontal well.
- The isotropic permeability of the reservoir and constant viscosity of the reservoir fluid.

- Transfer of fluid occurs only through the Macro-fracture to the Hydraulic fracture.

- Matrix has the spherical shape and contains most of the storage of the reservoir.

- The Fracture has negligible storage capacity but has high conductivity.

- The pressure in the linear axis of each continuum is independent to the other continuum. (Pseudo-function).

- Unsteady state (Transient) flow condition in the all regions.

**5.4 Development of the Mathematical Model**

One dimensional linear diffusion equation for the slightly compressible fluid

$$\frac{\partial^2 p}{\partial x^2} = \frac{\phi\, c_t \mu}{k} \frac{\partial \mathrm{p}}{\partial t} \tag{5.1}$$

Flux law is modified by the fractional derivative for incorporating the memory effect (Caputo 1999, Hossain *et. al.;* 2005, 2006, Raghavan, 2011; Chen and Raghavan, 2011, 2013, 2014). Fractional time derivative represents the sub-diffusion. The Sub-diffusion occurs when the previous time event affects the performance of the current fluid flow. According to the order of the derivative, the fractional time derivative of the pressure gradient includes a weighing factor to each time step of the flow history and measure the effects of time at a point in the flow medium. Consequently, the pressure gradients at those points are not instantaneous; rather, holds the impact of the longer time event. The diffusion process is slowed down due to the fractional time derivative. Alternatively, the fractional space derivative represents a faster diffusion than the conventional one. The modified flux law for this anomalous diffusion is written as (Chen and Raghavan, 2015):

$$u\,(x,t) = \frac{q}{A} = -\eta_{\alpha,\beta}\, \frac{\partial^{1-\alpha}}{\partial t^{1-\alpha}} \left[\frac{\partial^{\beta} p(x,t)}{\partial x^{\beta}}\right] \tag{5.2}$$

$0 < \alpha \leq 1\ and\ 0 < \beta \leq 1$; $\eta_{\alpha,\beta} = \frac{k_{\alpha,\beta}}{\mu}$ . $k_{\alpha,\,\beta}$ is defined as a dynamic constant. In conventional flux law, the permeability (k) has the dimension of $L^2$ but in modified flux

law the dynamic constant ($k_{\alpha,\beta}$) has the dimension of $L^{1+\beta}T^{1-\alpha}$. If $\alpha = 1$ and $\beta = 1$, then Eq. (5.2) yields the conventional flux law and the dynamic constant can be defined as permeability with the same dimension ($L^2$). The Caputo's definitions of fractional derivatives are: (Caputo, 1967, 1998)

$$\frac{\partial^{\alpha} p(x,t)}{\partial t^{\alpha}} = \frac{1}{\Gamma(1-\alpha)} \int_0^t (t-u)^{-\alpha} [\frac{\partial p(x,u)}{\partial u}] \partial u \tag{5.3}$$

$$\frac{\partial^{\beta} p(x,t)}{\partial x^{\beta}} = \frac{1}{\Gamma(1-\beta)} \int_0^x (x-v)^{-\beta} [\frac{\partial p(v,t)}{\partial v}] \partial u \tag{5.4}$$

'Γ' denotes the gamma function. By using the modified flux law (Eq. 5.2) in the continuity equation (Eq. 5.1):

$$\frac{\partial(-\rho\eta_{\alpha,\beta} \frac{\partial^{1-\alpha}}{\partial t^{1-\alpha}} \frac{\partial^{\beta} p(x,t)}{\partial x^{\beta}})}{\partial x} = -\phi\, c_t \rho\, \frac{\partial \mathrm{p}}{\partial t} \tag{5.5}$$

Taking $\frac{\partial^{\alpha-1}}{\partial t^{\alpha-1}}$ of both sides

$$\frac{\partial([\frac{\partial^{\beta} p(x,t)}{\partial x^{\beta}}])}{\partial x} = \frac{\phi\, c_t}{\eta_{\alpha,\beta}} \frac{\partial^{\alpha} \mathrm{p(x,t)}}{\partial t^{\alpha}} \tag{5.6}$$

Let $\eta_{\alpha,\beta} \neq f(x)$. This is the equation for one dimensional linear anomalous diffusion of the slightly compressible fluid.

For sub-diffusion flow $\beta = 1$; so, Eq. (5.6) reduces to

$$\frac{\partial^2 p(x,y)}{\partial x^2} = \frac{\phi\, c_t}{\eta_{\alpha,\beta}} \frac{\partial^{\alpha} \mathrm{p(x,t)}}{\partial t^{\alpha}} \tag{5.7}$$

For super diffusion $\alpha = 1$. Therefore, Eq. (5.6) yields

$$\frac{\partial(\frac{\partial^{\beta} p(x,t)}{\partial x^{\beta}})}{\partial x} = \frac{\phi\, c_t}{\eta_{\alpha,\beta}} \frac{\partial \mathrm{p(x,t)}}{\partial t} \tag{5.8}$$

### 5.4.1 Flow in the Outer Reservoir

Eq. 5.7 can be rewritten for the outer reservoir in terms of pressure drop. The order of the differentiation is related to the impact of the time event in the outer reservoir flow.

$$\frac{\partial^2 \Delta p_o}{\partial x^2} = \frac{(\phi\, c_t)_o \mu}{k_{\alpha o}} \frac{\partial^{\alpha o} \Delta p_o}{\partial t^{\alpha o}} \tag{5.9}$$

In dimensionless form:

$$\frac{\partial^2 p_{OD}}{\partial {x_D}^2} = \omega_{Ao}\, \lambda_{Ao} \frac{\partial^{\alpha o} p_{OD}}{\partial t_D^{\alpha o}} \tag{5.10}$$

$$\frac{\partial^2 p_{OD}}{\partial {x_D}^2} = M_{DA} \frac{\partial^{\alpha o} p_{OD}}{\partial t_D^{\alpha o}} \tag{5.11}$$

Where $M_{DA}$ is the dimensionless anomalous number. $\omega_{Ao}$ is the dimensional anomalous storability with a dimension of $L^{1-\alpha}T^{2-2\alpha}M^{\alpha-1}$. For classical diffusion $\alpha$=1, and $\omega_{Ao}$ changes to dimensionless storability ratio. $\lambda_{Ao}$ is the dimensional inter-porosity co-efficient and has the dimension of $L^{\alpha-1}T^{2\alpha-2}M^{1-\alpha}$. In the case of classical diffusion, also the $\lambda_{Ao}$ becomes the dimensionless inter-porosity. Anomalous number represents the fluid transfer phenomenon between two adjacent domains where normal diffusion occurs in the one domain and the anomalous diffusion occurs in the other domain.

Applying Laplace transformation on Eq. (5.11)

$$\frac{\partial^2 \bar{p}_{OD}}{\partial {x_D}^2} - M_{DA}\{s^{\alpha o} \bar{p}_{OD} - p_{OD}(x_D)\} = 0 \tag{5.12}$$

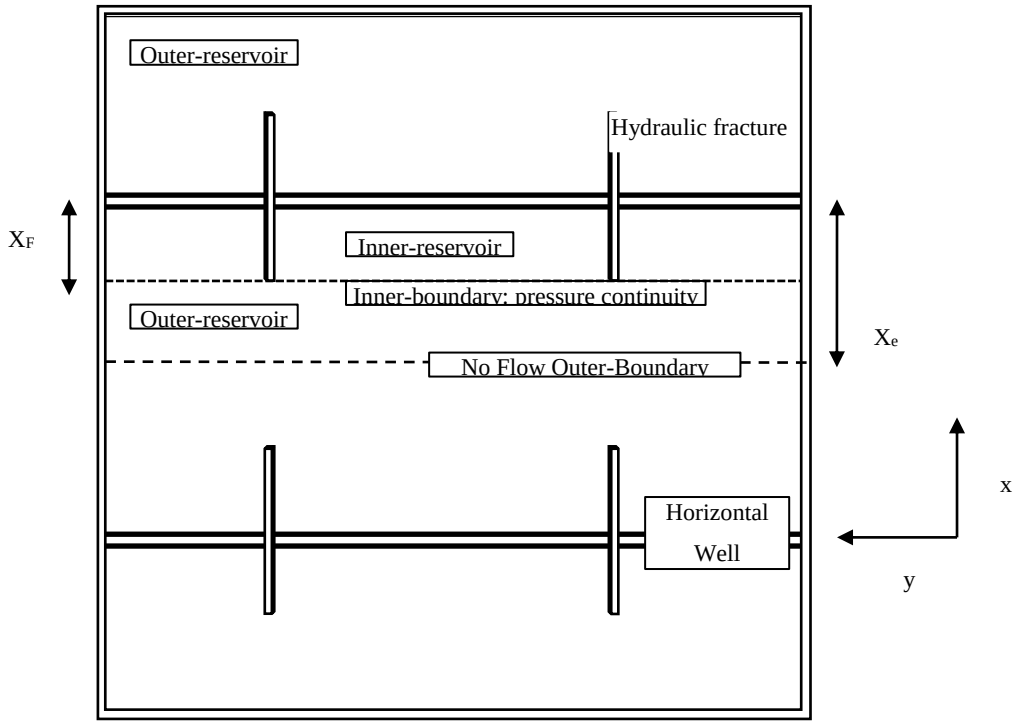


**Figure 5.7: boundary conditions of the outer reservoir**

At $t = 0$, the outer-reservoir pressure is the same as the initial pressure, so the pressure drop is zero at that time.

$$\Delta p_0(x, o) = 0 \tag{5.13}$$

$$p_{OD(x_D,0)} = 0 \tag{5.14}$$

If the spacing of two parallel horizontal reservoirs is $2x_e$, there is a no flow boundary at $x = x_e$. That implies

$$\frac{\partial \Delta p_o}{\partial x}_{|x=x_e} = 0 \tag{5.15}$$

$$\frac{\partial \bar{p}_{OD}}{\partial x_D}_{|x_D=x_{eD}} = 0 \tag{5.16}$$

The flow is linear in $x$ direction when it flows from the outer-reservoir to the inner-reservoir. The fluid transfer between the outer reservoir and the matrix of inner-reservoir is negligible; therefore, it is assumed that the fluid transfer occurs only through the macro-fracture. Pressure is continuous at the mutual boundary of the macro-fracture and the outer-reservoir; hence, the pressure of those two domains is equal at $x = x_{HF}$.

$$\Delta p_{0_{|x=x_{HF}}} = \Delta p_{MF_{|x=x_{HF}}} \tag{5.17}$$

$$\bar{p}_{0D_{|x_D=1}} = \bar{p}_{MFD_{|x_{D=1}}} \tag{5.18}$$

From Eq. (5.12) and Eq. (5.14)

$$\frac{\partial^2 \bar{p}_{OD}}{\partial {x_D}^2} - M_{DA} s^{\alpha o} \bar{p}_{OD} = 0 \tag{5.19}$$

The general solution of the Eq. (5.19)

$$\bar{p}_{OD} = Aexp\left(-\sqrt{\beta_o} x_D\right) + Bexp(\sqrt{\beta_o} x_D) \tag{5.20}$$

$\beta_o = M_{DA} s^{\alpha o}$. $\beta_o$ is the outer reservoir function that represents the heterogeneity of the reservoir.

For outer boundary condition (Eq. 5.16)

$$A = Bexp(2\sqrt{\beta_o} x_{eD}) \tag{5.21}$$

And

$$\bar{p}_{OD} = Bexp(\sqrt{\beta_o} x_{eD})\left((\exp(\sqrt{\beta_o}(x_{eD} - x_D) + \exp(-\sqrt{\beta_o}(x_{eD} - x_D))\right) \tag{5.22}$$

Inner boundary condition gives

$$B = \frac{\bar{p}_{MFD_{|x_{D=1}}}}{exp(\sqrt{\beta_o} x_{eD})\left((\exp(\sqrt{\beta_o}(x_{eD} - 1) + \exp\left(-\sqrt{\beta_o}(x_{eD} - 1)\right)\right)} \tag{5.23}$$

The final solution for the outer-reservoir

$$\bar{p}_{OD} = \bar{p}_{MFD_{|x_D=1}} \frac{\cosh(\sqrt{\beta_o}(x_{eD} - x_D))}{\cosh(\sqrt{\beta_o}(x_{eD} - 1))} \tag{5.24}$$

### 5.5.2 Case 1: Spherical Matrix Block with Fractured Surface

This model considers two different types of matrix block (Fig. 5.4 and Fig. 5.5). In the first case, the spherical matrix block with fractured surface is considered (Fig. 5.4)

#### 5.5.2.1 Core Matrix

In the case of isotropic formation, the radial flow can be assumed as a one-dimensional linear flow. So, the governing radial diffusion equation of the core matrix is

$$\frac{1}{r^2}\frac{\partial}{\partial r}\left(r^2 \frac{\partial \Delta p_{mc}}{\partial r}\right) = \frac{(\phi\, c_t)_{mc}\mu}{k_{mc}} \frac{\partial \Delta p_{mc}}{\partial t} \tag{5.25}$$

At the initial time the matrix has the same pressure of the initial pressure. At the center of the sphere, a finite pressure is assumed. At the contact surface of the core matrix and the cake fracture, there exists a continuity of the pressure because the flux is moved from the core to the surface layer of the matrix through the cake fracture. Therefore, the initial and the boundary conditions of the core matrix are

$$\Delta p_{mc}(r,0) = 0 \tag{5.26}$$

$$\Delta p_{mc}(0,t) = finite \tag{5.27}$$

$$\Delta p_{mc_{|r=r_{mc}}} = \Delta p_{fc_{|r=r_{mc}}} \tag{5.28}$$

For computational simplicity, a substitution is made for the $\partial \Delta p_{mc}$ by

$$w_{mcD}(r_D, t_D) = \Delta p_{mcD}(r_D, t_D) r_D \tag{5.29}$$

The general solution of the Eq. 5.25 given as

$$\bar{w}_{mcD} = Aexp\left(-\sqrt{\alpha_{mc}} r_D\right) + Bexp\left(\sqrt{\alpha_{mc}} r_D\right) \tag{5.30}$$

The final pressure solution of the core matrix is derived by using the boundary conditions (Eq. A.3.20)

$$\bar{p}_{mcD}(r_D, t_D) = \frac{1}{r_D} \frac{\bar{p}_{fcD} r_{mcD} \sinh\left(\sqrt{\alpha_{mc}} r_D\right)}{\sinh\left(\sqrt{\alpha_{mc}} r_{mcD}\right)} \tag{5.31}$$

#### 5.5.2.2 Flow in the cake matrix

In this model, the cake matrix is identified as the matrix formation in the surface area of the spherical matrix block that is bounded by the cake fracture. Figure 5.6 shows the general structure of the cake matrix and Fig. 5.8 illustrates the details description and the flow conditions. The formation of the cake matrix is approximated by a rectangular slab that has an equal length of surface-area depth and a thickness of $h_{cm}$. The governing flow equation in the fracture cake matrix

$$\frac{\partial^2 \Delta p_{cm}}{\partial \xi^2} = \frac{(\phi\, c_t)_{mc} \mu}{k_{mc}} \frac{\partial \Delta p_{cm}}{\partial t} \tag{5.32}$$

The fluid flux moves from the cake matrix to the cake fracture in the linear $\xi$ direction. A no flow boundary occurs at the mid-point of the matrix thickness as the fluxes moves concurrently to the two-opposite fracture from a single matrix slab. At the mutual

boundary of the cake fracture and the cake matrix, pressure continuity is assumed. The pressure drop at the interface is assumed to be negligible under the transient flow condition. Hence, the initial and boundary conditions for the cake matrix are

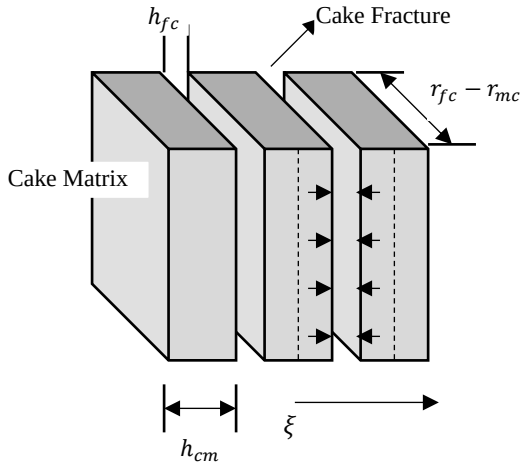


**Figure 5.8: Structure of the cake matrix**

$$\Delta p_{cm}(\xi, o) = 0 \tag{5.33}$$

$$\frac{\partial \Delta p_{cm}}{\partial \xi}_{|\xi=0} = 0 \tag{5.34}$$

$$\Delta p_{cm}{}_{\left|\xi=\frac{h_{cm}}{2}\right.} = \Delta p_{fc}{}_{\left|\xi=\frac{h_{cm}}{2}\right.} \tag{5.35}$$

The dimensionless form of the Eq. 5.32 after Laplace transformation

$$\frac{\partial^2 \bar{p}_{cmD}}{\partial {\xi_D}^2} - \frac{3\omega_{mc}}{\lambda_{cm}}\left\{s\bar{p}_{cmD}(\xi_D, s) - p_{cmD}(\xi_D, 0)\right\} = 0 \tag{5.36}$$

The general solution of Eq. 5.36

$$\bar{p}_{cmD} = Aexp\left(-\sqrt{\alpha_{cm}}\xi_D\right) + Bexp\left(\sqrt{\alpha_{cm}}\xi_D\right) \tag{5.37}$$

$Here\ \alpha_{cm} = \frac{3\omega_{mc}s}{\lambda_{cm}}$ and $\alpha_{cm}$ is the characteristic function that contains the heterogeneity at the cake matrix.

The pressure solution of the cake matrix with the assigned boundary conditions (Appendix A Eq. A.4.12)

$$\bar{p}_{cmD} = \frac{\Delta\bar{p}_{fcD} cosh\left(\sqrt{\alpha_{cm}}\xi_D\right)}{cosh\left(\sqrt{\alpha_{cm}}\right)} \tag{5.38}$$

### 5.5.2.3 Flow in Cake fracture

In the model, the cake fracture is a conduct that transfer the fluid flux from both the core matrix and the cake matrix to the micro-fracture. It has comparatively a high flow capacitance than the matrix so the fluid transfer from the cake matrix to the macro fracture can be ignored. Fluid flux between the cake matrix and the cake fracture is modeled by a dual-porosity mechanism; thus, the flux contribution of the cake matrix to the fracture, is evaluated by a source term ($q_{Source,cm}$) that is equivalent to the transient matrix influx per unit time per unit volume of the drainage area of the matrix at the outer boundary.

$$\frac{\partial^2 \Delta p_{fc}}{\partial r^2} = \frac{(\phi\, c_t)_{fc}\mu}{k_{fc}} \frac{\partial \Delta p_{fc}}{\partial t} + \frac{\mu}{k_{fc}} q_{Source,cm} \tag{5.39}$$

$q_{Source,cm}$ is the influx from the cake matrix per unit volume at unit time. The source term can be evaluated as (Kazemi 1969; Ahmadi 2011):

$$q_{Source,cm} = \frac{2k_{cm}}{\mu h_{cm}} \frac{\partial \Delta p_{cm}}{\partial \xi}\Big|_{\xi=\frac{h_{cm}}{2}} \tag{5.40}$$

The dimensionless flow equation with the source term and after Laplace transformation is

$$\frac{\partial^2 \bar{p}_{fcD}(r_D, s)}{\partial {r_D}^2} - \frac{3\omega_{fc}}{\lambda_{fc}}\left\{s\bar{p}_{fcD}(r_D, s) - p_{fcD}(r_D, 0)\right\} - \lambda_{fc}^{'} \frac{\partial \bar{p}_{cmD}}{\partial \xi_D}_{|\xi_D=1} = 0 \tag{5.41}$$

The initial condition for the Cake fracture

$$\Delta p_{fc}(r, o) = 0 \tag{5.42}$$

The inner boundary of the cake fracture is its mutual boundary with the core matrix. The matrix transfers the fluid flux solely to the fracture so at this common boundary there is a continuity of flux between the core matrix and the cake fracture. The surface area ratio of the two domains is $\frac{h_{fc}+h_{cm}}{h_{fc}}$. Fig. 5.9 illustrates the conceptual surface area both the cake matrix and the surface layer which is comprised of the cake matrix and the cake fracture. Therefore, the inner boundary condition of the cake fracture in Laplace domain

$$\left.\frac{\partial \bar{p}_{fcD}(r_D,s)}{\partial r_D}\right|_{(r_{mcD},s)} = \frac{k_{mc}(h_{fc}+h_{cm})}{k_{fc}h_{fc}} \left.\frac{\partial \bar{p}_{mcD}(r_D,s)}{\partial r_D}\right|_{(r_{mcD},s)} \tag{5.43}$$

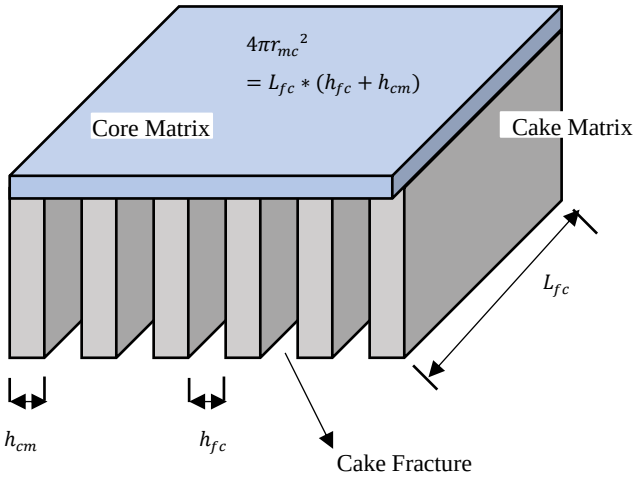


**Figure 5.9: The conceptual surface area of the core-matrix and the surface layer**

Pressure solution of the core matrix gives

$$\left.\frac{\partial \bar{p}_{mcD}}{\partial r_D}\right|_{(r_{mcD},s)} = \bar{p}_{fcD|r_{mcD}} \left\{\sqrt{\alpha_{mc}}\coth\left(\sqrt{\alpha_{mc}}r_{mcD}\right) - \frac{1}{r_{mcD}}\right\} \tag{5.44}$$

The pressure solution of the cake matrix yields

$$\left.\frac{\partial \bar{p}_{cmD}}{\partial \xi_D}\right|_{(\xi_D=1)} = \bar{p}_{fcD|\xi_D=1}\sqrt{\alpha_{cm}}\tanh\left(\sqrt{\alpha_{cm}}\right) \tag{5.45}$$

The inner boundary condition (5.43) with the core matrix pressure derivative

$$\left.\frac{\partial \bar{p}_{fcD}}{\partial r_D}\right|_{(r_{mcD},s)} = \bar{p}_{fcD|r_{mcD}}\beta_{mc} \tag{5.46}$$

Here, $\beta_{mc} = \frac{k_{mc}(h_{fc}+h_{cm})}{k_{fc}h_{fc}}\left\{\sqrt{\alpha_{mc}}\coth\left(\sqrt{\alpha_{mc}}r_{mcD}\right) - \frac{1}{r_{mcD}}\right\}$

The cake fracture maintains a pressure continuity with the micro-fracture at its outer boundary because it is assumed that a negligible pressure drop is occurred at the interface under the transient flow condition.

$$\Delta p_{fc}\Big|_{r=\frac{y_f}{2}} = \Delta p_{mf}\Big|_{r=\frac{y_f}{2}} \tag{5.47}$$

The assumption of pseudo-pressure function states that the pressure value of the cake fracture is independent of $\xi$ axis, i.e; $\bar{p}_{fcD} \neq f(\xi)$. Eq. 5.41, Eq. 5.42 and Eq. 5.45 gives

$$\frac{\partial^2 \bar{p}_{fcD}}{\partial {r_D}^2} - \alpha'_{fc}\bar{p}_{fcD} = 0 \tag{5.48}$$

$Here, \alpha'_{fc} = \alpha_{fc} + \lambda'_{fc}\sqrt{\alpha_{cm}}\tanh(\sqrt{\alpha_{cm}})$ and the function $\alpha'_{fc}$ is the characteristic function of the heterogeneous character of the cake fracture.

The general solution of the Eq. 5.48

$$\bar{p}_{fcD} = Aexp\left(-\sqrt{\alpha'_{fc}}r_D\right) + Bexp(\sqrt{\alpha'_{fc}}r_D) \tag{5.49}$$

The inner boundary condition is implemented in the solution by the differentiating of the Eq. 5.49 and evaluating it at $r_{D=}r_{mcD}$ that following a substitution in Eq. 5.44. On the contrary, Eq. 5.49 is used for the outer boundary condition. Detail derivation is given in the Appendix A.

The final pressure solution for the cake fracture from Appendix A, Eq. A.5.28

$$\bar{p}_{fcD} = \bar{p}_{mfD_{|r_D=1}} \frac{1}{\beta_{fc}} \left\{ \left( \frac{\sqrt{\alpha'_{fc}} - \beta_{mc}}{\sqrt{\alpha'_{fc}} + \beta_{mc}} \right) exp\left(\sqrt{\alpha'_{fc}}(r_{mcD} - r_D)\right) + exp\left(-\sqrt{\alpha'_{fc}}(r_{mcD} - r_D)\right) \right\} \tag{5.50}$$

$$Here, \beta_{fc} = \left( \frac{\sqrt{\alpha'_{fc}} - \beta_{mc}}{\sqrt{\alpha'_{fc}} + \beta_{mc}} \right) exp\left(\sqrt{\alpha'_{fc}}(r_{mcD} - 1)\right) + exp\left(-\sqrt{\alpha'_{fc}}(r_{mcD} - 1)\right)$$

### 5.5.3 Flow in the Micro-fracture

One dimensional linear flow is assumed in the micro-fracture at the transient condition. A source of flux enters in the micro-fracture at $r = \frac{y_f}{2}$. According to the Swaan O (1976), at the transient condition, the matrix flux is distributed in the one-half thickness of the fracture in an instantaneous and uniform distribution. In case of linear flow, it can be evaluated as the half of the fracture volume that encloses the matrix. Due to the simplified

idealization of matrix, the spherical matrix can be treated as a parallelepiped and isotropic matrix block with a dimension of $y_f$ and a flow symmetry at the center of the block (Fig. 5.10). As mentioned in the previous section, the cake fracture is the only medium that transfers the flux, the source term definition only contains the intrinsic properties of the fracture. Although Kazemi's (1969) definition is appropriate for the block matrix, in this study Swaan O's (1976) definition is used since the original shape of the matrix is spherical and the later definition is more appropriate for the spherical- shaped formation. So, the matrix influx to the micro-fracture is

$$q_{Source,fc} = \frac{2k_{fc}h_{fc}}{\mu h_{mf}(h_{cm}+h_{fc})}\frac{\partial \Delta p_{fc}}{\partial r}\Big|_{r=\frac{y_f}{2}} \tag{5.51}$$

The fluid flow equation for the micro-fracture

$$\frac{\partial^2 \Delta p_{mf}}{\partial z^2} = \frac{(\phi\, c_t)_{mf}\mu}{k_{mf}}\frac{\partial \Delta p_{mf}}{\partial t} + \frac{2k_{fc}h_{fc}}{k_{mf}h_{mf}(h_{cm}+h_{fc})}\frac{\partial \Delta p_{fc}}{\partial r}\Big|_{r=\frac{y_f}{2}} \tag{5.52}$$

Initial condition for the micro-fracture

$$\Delta p_{mf}(z,o) = 0 \tag{5.53}$$

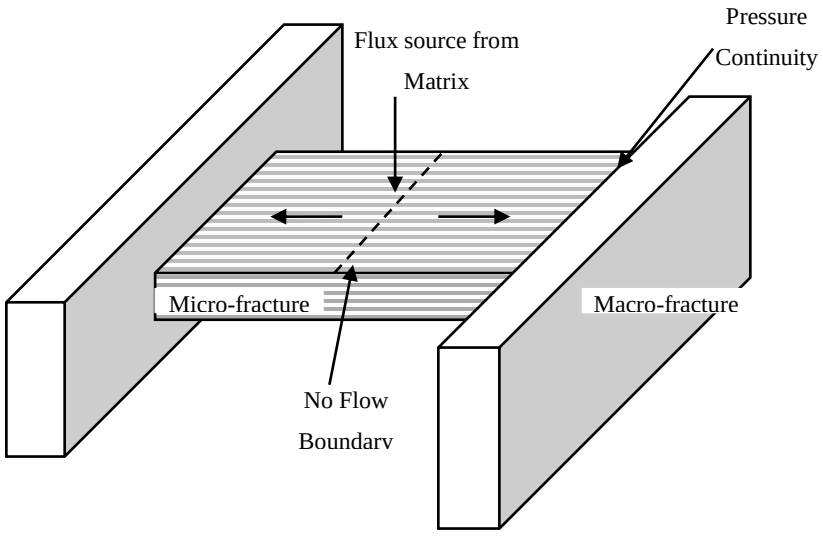


**Figure 5.10: Boundary Conditions for the Micro-fracture. Single fracture is shown for simplicity.**

The micro-fracture is connected to the macro-fracture at its both end (Figure 5.10). Therefore, the flow symmetry creates a no flow boundary at the mid-point of the matrix block. This inner boundary condition is

$$\frac{\partial \Delta p_{mf}}{\partial z}_{|z=0,t} = 0 \tag{5.54}$$

At the outer boundary of the micro-fracture, there is a continuity of pressure at the common boundary of the micro and macro fracture. Micro-fracture only communicates with the macro-fracture and for the simplicity the pressure drop at the interface is ignored.

$$\Delta p_{mf}\Big|_{z=\frac{L_f}{2}} = \Delta p_{MF}\Big|_{z=\frac{L_f}{2}} \tag{5.55}$$

Differentiating Eq. 5.50 and evaluating at $r_D = 1$ gives

$$\frac{\partial \bar{p}_{fcD}}{\partial r_D}_{|(r_D=1,s)} = -\bar{p}_{mfD_{|r_D=1}} \beta'_{fc} \tag{5.56}$$

Here, $\beta'_{fc} = \frac{1}{\beta_{fc}} \left\{ \left( \frac{\sqrt{\alpha'_{fc}} - \beta_{mc}}{\sqrt{\alpha'_{fc}} + \beta_{mc}} \right) \sqrt{\alpha'_{fc}} exp\left( \sqrt{\alpha'_{fc}} (r_{mcD} - 1) \right) - \sqrt{\alpha'_{fc}} exp\left( -\sqrt{\alpha'_{fc}} (r_{mcD} - 1) \right) \right\}$

The dimensionless form of the Eq. 5.52 at Laplace domain with the initial condition and the value Eq. 5.56

$$\frac{\partial^2 \bar{p}_{mfD}}{\partial {z_D}^2} - \beta_{mf} \bar{p}_{mfD} = 0 \tag{5.57}$$

Here, $\beta_{mf} = \frac{3\omega_{mf} s}{\lambda_{mf}} - \beta'_{fc} \lambda_{fcf}$ and it shows the deviated behavior of the micro-fracture due to its homogeneous character.

The general pressure solution of the micro-fracture

$$\bar{p}_{mfD} = A exp\left( -\sqrt{\beta_{mf}} z_D \right) + B exp\left( \sqrt{\beta_{mf}} z_D \right) \tag{5.58}$$

The final pressure solution of the micro fracture by the evaluation of the pressure conditions (Appendix A Eq. A.6.20)

$$\bar{p}_{mfD} = \bar{p}_{MFD_{|z_D=1}} \frac{cosh\,(\sqrt{\beta_{mf}} z_D)}{cosh\,(\sqrt{\beta_{mf}})} \tag{5.59}$$

### 5.5.4 Flow in the Macro-fracture

The characteristic flow in the macro-fracture is a two-dimensional linear flow. In the model, macro-fracture is assumed as a conduit that has the higher flow capacity than the macro-fracture and a continuous-extend over the whole inner reservoir in $x$ direction and in $y$ direction. At its outer boundary in the $x$ direction, a flux enters by maintaining a flux-continuity condition with the outer reservoir. A flux source, alternatively, from the macro-fracture. Both the macro-fracture and the micro-fracture have rectangular-block structure; therefore, at the contact surface, the source term is evaluated according to the definition of Kazemi (1969). The governing flow equation in the macro-fracture is

$$\frac{\partial^2 \Delta p_{MF}}{\partial x^2} + \frac{\partial^2 \Delta p_{MF}}{\partial y^2} = \frac{(\phi\, c_t)_{MF} \mu}{k_{MF}} \frac{\partial \Delta p_{MF}}{\partial t} + \frac{\mu}{k_{MF}} q_{Source,mf} \tag{5.60}$$

Under the transient flow condition transient flow, the flow from unit volume of the micro-fracture at unit time

$$q_{Source,mf} = \frac{k_{mf}}{\frac{L_f}{2}\mu} \frac{\partial \Delta p_{mf}}{\partial z}\Big|_{z=\frac{L_f}{2}} \tag{5.61}$$

An integration in the $x$ direction gives the total flow in that axis.

$$\frac{1}{x_{HF}} \frac{\partial \Delta p_{MF}}{\partial x} + \frac{\partial^2 \Delta p_{MF}}{\partial y^2} - \frac{2}{L_f} \frac{k_{mf}}{k_{MF}} \frac{\partial \Delta p_{mf}}{\partial z}\Big|_{z=\frac{L_f}{2}} = \frac{(\phi\, c_t)_{MF} \mu}{k_{MF}} \frac{\partial \Delta p_{MF}}{\partial t} \tag{5.62}$$

In case of linear flow, the pseudo function assumption reveals that the change of the pressure in the $y$ direction is independent of the $x$ direction.

In dimensionless form of the Eq. 5.62

$$\frac{\partial p_{MFD}}{\partial x_D} + \frac{\partial^2 p_{MFD}}{\partial {y_D}^2} - \frac{\lambda_{mf}}{3} \frac{\partial p_{mfD}}{\partial z_D}_{|z_D=1} = \frac{\partial p_{MFD}}{\partial t_D} \tag{5.63}$$

The initial condition

$$\Delta p_{MF}(x, y, o) = p_i \tag{5.64}$$

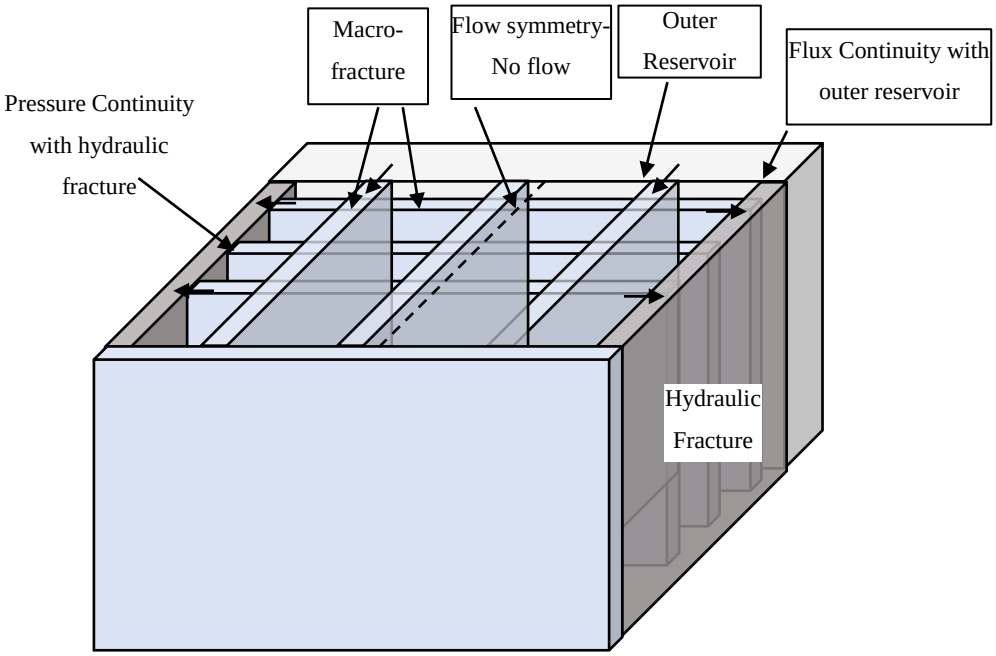


**Figure 5. 11: Boundary Conditions for the macro-fracture. For Simplicity, a limited number of fractures is shown.**

The fluid flows linearly from the outer reservoir to the inner reservoir only through the macro-fracture in the $x$ direction. Thus, at the common-boundary of the outer reservoir and the macro-fracture ($x = x_{HF}$), there exists a flow-continuity. Alternatively, a no-flow boundary condition occurs at the mid-point ($y = y_e$) of the inner reservoir in the $y$ direction because the inner reservoir simultaneously drains the fluid toward the two opposite hydraulic fractures (Fig. 5.11).

Thus, Inner boundary condition in the $x$ direction for the Macro-fracture

$$q_0(x_{HF}, t) = q_{MF}(x_{HF}, t) \tag{5.65}$$

$$\frac{k_{\alpha o}(h_{MF} + L_f)}{\mu} \frac{\partial^{1-\alpha o}}{\partial t^{1-\alpha o}} \left(\frac{\partial \Delta p_0}{\partial x}\right)_{x=x_{HF}} = \frac{k_{MF} h_{MF}}{\mu} \left(\frac{\partial \Delta p_{MFD}}{\partial x}\right)_{x=x_{HF}} \tag{5.66}$$

The condition is transferred in the Laplace domain as

$$\left(\frac{\partial \bar{p}_{MFD}(x, y, s)}{\partial x_D}\right)_{x_D=1} = C_{OMF} \left(\frac{(\phi\, c_t)_{MF} \mu x_{HF}^2}{k_{MF}}\right)^{\alpha o - 1} s^{1-\alpha o} \left(\frac{\partial \bar{p}_{oD}(x, y, s)}{\partial x_D}\right)_{x_D=1} \tag{5.67}$$

Here, $C_{OMF} = \frac{k_{\alpha o}(h_{MF}+L_f)}{k_{MF}h_{MF}}$

Differentiation of the Eq. 5.24 and 5.59 yields

$$\left(\frac{\partial \bar{p}_{oD}}{\partial x_D}\right)_{x_D=1} = -\bar{p}_{MFD_{|x_D=1}}\beta_{OMF} \tag{5.68}$$

Here, $\beta_{OMF} = \sqrt{\beta_o}\tanh\left(\sqrt{\beta_o}(x_{eD}-1)\right)$

$$\frac{\partial \bar{p}_{mfD}}{\partial z_D}_{|z_D=1} = \bar{p}_{MFD_{|z_D=1}}\sqrt{\beta_{mf}}\tanh\left(\sqrt{\beta_{mf}}\right) \tag{5.69}$$

From the Eq. 5.67 and Eq. 5.68

$$\left(\frac{\partial \bar{p}_{MFD}}{\partial x_D}\right)_{x_D=1} = -\beta_{OMFD}\bar{p}_{MFD_{|x_D=1}} \tag{5.70}$$

Here, $\beta_{OMFD} = C_{OMF}\left(\frac{(\phi\, c_t)_{MF}\mu x_{HF}^2}{k_{MF}}\right)^{\alpha o-1} s^{1-\alpha o}\beta_{OMF}$

At the inner boundary of the $y$ direction, a no flow boundary is created due to the flow symmetry.

$$\frac{\partial \Delta p_{MF}}{\partial y}_{|y=y_e} = 0 \tag{5.71}$$

Pressure is continuous at the interface of the macro-fracture and the outer reservoir. So, at the outer boundary of the macro-fracture in the y direction

$$\Delta p_{MF}|_{y=\frac{w}{2}} = \Delta p_{HF}|_{y=\frac{w}{2}} \tag{5.72}$$

Assuming the pseudo-function assumption i.e.; $\bar{p}_{MFD_{|x_D=1}} = \bar{p}_{MFD_{|z_D=1}} = \bar{p}_{MFD}$.

Transforming the Eq. 5.63 in Laplace domain and using the Eq. 5.64, Eq. 5.69, Eq. 5.70

$$\frac{\partial^2 \bar{p}_{MFD}}{\partial {y_D}^2} - \beta_{MF}\bar{p}_{MFD} = 0 \tag{5.73}$$

Here, $\beta_{MF} = \beta_{OMFD} + \frac{\lambda_{mf}}{3}\sqrt{\beta_{mf}}\tanh\left(\sqrt{\beta_{mf}}\right) + s$. The function $\beta_{MF}$ represents the non-homogeneity in the macro-fracture.

The final pressure solution of the Eq. 5.71 is derived by the implementation of the boundary conditions (Eq. 5.71 and Eq. 5.72). Appendix A, Eq. A.7.31

$$\bar{p}_{MFD} = \bar{p}_{HFD}|_{y_D=\frac{w_D}{2}} \frac{\cosh\left(\sqrt{\beta_{MF}}(y_{eD} - y_D)\right)}{\cosh\left(\sqrt{\beta_{MF}}(y_{eD} - \frac{w_D}{2})\right)} \tag{5.74}$$

### 5.5.5 Flow in the Hydraulic Fracture

The stimulation process generates a high conductive region in the hydraulic fracture zone by generating new fracture and connecting the isolated fracture and vugs. The induced connectivity alters the flow capacity of formation. Therefore, the contribution of the space event becomes significant. The consequential faster flow in the hydraulic fracture can be defined as super diffusion. A fractional space-derivative represents that faster flow and the order of differentiation is related to the magnitude of the space-event's influence. Eq. 5.8 is the characteristics equation for the super-diffusion and in the case of the hydraulic fracture flow it can be written as

$$\frac{\partial}{\partial x}\left(\frac{\partial^\beta \Delta p_{HF}}{\partial x^\beta}\right) + \frac{\partial}{\partial y}\left(\frac{\partial^\beta \Delta p_{HF}}{\partial y^\beta}\right) = \frac{(\phi\, c_t)_{HF}\mu}{k_\beta}\, \frac{\partial \Delta p_{HF}}{\partial t} \tag{5.75}$$

A single fracture is related to two inner reservoirs in the $y$ direction, thus, it is assumed that the flux from an inner reservoir is distributed from the boundary of the hydraulic fracture to the half of its width. An integration from the mid-point to the outer boundary ($\frac{w}{2}$) gives the total flow at the $y$ direction. The linear flow assumption implies that the pressure changes in the $x$ direction is independent of the $y$ direction.

$$\frac{\partial}{\partial x}\left(\frac{\partial^\beta \Delta p_{HF}}{\partial x^\beta}\right) + \frac{2}{w}\left(\frac{\partial^\beta \Delta p_{HF}}{\partial y^\beta}\right)_{y=\frac{w}{2}} = \frac{(\phi\, c_t)_{HF}\mu}{k_\beta}\, \frac{\partial \Delta p_{HF}}{\partial t} \tag{5.76}$$

Dimensionless form of the Eq. 5.76 is

$$\frac{\partial}{\partial x_D}\left(\frac{\partial^\beta p_{HFD}}{\partial {x_D}^\beta}\right) + \frac{2}{w_D}\left(\frac{\partial^\beta p_{HFD}}{\partial {y_D}^\beta}\right)_{y_D=\frac{w_D}{2}} = M_{DAHF}\frac{\partial p_{HFD}}{\partial t_D} \tag{5.77}$$

Initial condition of the hydraulic fracture

$$\Delta p_{HF}(x, y, o) = 0 \tag{5.78}$$

Macro-fracture flux is evaluated at the mutual boundary of the hydraulic fracture and the macro-fracture is assumed to be continuous so at the outer boundary ($y = \frac{w}{2}$) of the hydraulic fracture, both fluxes have equal magnitude.

$$\frac{k_\beta(h_{MF}+L_f)}{\mu}\left(\frac{\partial^\beta \Delta p_{HF}}{\partial y^\beta}\right)_{y=\frac{w}{2}} = \frac{k_{MF}h_{MF}}{\mu}\left(\frac{\partial \Delta p_{MF}}{\partial y}\right)_{y=\frac{w}{2}} \tag{5.79}$$

The dimensionless form of the outer boundary condition in Laplace domain

$$\left(\frac{\partial^\beta \bar{p}_{HFD}}{\partial {y_D}^\beta}\right)_{y_D=\frac{w_D}{2}} = \lambda'_{AF}\left(\frac{\partial \bar{p}_{MFD}}{\partial y_D}\right)_{y_D=\frac{w_D}{2}} \tag{5.80}$$

Differentiating the pressure solution of the macro-fracture and evaluating at $y_D = \frac{w_D}{2}$ gives

$$\left(\frac{\partial \bar{p}_{MFD}}{\partial y_D}\right)_{y_D=\frac{w_D}{2}} = -\sqrt{\beta_{MF}}\tanh\left(\sqrt{\beta_{MF}}(y_{eD}-\frac{w_D}{2})\right)\bar{p}_{HFD}|_{y_D=\frac{w_D}{2}} \tag{5.81}$$

From the Eq. 5.80 and Eq. 5.81

$$\left(\frac{\partial \bar{p}_{HFD}}{\partial {y_D}^\beta}\right)_{y_D=\frac{w_D}{2}} = -\beta_{MHF}\bar{p}_{HFD}|_{y_D=\frac{w_D}{2}} \tag{5.82}$$

Here $\beta_{MHF} = \lambda'_{AF}\sqrt{\beta_{MF}}\tanh\left(\sqrt{\beta_{MF}}(y_{eD}-\frac{w_D}{2})\right)$

Substituting the initial and the boundary condition in the Laplace transform form of the Eq. 5.77

$$\frac{\partial}{\partial x_D}\left(\frac{\partial^\beta \bar{p}_{HFD}}{\partial {x_D}^\beta}\right) - \beta_{HF}\bar{p}_{HFD} = 0 \tag{5.83}$$

Here $\beta_{HF} = \frac{2}{w_D}\beta_{MHF} + M_{DAHF}s$

The Laplace transformation of Eq. 5.83 for the space $x$

$$\tilde{s}\left[\tilde{s}^\beta \bar{\bar{p}}_{HFD}(s,\tilde{s}) - \tilde{s}^{\beta-1}\bar{p}_{HFD}(0,s)\right] - \left(\frac{\partial^\beta \bar{p}_{HFD}(x_D,s)}{\partial {x_D}^\beta}\right)_{x_D=0} - \beta_{HF}\bar{\bar{p}}_{HFD}(s,\tilde{s}) = 0 \tag{5.84}$$

$$\bar{\bar{p}}_{HFD}(s,\tilde{s}) = \frac{\tilde{s}^\beta}{\tilde{s}^{\beta+1}-\beta_{HF}}\bar{p}_{HFD}(0,s) + \frac{1}{\tilde{s}^{\beta+1}-\beta_{HF}}\left(\frac{\partial^\beta \bar{p}_{HFD}(x_D,s)}{\partial {x_D}^\beta}\right)_{x_D=0} = 0 \tag{5.85}$$

Inverting Eq. 5.85

$$\bar{p}_{HFD}(x_D, s) = \bar{p}_{HFD}(0, s) E_{\beta+1}\left(\beta_{HF} {x_D}^{\beta+1}\right) + {x_D}^{\beta} E_{\beta+1,\beta+1}(\beta_{HF} {x_D}^{\beta+1}) \left(\frac{\partial \bar{p}_{HFD}(x_D, s)}{\partial {x_D}^{\beta}}\right)_{x_D=0} \quad (5.86)$$

At the inner boundary of the hydraulic fracture at $x = 0$, fluid is flows from the fracture to the horizontal well. If constant flow rate at the well-bore is assumed, then

$$u = -\frac{k_\beta}{\mu}\left(\frac{\partial^\beta \Delta p_{HF}}{\partial x^\beta}\right)_{x=0} \quad (5.87)$$

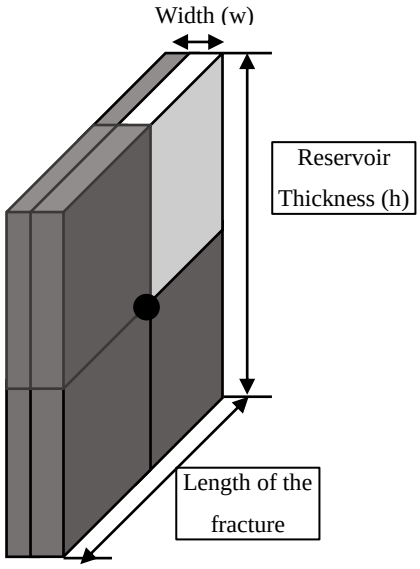


**Figure 5.12: Simplified structure of the hydraulic fracture. The shaded area is the representative zone of the model.**

To determine the total flow, Eq. 5.87 has to integrate along the width and the thickness of the reservoir. An Integration is done alone the $y$ axis from the center to $\frac{w}{2}$ and at the half of the thickness of the reservoir. The integrated result at Laplace domain

$$\left(\frac{\partial^\beta \bar{p}_{HFD}}{\partial {x_D}^{\beta}}\right)_{x_D=0} = -\frac{\pi}{c_{AFD} s} \quad (5.88)$$

Substituting inner boundary condition in Eq.5.86

$$\bar{p}_{HFD}(x_D, s) = \bar{p}_{HFD}(0, s) E_{\beta+1}\left(\beta_{HF} {x_D}^{\beta+1}\right) - \frac{\pi}{c_{AFD} s} {x_D}^{\beta} E_{\beta+1,\beta+1}(\beta_{HF} {x_D}^{\beta+1}) \tag{5.89}$$

The outer boundary of the Hydraulic fracture in the $x$ direction is the tip of the hydraulic fracture. It is assumed that no flow is transferred at this area so the outer boundary condition

$$\frac{\partial \Delta p_{HF}}{\partial x}_{|x=x_{HF},t} = 0 \tag{5.90}$$

Differentiating the Eq. 5.88 yields (Hombole *et. al.*, 2011, Fomin *et. al.*, 2010)

$$\frac{d\bar{p}_{HFD}(x_D, s)}{dx} = \bar{p}_{HFD}(0, s) \beta_{HF} {x_D}^{\beta} E_{\beta+1,\beta+1}\left(\beta_{HF} {x_D}^{\beta+1}\right) - \frac{\pi}{c_{AFD} s} {x_D}^{\beta-1} E_{\beta+1,\beta}\left(\beta_{HF} {x_D}^{\beta+1}\right) \tag{5.91}$$

$$\bar{p}_{HFD}(0, s) = \frac{\pi E_{\beta+1,\beta}(\beta_{HF})}{c_{AFD} s \beta_{HF} E_{\beta+1,\beta+1}(\beta_{HF})} \tag{5.92}$$

Substitute the value of Eq. 5.92 in Eq. 5.89

$$\bar{p}_{HFD}(x_D, s) = \frac{\pi}{c_{AFD} s} \left\{ \frac{E_{\beta+1,\beta}(\beta_{HF})}{\beta_{HF} E_{\beta+1,\beta+1}(\beta_{HF})} E_{\beta+1}\left(\beta_{HF} {x_D}^{\beta+1}\right) - {x_D}^{\beta} E_{\beta+1,\beta+1}\left(\beta_{HF} {x_D}^{\beta+1}\right) \right\} \tag{5.93}$$

This is the expression for the dimensionless hydraulic fracture pressure for the constant terminal rate flow.

At $x_D = 0$ the hydraulic fracture pressure will be the bottom-hole pressure. The expression can be deduced from the Eq. 5.93

$$\bar{p}_{wD}(x_D, s) = \frac{\pi}{c_{AFD} s} \left\{ \frac{E_{\beta+1,\beta}(\beta_{HF})}{\beta_{HF} E_{\beta+1,\beta+1}(\beta_{HF})} \right\} \tag{5.94}$$

This is the expression for the dimensionless bottom-hole pressure for the constant terminal rate flow.

### 5.5.6 Case 2: Rectangular Matrix Block

#### 5.5.6.1 Block Matrix Flow

The geometry of the matrix block is shown in the Fig. 5.5. The flow equation in the matrix block is

$$\frac{\partial^2 \Delta p_m}{\partial \zeta^2} = \frac{(\phi\, c_t)_m \mu}{k_{mc}} \frac{\partial \Delta p_m}{\partial t} \tag{5.95}$$

At $t = 0$, the same pressure at every domain of the reservoir.

$$\Delta p_m(\zeta, o) = 0$$

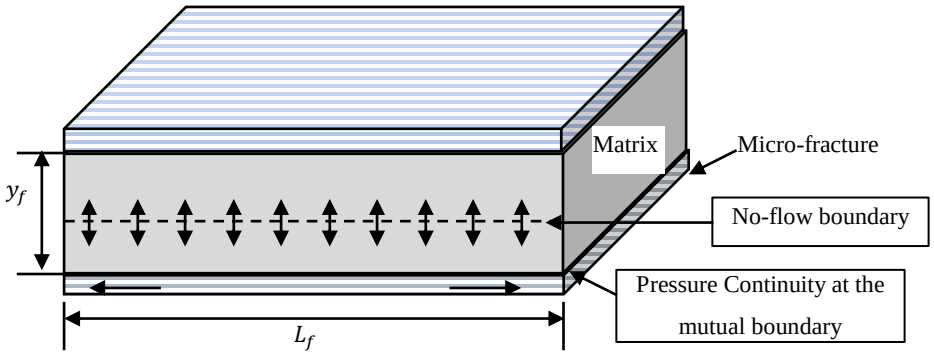


**Figure 5.13: Boundary Conditions for the block matrix and the micro-fracture**

Each matrix block is connected with two micro-fracture and the flow only occurs at the $\zeta$ direction because of the assumption of linear flow (Fig. 5.13). Hence, there is a no flow boundary at the middle of the $\zeta$ axis, i.e. $\zeta = 0$. So,

$$\frac{\partial \Delta p_m}{\partial \zeta}_{|\zeta=0} = 0 \tag{5.96}$$

At the outer boundary of the matrix block, it maintains a constant pressure relationship with the micro-fracture.

$$\Delta p_m\Big|_{\zeta=\frac{y_f}{2}} = \Delta p_{mf}\Big|_{\zeta=\frac{y_f}{2}} \tag{5.97}$$

The dimensionless flow equation for the matrix block after implementing the Laplace transform and applying the initial condition

$$\frac{\partial^2 \bar{p}_{mD}(\zeta_D, s)}{\partial \zeta_D{}^2} - \frac{3\omega_m}{\lambda_m} s\bar{p}_{mD}(\zeta_D, s) = 0 \tag{5.98}$$

$Here\ \alpha_m = \frac{3\omega_m s}{\lambda_m}$

The final pressure solution for the block matrix (Appendix)

$$\bar{p}_{mD} = \frac{\bar{p}_{mD} cosh\left(\sqrt{\alpha_m}\zeta_D\right)}{cosh\left(\sqrt{\alpha_m}\right)} \tag{5.99}$$

### 5.5.6.2 Flow in the Micro-fracture

The contribution of the matrix flux in the micro-fracture flow is a source term that comes from the matrix block. Therefore, a change in the matrix geometry only updates that flux-source of the matrix. For a rectangular block shaped matrix, the transient source term is defined according to the kazemi's (1969) definition. In this case, the flux exchange area of the matrix and the fracture is equal to the block dimension.

$$q_{Source,m} = \frac{k_m}{\frac{y_f}{2}\mu} \frac{\partial \Delta p_m}{\partial \zeta} \Big|_{\zeta=\frac{y_f}{2}} \tag{5.100}$$

The fluid flow equation for the micro-fracture

$$\frac{\partial^2 \Delta p_{mf}}{\partial z^2} = \frac{(\phi\, c_t)_{mf}\mu}{k_{mf}} \frac{\partial \Delta p_{mf}}{\partial t} + \frac{\mu}{k_{mf}} q_{Source,m} \tag{5.101}$$

The dimensionless form of Eq. 5.101 after substituting Eq. 5.100

$$\frac{\partial^2 p_{mfD}}{\partial {z_D}^2} = \frac{3\omega_{mf}}{\lambda_{mf}} \frac{\partial p_{mfD}}{\partial t_D} + \lambda_{mf}^{'} \frac{\partial p_{mD}}{\partial \xi_D}_{|\xi_D=1} \tag{5.102}$$

The differentiation of Eq. 5.99 yields

$$\frac{\partial \bar{p}_{mD}}{\partial {\zeta_D}}_{|\zeta_D=1} = \bar{p}_{mfD}\sqrt{\alpha_m}\tanh\left(\sqrt{\alpha_m}\right) \tag{5.103}$$

By Laplace transformation and using the same initial condition (Eq. 5.53) provide the flow equation as

$$\frac{\partial^2 \bar{p}_{mfD}}{\partial {z_D}^2} - \beta'_{mf}\bar{p}_{mfD} = 0 \tag{5.104}$$

$Here,\ \beta'_{mf} = \frac{3\omega_{mf}s}{\lambda_{mf}} + \beta_m$. The $\beta_{mf}$is the modified domain-function for the micro-fracture that is related with a rectangular block. The subsequent calculation in the remaining domains is same as the spherical matrix block.

The final pressure solution of the macro-fracture with the same boundary conditions (Eq. 5.54 and Eq. 5.55)

$$\bar{p}_{mfD} = \bar{p}_{MFD_{|z_D=1}} \frac{cosh\,(\sqrt{\beta'_{mf}} z_D)}{cosh\,(\sqrt{\beta'_{mf}})} \tag{5.105}$$

**5.6 Validation of the expression**

For $\beta = 1$ the flow will be the classical flow equation. Substituting the value of $\beta = 1$ in the Eq. 5.94

$$\bar{p}_{wD}(x_D, s) = \frac{\pi}{c_{AFD} s} \left\{ \frac{E_2(\beta_{HF})}{\beta_{HF} E_{2,2}(\beta_{HF})} \right\} \tag{5.106}$$

$$\bar{p}_{wD}(x_D, s) = \frac{\pi}{c_{AFD} s \sqrt{\beta_{HF}} \tanh(\sqrt{\beta_{HF}})} \tag{5.107}$$

This is the similar expression for the multi-continuum reservoir flow (Brown et. al., 2009. Ozkan et. al., 2010, 2011, Alibini 2016)

If $\beta_{HF} = 1$ then from the asymptotic expression of $\tanh(1)$, it can be shown that the equation (129) becomes:

$$\bar{p}_{wD}(x_D, s) = \frac{\pi}{c_{AFD} s} \tag{5.108}$$

This is the general expression for the bottom-hole pressure at constant flow rate for the linear reservoir.

The response of the model is compared with the Brawn et. al. (2011) model in figure 5.14. The response of the both models is nearly identical for a $\alpha_o$ value of 1 and β value of 0.95. The permeability of the microfracture is assumed to be very lower (0.1) than the micro-fracture, so the inner reservoir becomes a dual porosity system like as Brawn's model. The response it adjusted by altering the compressibility values of the matrix and the macro-fracture of the multi-continuum anomalous model. For a value of the compressibility and the permeability of the continuum, the both models behave as same. The matching of the curve is the evident of the consistency of the result. Because of the

effect of space (β=0.95) there is a difference is remaining in the response at the early time.

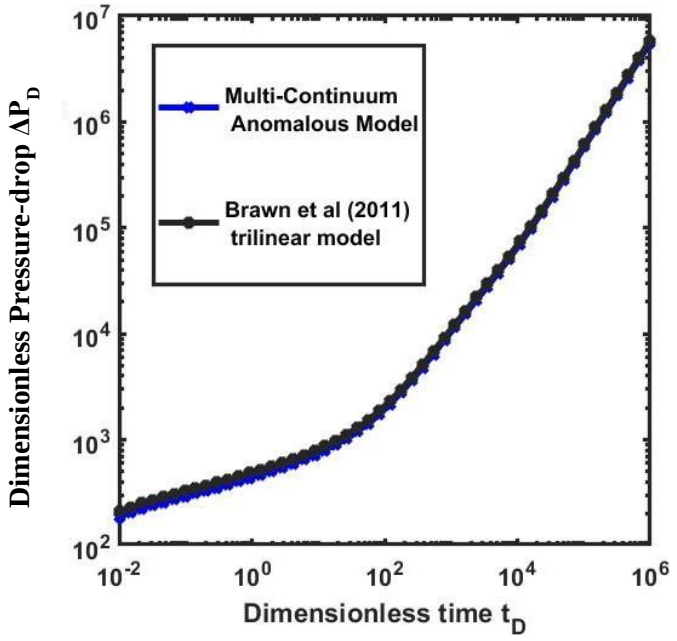


**Figure 5.14: Comparison of Multi-Continuum Anomalous Model and the Brawn et al (2011) trilinear model.**

## 5.7 Results and Analysis

This section describes the response of the model. Table 5.1 summarized all the data that are used for the response analysis.

**Table 5.1: Synthetic data for the model analysis**

| Parameters | Value | Parameters | Value |
|---|---|---|---|
| Reservoir thickness, h, ft | 250 | Macro fracture total compressibility, $c_{MF}$, Psi$^{-1}$ | 5E-3 |
| Wellbore radius, $r_w$, ft | 0.25 | Thickness of the macro-fracture, $h_{MF}$,ft | 0.009 |
| Horizontal well lengthy, $L_H$, ft | 3100 | Micro fracture porosity, $\phi_{mf}$,fraction | 0.45 |
| Spacing of macro-fracture, $L_F$, ft | 10 | Micro-fracture permeability, $K_{mf}$, md | 20 |
| Number of hydraulic fracture, $n_{HF}$ | 10 | Micro fracture total compressibility, $c_{mf}$,Psi$^{-1}$ | 5E-3 |
| Number of Macro-fracture, $n_{MF}$ | 25 | Thickness of the micro-fracture, $h_{mf}$,ft | 0.006 |
| Number of Micro-fracture, $n_{mf}$ | 50 | Spacing between two fractures, $y_f$, ft | 5 |
| Distance between hydraulic fractures, $d_F$,ft | 300 | Cake fracture porosity, $\phi_{fc}$, fraction | 0.40 |
| Distance to boundary parallel to well, $x_e$,ft | 350 | Cake fracture permeability, $K_{fc}$,md | 10 |
| Drainage area length, $y_e$,ft | 150 | Cake fracture total compressibility, $c_{fc}$,Psi$^{-1}$ | 2E-4 |
| Viscosity, μ, cp | 0.3 | Mico-fracture thickness, $h_{fc}$, ft | 0.003 |
| Constant flow rate, q, Stb/Day | 300 | Radius of the matrix core, $r_{mc}$, ft | 2 |
| Hydraulic fracture porosity, $\phi_{HF}$,fraction | 0.40 | Thickness of the cake matrix slab, $h_{cm}$, ft | $0.2 * r_{mc}$ |
| Phenomenological coefficient, $K_{\beta}$, md-hr$^{1-\alpha}$ | 50000 | Core matrix porosity, $\phi_{mc}$,fraction | 0.05 |
| Hydraulic fracture total compressibility, $c_{HF}$, Psi$^{-1}$ | 1E-4 | Core matrix permeability, $K_{mc}$,md | 1E-4 |
| Hydraulic fracture half length, $x_{HF}$,ft | 250 | Core matrix total compressibility, $c_{mc}$,Psi$^{-1}$ | 1E-4 |
| Hydraulic fracture width, w, ft | 0.01 | Outer reservoir porosity, $\phi_o$, fraction | 0.05 |
| Memory Parameter (Space), β | 0.8 | Phenomenological coefficient, $K_{\alpha}$,md-hr$^{1-\alpha}$ | 1.2 |
| Macro fracture porosity, $\phi_{MF}$,fraction | 0.60 | Outer reservoir total compressibility, $c_o$ Psi$^{-1}$ | 1E-4 |
| Macro-fracture permeability, $K_{MF}$, md | 1000 | Memory Parameter, $\alpha_o$ | 0.9 |

### 5.7.1 Dimensionless pressure drops

The dimensionless pressure response of the homogeneous reservoir is a single slope line. It is an evident that the response curve has more than one slope in the dual or triple continuum reservoir (warren and Root, 1968, Abdassah and Ershaghi, 1986). The response curve of tri-linear models also shows a slope change at the transition of the earlier and the intermediate to late time response (Brawn, 2009; Ozkan *et al.*, 2011,2012, Albinali *et al.*, 2016a, 2016b). Figure 5.15 and figure 5.16 shows the dimensionless pressure response and the pressure drop profile of the model, both have two distinguishable slopes. With a value of 0.75, the initial slope holds the contributions of the hydraulic fracture and the macro-fracture whereas the second slope changes according to the late time pressure response. Due to low permeability of the matrix and high storage capacity, the late time response is dominated by the matrix flow parameters.

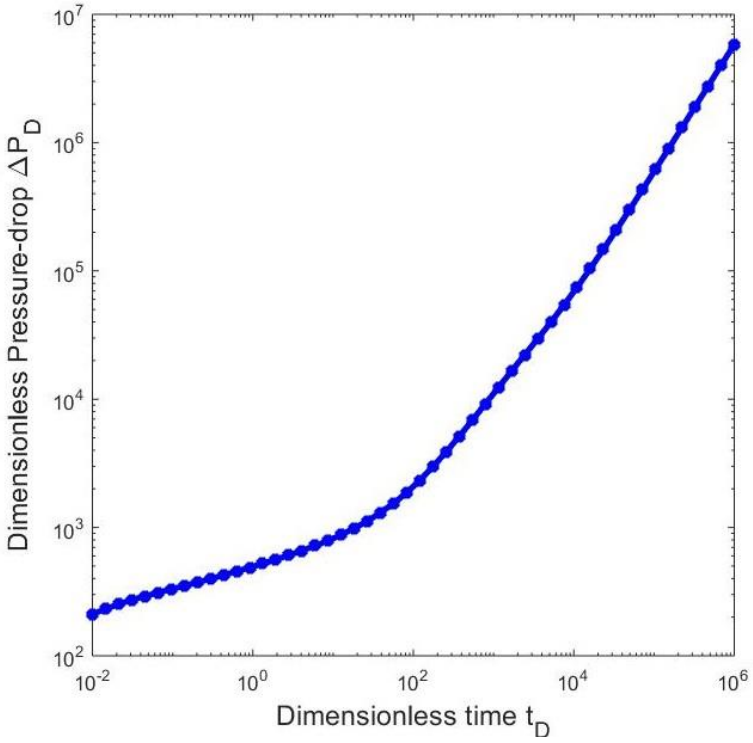


**Figure 5.15: Dimensionless wellbore pressure for the Multi-Continuum Anomalous Model**

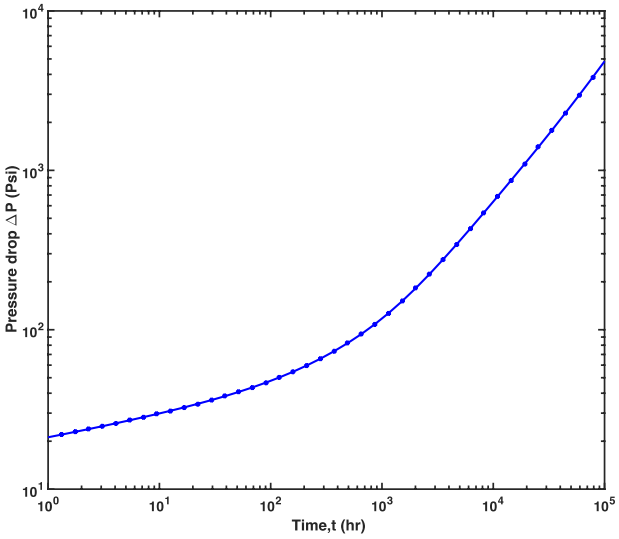


**Figure 5.16: Wellbore pressure drop for the Multi-Continuum Anomalous Model**

### 5.7.2 Effect of the Hydraulic fracture-permeability

The hydraulic fracture is the only conduit that feeds the well; therefore, the permeability of the hydraulic fracture affects the pressure response. The model considers super-diffusion in the hydraulic fracture. Thus, the flux law has a phenomenological constant of the dimension of $L^{1+\beta}$. Figure 5.17 shows the effect of the hydraulic fracture perviousness on the pressure response of the well. For a constant rate production, the pressure drop is decreases for a higher phenomenological constant of the hydraulic fracture. Although the hydraulic fracture is extended for a smaller area compare to the inner reservoir, the perviousness of the fracture alters the pressure drop at the early and intermediate time. It is important to note that the higher value of the perviousness shows an earlier boundary effect than the lower one.

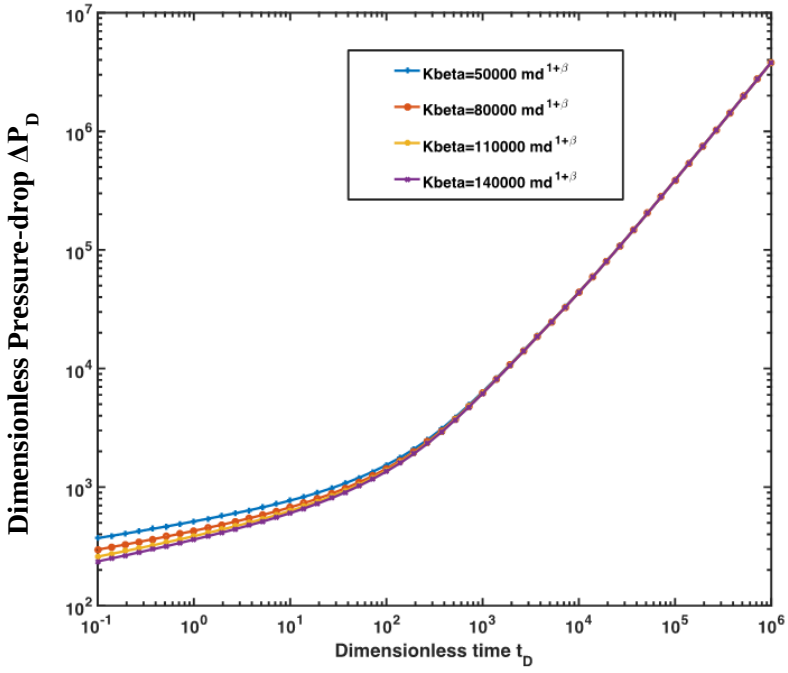


**Figure 5.17: Dimensionless wellbore pressure drop for the different values of the phenomenological constant ($K_{beta}$)**

### 5.7.3 Effect of the Super diffusion

The effect of the super-diffusion is evaluated according to the order of the space derivative. As the value of $\beta$ decreases from the unity, the space event becomes more significant; hence, the flow will be accelerated at the same pressure gradient. Fig. 5.18 shows how the faster flow influences the pressure response of the reservoir. The single most marked observation to emerge from the figure (Fig.5.18) is the impact of the super-diffusion is prolonged from the very early time to the late time. This result has further strengthened the hypothesis that the space event in the hydraulic fracture can significantly alter the flow characteristics. For a conventional flow ($\beta = 1$), pressure drop is higher than the super-diffusion flow. At the intermediate time, the pressure drop variation is more significant because the macro-fracture and the matrix starts to response to the pressure gradient and that provides a constant flow rate without

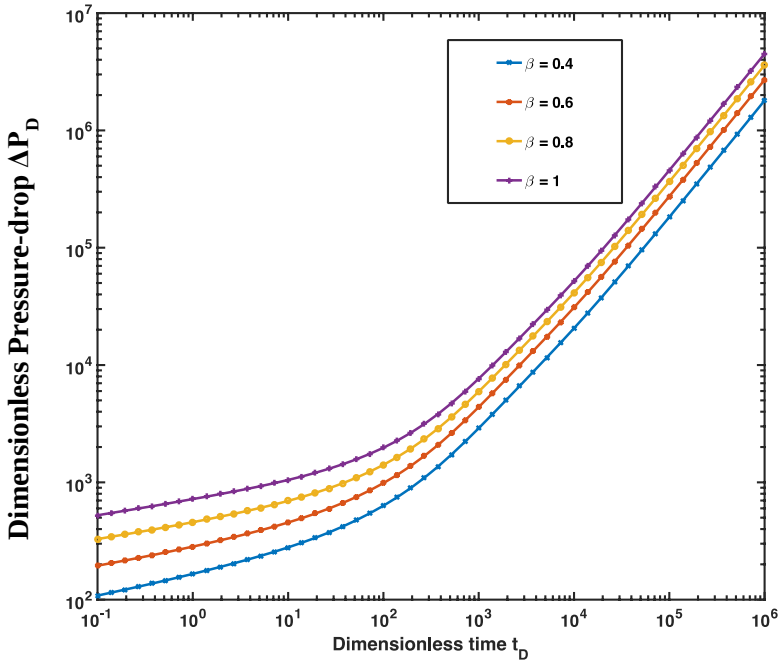


**Figure 5.18: Dimensionless wellbore pressure drop for the different values of the $\beta$ (Degree of super-diffusion)**

### 5.7.4 Effect of the Macro-fracture

Fig. 5.19 shows the effect of the micro-fracture permeability on the pressure response. Micro-fracture is the dominant conduit in the inner reservoir region; thus, the permeability-alteration in the micro-fracture changes the pressure response from the earlier time to the late time of the production ($t_D = 10.6E4$). However, at the intermediate time, the macro-fracture permeability causes the most variation in the pressure response. At later time the flow capacitance of the macro-fracture reaches to the maximum and the flow is influenced by the boundary effect.

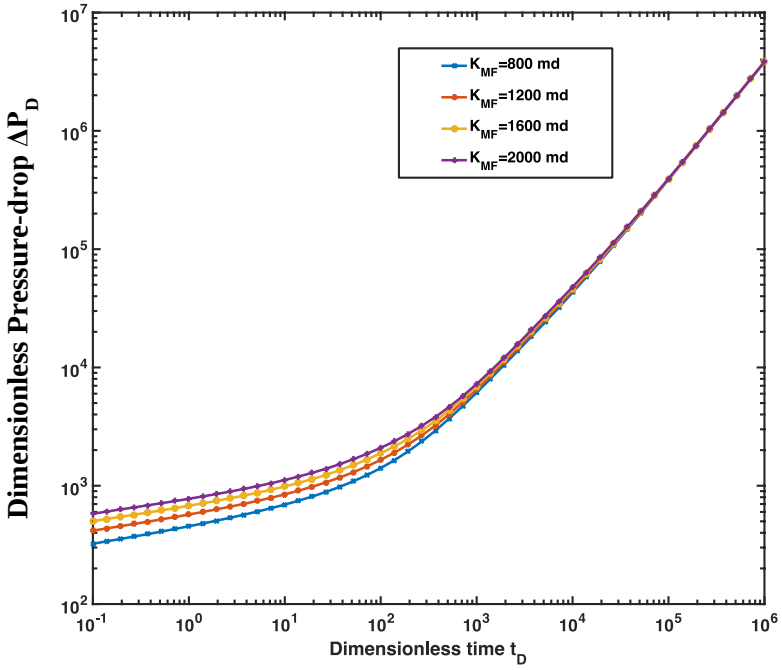


**Figure 5.19: Dimensionless wellbore pressure drop for the different values of the macro-fracture permeability ($K_{MF}$)**

### 5.7.5 Effect of the Micro-fracture

Micro-fracture is an intermediate zone between the source matrix and the hydraulic fracture; moreover, it has a small relative volume. Fig. 5.20 shows the pressure response variation due to the alteration of the micro-fracture permeability. From the figure it is observed that the micro-fracture flow capacity only affects the overall response only at an intermediate time, from $t_D = 1E-3$ to $t_D = 1E2$ , and the it creates a very slight variation in the pressure response. The response also shows that the pressure drop is decreasing while the micro-fracture permeability is increased.

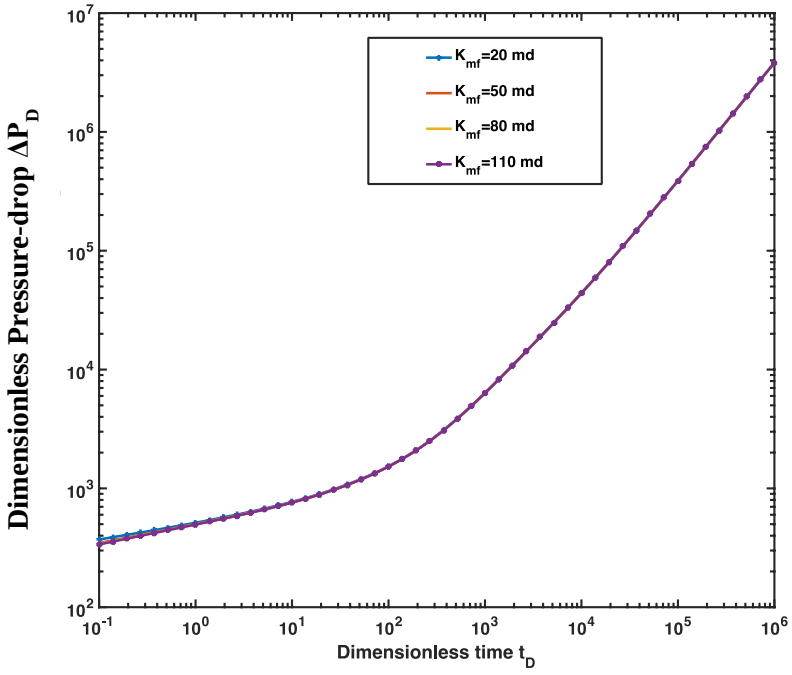


**Figure 5.20: Dimensionless wellbore pressure drop for the different values of the micro-fracture permeability ($K_{mf}$)**

### 5.7.6 Effects of the inner reservoir extend

The tip of the hydraulic fracture that bounded the inner reservoir area has a dissimilar effect at different flow time of the reservoir which is shown in the Fig. 5.21. A high-stimulated zone creates a high pressure-drop at the early time whereas at intermediate time the matrix and the macro-fracture regulate the flow. Therefore, at that time the pressure-drop due to the size of the stimulated zone is lower. At the late time, it is required a lower bottom hole pressure to maintain a constant flow rate from a reservoir with a long areal extend of the inner reservoir.

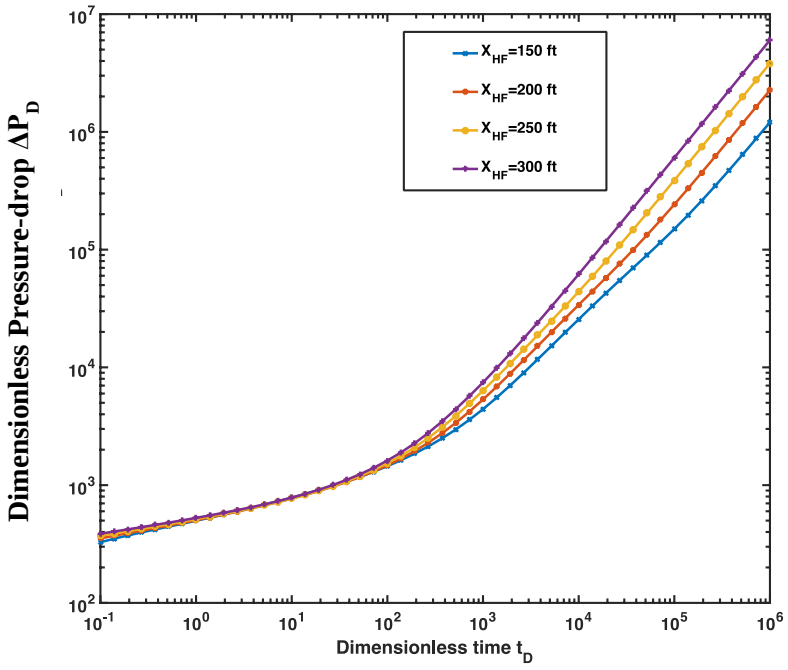


**Figure 5.21: Dimensionless wellbore pressure drop variations for the extend of the inner reservoir and the hydraulic fracture ($X_{HF}$).**

### 5.7.7 Effect of the matrix permeability

A change of the flow parameters in the matrix causes the change in the pressure response at intermediate to late time period. Figure 5.22 shows that an increment of the matrix permeability can reduce the pressure drop at a significant rate at intermediate time and boundary effect initiates earlier. Moreover, the findings demonstrate that the macro-fracture can influence at the early-intermediate-transient time whereas the matrix has the most impact at the late intermediate time. The matrix is acted as the main fluid source, so the conductivity of the matrix regulates the flow of the reservoir after reaching the pressure pulse to the matrix.

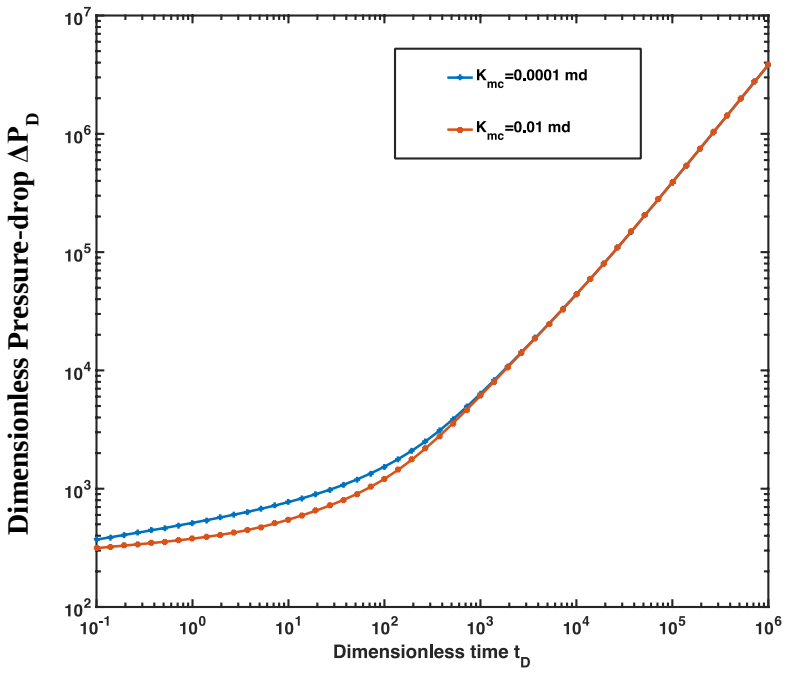


**Figure 5.22: Dimensionless wellbore pressure response for the different values of the core-matrix permeability ($K_{mc}$)**

### 5.7.8 Effect of the Outer reservoir

The effect of the outer reservoir is shown in the Fig. 5.23. Since the most influential character of the outer reservoir is the sub-diffusion, the anomalous parameter, termed the phenomenological constant and the order of the time derivative control the pressure response at this model. The lower value of the anomalous parameters makes an extra pressure drop at the late early to early intermediate time ($t_D = 1E-4\ to\ 5E-1$). These findings significantly differ from the previous results reported in the literature (Brawn, 2009; Ozcan, 2011; Ozkan *et. al,* 2012). The study shows an impact of the outer reservoir at earlier time because the frequency of the macro-fracture is higher in the inner reservoir region and the extend of the inner reservoir is smaller than the previous studies. Therefore, the pressure response travels faster in the multi-continuum anomalous model. The findings also validate the time impact on fluid flow that causes a slower flow; thus, yields a reduction in pressure.

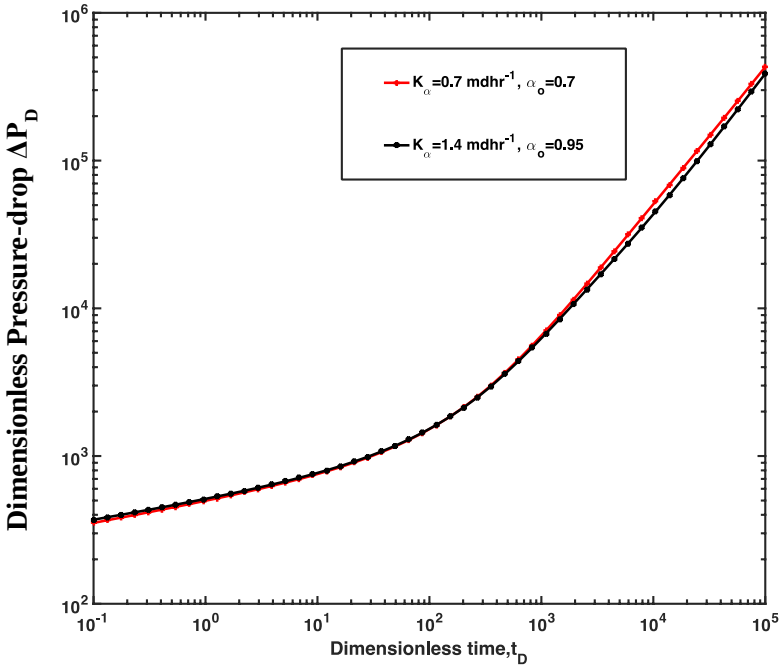


**Figure 5.23: Variations of the Dimensionless wellbore pressure drop with the sub-diffusion parameter ($K_\alpha, \alpha$).**

### 5.7.9 Effect of the hydraulic fracture density

The study assumes a no-flow boundary at the mid-point ($y = Y_e$) of two adjacent hydraulic fractures. Therefore, the outer boundary of the inner reservoir increases as the number of hydraulic fracture decreases. Figure 5.24 illustrates the effect of the hydraulic fracture density. No significant difference is observed at the early and the intermediate time. A variation of the pressure drop occurs when the boundary effect is identified in the flow. A high density of the hydraulic fracture triggers to an earlier boundary effect.

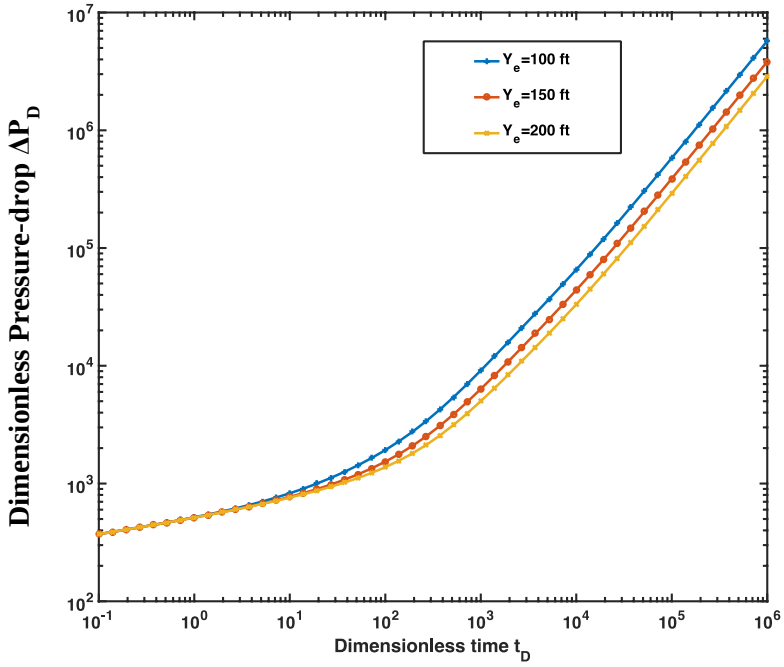


**Figure 5.24: Dimensionless wellbore pressure loss variation with the density of the macro-fracture.**

### 5.7.10 Effect of the density of the macro-fracture

The most remarkable result to emerge from the model response is that the influence of the density of the macro-fracture. In the model, matrix is the source of the fluid; however, the tight formation of the matrix has a poor conductivity. Consequently, with a relative higher conductivity, the macro-fracture controls the fluid flows to the hydraulic fracture. Figure 5.25 reveals that the impact of the macro-fracture density in term of dimensionless pressure. A denser macro-fracture maintains the constant flow rate through a lower pressure drop in the reservoir. Although the boundary effect starts earlier for the denser macro-fracture, due to its high conductivity lower pressure drop sustains at the late time.

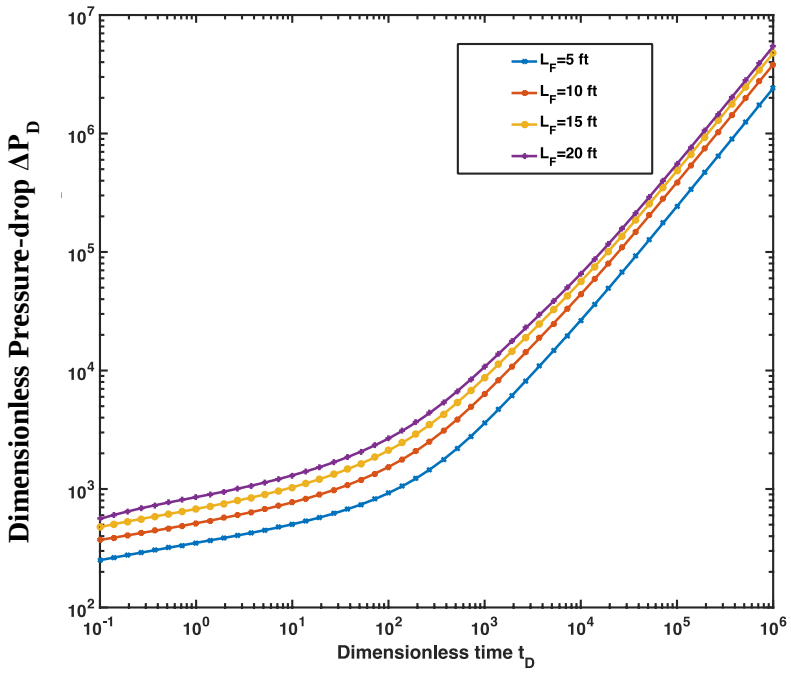


**Figure 5.25: Effect of the macro-fracture density on the dimensionless bottom-hole pressure response of the model.**

### 5.8 Chapter Summary

A multi-continuum anomalous model is developed in this chapter. A logical combination of flow conditions is used in a modified physical structure. Either the pressure continuity or the flow continuity condition controls the inter-porosity flow between different domains. The solution for the pressure is derived in the Laplace domain and then it is inversed by Stehfest algorithm. The response analysis of the model shows the following major findings:

a. The response curve has two distinguish slope that are related to the flow parameters of the domains.
b. The influence of the super-diffusion in the hydraulic fracture is remarkable as it alters the pressure response during the whole life of the reservoir.
c. The sub-diffusion impact is significant at the late time response and increases with the time.

d. Macro-fracture permeability regulates the pressure drop in the reservoir as it is the main conduit in the inner reservoir.
e. Matrix permeability can influence the pressure response at the late early to intermediate time.
f. The density of the macro-fracture has a significant impact both in the early and the late time.

**Symbol**

| | |
|---|---|
| h | Reservoir thickness, ft |
| $r_w$ | Wellbore radius, ft |
| $L_H$ | Horizontal well lengthy, ft |
| $L_F$ | Spacing of macro-fracture, ft |
| $n_f$ | Number of hydraulic fracture, f |
| $d_F$ | Distance between hydraulic fractures, ft |
| $x_e$ | Distance to boundary parallel to well, ft |
| $y_e$ | Drainage area length, ft |
| μ | Viscosity, cp |
| q | Constant flow rate, Stb/day |
| $\phi_{HF}$ | Hydraulic fracture porosity, fraction |
| $K_\beta$ | Phenomenological coefficient, md-hr$^{1-\alpha}$ |
| $c_{HF}$ | Hydraulic fracture total compressibility, Psi$^{-1}$ |
| $x_{HF}$ | Hydraulic fracture half length, ft |
| w | Hydraulic fracture width, ft |
| β | Memory Parameter (Space) |
| $\phi_{MF}$ | Macro fracture porosity, fraction |
| $K_{MF}$ | Macro-fracture permeability, md |
| $c_{MF}$ | Macro fracture total compressibility, Psi$^{-1}$ |
| $h_{MF}$ | Thickness of the macro-fracture, ft |
| $\phi_{mf}$ | Micro fracture porosity, fraction |
| $K_{mf}$ | Micro-fracture permeability, md |

$c_{mf}$ Micro fracture total compressibility, $Psi^{-1}$

$h_{mf}$ Thickness of the micro-fracture, ft

$y_f$ Spacing between two fractures, ft

$\phi_{fc}$ Cake fracture porosity, fraction

$K_{fc}$ Cake fracture permeability, md

$c_{fc}$ Cake fracture total compressibility, $Psi^{-1}$

$h_{fc}$ Mico-fracture thickness,

$r_{mc}$ Radius of the matrix core, ft

$h_{cm}$ Thickness of the cake matrix slab, ft

$\phi_{mc}$ Core matrix porosity, fraction

$K_{mc}$ Core matrix permeability, md

$c_{mc}$ Core matrix total compressibility, $Psi^{-1}$

$\phi_o$ Outer reservoir porosity, fraction

$K_\alpha$ Phenomenological coefficient, $md\text{-}hr^{1-\alpha}$

$c_o$ Outer reservoir total compressibility, $Psi^{-1}$

$\alpha_o$ Memory Parameter,

***Model Constant***

$$x_D = \frac{x}{x_{HF}}$$

$$x_{eD} = \frac{x_e}{x_{HF}}$$

$$y_D = \frac{y}{x_{HF}}$$

$$y_{eD} = \frac{y_e}{x_{HF}}$$

$$w_D = \frac{w}{x_{HF}}$$

$$r_D = \frac{r}{\frac{y_f}{2}}$$

$$\xi_D = \frac{\xi}{\frac{h_{cm}}{2}}$$

$$z_D = \frac{z}{\frac{L_f}{2}}$$

$$\zeta_D = \frac{\zeta}{\frac{y_f}{2}}$$

$$c_{AFD} = \frac{k_\beta w B}{k_{MF} {x_{HF}}^\beta}$$

$$c_{HFD} = \frac{B w k_{HF}}{\pi k_{MF} x_{HF}}$$

$$\lambda_{Ao} = \frac{k_{MF}^{\alpha o} \mu x_{HF}^2}{k_{\alpha o} \mu^{\alpha o} x_{HF}^{2\alpha}}$$

$$\lambda_{mc} = \frac{12 x_{HF}^2 k_{mc}}{y_f^2 k_{MF}}$$

$$\lambda_{cm} = \frac{12 x_{HF}^2 k_{mc}}{h_{cm}^2 k_{MF}}$$

$$\lambda_{fc} = \frac{12 x_{HF}^2 k_{fc}}{y_f^2 k_{MF}}$$

$$\lambda'_{fc} = \frac{k_{cm} {y_f}^2}{k_{fc}\, h_{cm}^2}$$

$$\lambda_{fcf} = \frac{{L_f}^2 k_{fc} h_{fc}}{k_{mf} y_f h_{mf} (h_{cm} + h_{fc})}$$

$$\lambda_{mf} = \frac{12 {x_{HF}}^2}{L_f^2} \frac{k_{mf}}{k_{MF}}$$

$$\lambda_{AF} = \frac{k_{MF} {x_{HF}}^\beta}{k_\beta x_{HF}}$$

$$\lambda'_{AF} = \frac{k_{MF} h_{MF}}{k_\beta (h_{MF} + L_f)} \frac{{x_{HF}}^\beta}{x_{HF}}$$

$$\lambda'_{mf} = \frac{L_f^2 k_m}{{y_f}^2 k_{mf}}$$

$$\lambda_m = \frac{12x_{HF}^2 k_m}{{y_f}^2 k_{MF}}$$

$$\lambda'_{HF} = \frac{k_{MF} h_{MF}}{k_{HF}(h_{MF} + L_f)}$$

$$\eta_{HFD} = \frac{(\phi\, c_t)_{HF}}{(\phi\, c_t)_{MF}} \frac{k_{MF}}{k_{HF}}$$

$$\omega_{Ao} = \frac{(\phi\, c_t)_o}{(\phi\, c_t)_{MF}^{\alpha o}}$$

$$\omega_{mc} = \frac{(\phi\, c_t)_{mc}}{(\phi\, c_t)_{MF}}$$

$$\omega_{fc} = \frac{(\phi\, c_t)_{fc}}{(\phi\, c_t)_{MF}}$$

$$\omega_{mf} = \frac{(\phi\, c_t)_{mf}}{(\phi\, c_t)_{MF}}$$

$$\omega_{HF} = \frac{(\phi\, c_t)_{HF}}{(\phi\, c_t)_{MF}}$$

$$C_{OMF} = \frac{k_{\alpha o}(h_{MF} + L_f)}{k_{MF} h_{MF}}$$

$$M_{DA} = \omega_{Ao} * \lambda_{Ao}$$

$$M_{DAHF} = \omega_{HF} \lambda_{AF}$$

$$\alpha_{mc} = \frac{3\omega_{mc} s}{\lambda_{mc}}$$

$$\alpha_{cm} = \frac{3\omega_{mc} s}{\lambda_{cm}}$$

$$\alpha_m = \frac{3\omega_m s}{\lambda_m}$$

$$\alpha_{fc} = \frac{3\omega_{fc} s}{\lambda_{fc}}$$

$$\alpha'_{fc} = \alpha_{fc} + \lambda'_{fc} \sqrt{\alpha_{cm}} \tanh\left(\sqrt{\alpha_{cm}}\right)$$

$$\eta_{HFD} = \frac{(\phi\, c_t)_{HF}}{(\phi\, c_t)_{MF}} \frac{k_{MF}}{k_{HF}}$$

$$\beta_o = M_{DA} s^{\alpha o}$$

$$\beta_{mc} = \frac{k_{mc}(h_{fc} + h_{cm})}{k_{fc}h_{fc}}\left\{\sqrt{\alpha_{mc}}\coth\left(\sqrt{\alpha_{mc}}r_{mcD}\right) - \frac{1}{r_{mcD}}\right\}$$

$$\beta_m = \lambda'_{mf}\sqrt{\alpha_m}\tanh\left(\sqrt{\alpha_m}\right)$$

$$\beta'_{mf} = \frac{3\omega_{mf}s}{\lambda_{mf}} + \beta_m$$

$$\beta_{fc} = \left(\frac{\sqrt{\alpha'_{fc}} - \beta_{mc}}{\sqrt{\alpha'_{fc}} + \beta_{mc}}\right)exp\left(\sqrt{\alpha'_{fc}}(r_{mcD} - 1)\right) + exp\left(-\sqrt{\alpha'_{fc}}(r_{mcD} - 1)\right)$$

$$\beta'_{fc} = \frac{1}{\beta_{fc}}\left\{\left(\frac{\sqrt{\alpha'_{fc}} - \beta_{mc}}{\sqrt{\alpha'_{fc}} + \beta_{mc}}\right)\sqrt{\alpha'_{fc}}exp\left(\sqrt{\alpha'_{fc}}(r_{mcD} - 1)\right)\right.$$

$$\left. - \sqrt{\alpha'_{fc}}exp\left(-\sqrt{\alpha'_{fc}}(r_{mcD} - 1)\right)\right\}$$

$$\beta_{mf} = \frac{3\omega_{mf}s}{\lambda_{mf}} - \beta'_{fc}\lambda_{fcf}$$

$$\beta_{OMF} = \sqrt{\beta_o}\tanh\left(\sqrt{\beta_o}(x_{eD} - 1)\right)$$

$$\beta_{OMFD} = C_{OMF}\left(\frac{(\phi\, c_t)_{MF}\mu x_{HF}^2}{k_{MF}}\right)^{\alpha o - 1} s^{1-\alpha o}\beta_{OMF}$$

$$\beta_{MF} = \beta_{OMFD} + \frac{\lambda_{mf}}{3}\sqrt{\beta_{mf}}\tanh\left(\sqrt{\beta_{mf}}\right) + s$$

$$\beta_{MHF} = \lambda'_{AF}\sqrt{\beta_{MF}}\tanh\left(\sqrt{\beta_{MF}}(y_{eD} - \frac{w_D}{2})\right)$$

$$\beta'_{MHF} = \lambda'_{HF}\sqrt{\beta_{MF}}\tanh\left(\sqrt{\beta_{MF}}(y_{eD} - \frac{w_D}{2})\right)$$

$$\beta_{HF} = \frac{2}{w_D}\beta_{MHF} + M_{DAHF}s$$

$$\beta'_{HF} = \frac{2}{w_D}\beta'_{MHF} + \eta_{HFD}s$$

## References


Albinali, A. (2016a). Analytical solution for anomalous diffusion in fractured nanoporous reservoirs. Colorado School of Mines.

Abdassah, D., & Ershaghi, I. (1986). Triple-porosity systems for representing naturally fractured reservoirs. SPE Formation Evaluation, 1(02), 113-127.

Alahmadi, H. A. H. (2010). A Triple-porosity model for fractured horizontal wells (Doctoral dissertation, Texas A & M University).

Albinali, A., & Ozkan, E. (2016b, May). Analytical Modeling of Flow in Highly Disordered, Fractured Nano-Porous Reservoirs. In SPE Western Regional Meeting. Society of Petroleum Engineers.

Albinali, A., Holy, R., Sarak, H., & Ozkan, E. (2016). Modeling of 1D Anomalous Diffusion in Fractured Nanoporous Media. Oil & Gas Science and Technology–Revue d'IFP Energies nouvelles, 71(4), 56.

Apaydin, O. G., Ozkan, E., & Raghavan, R. S. (2011, January). Effect of discontinuous microfractures on ultratight matrix permeability of a dual-porosity medium. In Canadian Unconventional Resources Conference. Society of Petroleum Engineers.

Brown, M., Ozkan, E., Raghavan, R., & Kazemi, H. (2011). Practical solutions for pressure-transient responses of fractured horizontal wells in unconventional shale reservoirs. SPE Reservoir Evaluation & Engineering, 14(06), 663-676.

de Swaan O, A. (1976). Analytic solutions for determining naturally fractured reservoir properties by well testing. Society of Petroleum Engineers Journal, 16(03), 117-122.

El-Banbi, A. H., & Wattenbarger, R. A. (1998, January). Analysis of linear flow in gas well production. In SPE Gas Technology Symposium. Society of Petroleum Engineers.

Fomin, S. E. R. G. E. I., Chugunov, V., & Hashida, T. O. S. H. I. Y. U. K. I. (2011). Mathematical modeling of anomalous diffusion in porous media. Fract. Differ. Calc, 1(1), 1-28.

Haubold, H. J., Mathai, A. M., & Saxena, R. K. (2011). Mittag-Leffler functions and their applications. Journal of Applied Mathematics, 2011.

Holy, R. W., & Ozkan, E. (2016, May). A Practical and Rigorous Approach for Production Data Analysis in Unconventional Wells. In SPE Low Perm Symposium. Society of Petroleum Engineers.

Kazemi, H. (1969). Pressure transient analysis of naturally fractured reservoirs with uniform fracture distribution. Society of petroleum engineers Journal, 9(04), 451-462.

Ozcan, O. (2014). Fractional diffusion in naturally fractured unconventional reservoirs. Colorado School of Mines.

Ozkan, E., Brown, M. L., Raghavan, R., & Kazemi, H. (2011). Comparison of fractured-horizontal-well performance in tight sand and shale reservoirs. SPE Reservoir Evaluation & Engineering, 14(02), 248-259.

Raghavan, R. (2011). Fractional derivatives: application to transient flow. Journal of Petroleum Science and Engineering, 80(1), 7-13.

Stehfest, H. (1970). Algorithm 368: Numerical inversion of Laplace transforms [D5]. Communications of the ACM, 13(1), 47-49.

Warren, J. E., & Root, P. J. (1963). The behavior of naturally fractured reservoirs. Society of Petroleum Engineers Journal, 3(03), 245-255.

Wattenbarger, R. A. (2007). Some Reservoir Performance Aspects of Unconventional Gas Production. In Private conference presentation.

# Chapter 6 Conclusions and Recommendations

In this research, a solution for a linear multi-continuum anomalous diffusion model is derived and analyzed. The following conclusions are made from the research:

All the fluid flow with memory impact is the non-Darcy flow but all the non-Darcy flow is not the memory based anomalous flow. The appropriate parameterization, conceptualization of memory impact, high non-linearity in the governing equation and numerical solution in an efficient way, are the unsolved difficulties for the proper establishment of this idea in the petroleum field.

The continuum-based models consider the physical structure of the reservoir; therefore, it requires additional reservoir parameters for the new continuum. Alternatively, anomalous diffusion approach requires less parameter compared to the continuum approaches, but a high uncertainty exists in the precise determination of the order of the differentiation or the fractal exponent. A combination of the continuum approach and the anomalous diffusion is one of the best alternatives for fluid flow modelling in the naturally fractured reservoir.

The model with the combination of the anomalous diffusion and continuum approach gives more flexibility in the modeling of fluid flow in fractured reservoir. The response curve has two distinct slope that are related to the flow parameters of the domains. The influence of the super-diffusion in the hydraulic fracture is remarkable as it alters the pressure response during the whole life of the reservoir. The sub-diffusion impact is significant at the late stage response of a reservoir and increases with the time. Macro-fracture permeability regulates the pressure drop in the reservoir as it is the main conduit in the inner reservoir. Matrix permeability can influence the pressure response at the late early to intermediate time. The density of the macro-fracture has a significant impact both in the early and the late time.

The following recommendations are made for the future research:

a. The implementation of the anomalous diffusion model in the reservoir analysis requires a proper procedure for the determination of the memory parameters.
b. A numerical investigation should be done with all the possible boundary conditions to determine the anomalous behavior impact in the reservoir flow.
c. Future studies on the multi-continuum anomalous model require a numerical investigation of the model so that it can be applied with a variation of the parameters.
d. The analysis of the boundary dominated flow in the multi-continuum anomalous model will enable the performance analysis of a fractured reservoir with higher matrix permeability

# Appendix A

## A.1 Derivation of the Continuity Equation for the Anomalous Diffusion

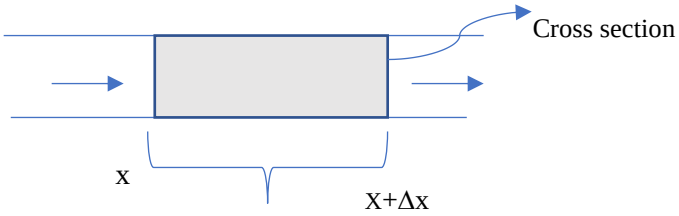


$$m = \frac{Mass\ of\ component\ in\ bulk\ volume}{Bulk\ volume}$$

$$= \rho\ \frac{V}{V_B} \qquad \text{[All are in the reservoir condition]}$$

$$= \rho\phi \quad \text{[For single phase flow } V^R = V^0\text{]}$$

Volumetric flux, u = Volume/Area*time

Mass flowing at x = $(\rho u)_x$

Mass flowing out at x +Δx = $(\rho u)_{x+\Delta x}$

During the time of Δt, the overall flow = $[(\rho u)_x - (\rho u)_{x+\Delta x}]\ A\Delta t$

For a time-interval Δt, the accumulation of mass inside volume (AΔx) is = $\Delta m A\Delta x$

According to the law of mass conservation:

$[(\rho u)_x - (\rho u)_{x+\Delta x}]\ A\Delta t = \Delta m A\Delta x$

Dividing by ΔxΔt:

$$\frac{[\ (\rho u)_x - (\rho u)_{x+\Delta x}\ ]}{\Delta x} = \frac{\Delta\rho\phi}{\Delta t} \qquad \text{(A.1.1)}$$

$$\frac{\partial(\rho u)}{\partial x} = -\frac{\partial\rho\phi}{\partial t} \quad [\ \Delta x \rightarrow 0, \Delta t \rightarrow 0] \qquad \text{(A.1.2)}$$

This is the continuity equation for the one-dimensional flow of a single-phase fluid. All the parameters are in reservoir condition.

Equation (A.1.1) can be rewritten as follow by the chain rule:

$$\frac{\partial(\rho u)}{\partial x} = -\phi(\frac{\partial \rho}{\partial p}\frac{\partial p}{\partial t}) \quad \text{(A.1.3)}$$

The definition of the compressibility

$$c_t = -\frac{1}{V}\frac{\partial V}{\partial p} \quad \text{(A.1.4)}$$

$$c_t = -\rho(\frac{\partial(\frac{1}{\rho})}{\partial p}) \quad \text{(A.1.5)}$$

$$c_t = \frac{1}{\rho}\frac{\partial \rho}{\partial p} \quad \text{(A.1.6)}$$

$$c_t \rho = \frac{\partial \rho}{\partial p} \quad \text{(A.1.7)}$$

Using the expression for the compressibility in the Eq. A.1. 2

$$\frac{\partial(\rho u)}{\partial x} = -\phi\, c_t \rho \frac{\partial p}{\partial t} \quad \text{(A.1.8)}$$

For the conventional approach Darcy's law is valid as a flux law

$$u = \frac{q}{A} = -\frac{k}{\mu}\frac{\partial p}{\partial x} \quad \text{(A.1.9)}$$

Eq. A.1. 8 yields

$$\frac{\partial(\rho\frac{\partial p}{\partial x})}{\partial x} = \frac{\phi\, c_t \rho \mu}{k}\frac{\partial p}{\partial t} \quad \text{(A.1.10)}$$

[For the slightly compressible fluid $\mu \neq f(x)$ and for the homogeneous reservoir $k \neq f(x)$]

$$\rho\frac{\partial^2 p}{\partial x^2} + \frac{\partial p}{\partial x}\frac{\partial \rho}{\partial x} = \frac{\phi\, c_t \rho \mu}{k}\frac{\partial p}{\partial t} \quad \text{(A.1.11)}$$

$$\rho\frac{\partial^2 p}{\partial x^2} + \frac{\partial p}{\partial x}\frac{\partial p}{\partial x}\frac{\partial \rho}{\partial p} = \frac{\phi\, c_t \rho \mu}{k}\frac{\partial p}{\partial t} \quad \text{(A.1.12)}$$

$$\rho\frac{\partial^2 p}{\partial x^2} + c_t \rho(\frac{\partial p}{\partial x})^2 = \frac{\phi\, c_t \rho \mu}{k}\frac{\partial p}{\partial t} \quad \text{(A.1.13)}$$

$$\rho(\frac{\partial^2 p}{\partial x^2} + c_t\left(\frac{\partial p}{\partial x}\right)^2) = \frac{\phi\, c_t \rho \mu}{k}\frac{\partial p}{\partial t} \quad \text{(A.1.14)}$$

$$\frac{\partial^2 p}{\partial x^2} = \frac{\phi\, c_t \mu}{k}\frac{\partial p}{\partial t} \quad \text{(A.1.15)}$$

For slightly compressible fluid $c_t\left(\frac{\partial p}{\partial x}\right)^2 = c_t\left(\frac{q\mu}{kA}\right)^2 \ll 1$. This is the equation for the one-dimensional linear diffusion of the slightly compressible fluid.

The modified flux law (Chen and Raghavan, 2015)

$$u\,(x,t) = \frac{q}{A} = -\eta_{\alpha,\beta}\,\frac{\partial^{1-\alpha}}{\partial t^{1-\alpha}}\left[\frac{\partial^{\beta} p(x,t)}{\partial x^{\beta}}\right] \tag{A.1.16}$$

where $0 < \alpha \leq 1\ and\ 0 < \beta \leq 1;\ \eta_{\alpha,\beta} = \frac{k_{\alpha,\beta}}{\mu}$

By using the modified flux law (Eq. A.1.16) in the continuity equation (Eq. A.1.15)

$$\frac{\partial\left(-\rho\eta_{\alpha,\beta}\,\frac{\partial^{1-\alpha}}{\partial t^{1-\alpha}}\frac{\partial^{\beta} p(x,t)}{\partial x^{\beta}}\right)}{\partial x} = -\phi\, c_t \rho\,\frac{\partial \mathrm{p}}{\partial t} \tag{A.1.17}$$

Taking $\frac{\partial^{\alpha-1}}{\partial t^{\alpha-1}}$ of both sides

$$\frac{\partial\left(\left[\frac{\partial^{\beta} p(x,t)}{\partial x^{\beta}}\right]\right)}{\partial x} = \frac{\phi\, c_t}{\eta_{\alpha,\beta}}\,\frac{\partial^{\alpha}\mathrm{p(x,t)}}{\partial t^{\alpha}} \tag{A.1.18}$$

Let $\eta_{\alpha,\beta} \neq f(x)$. This is the equation for one dimensional linear anomalous diffusion of the slightly compressible fluid.

For sub-diffusion flow β =1

$$\frac{\partial^2 p(x,y)}{\partial x^2} = \frac{\phi\, c_t}{\eta_{\alpha,\beta}}\,\frac{\partial^{\alpha}\mathrm{p(x,t)}}{\partial t^{\alpha}} \tag{A.1.19}$$

For super diffusion α = 1

$$\frac{\partial\left(\frac{\partial^{\beta} p(x,t)}{\partial x^{\beta}}\right)}{\partial x} = \frac{\phi\, c_t}{\eta_{\alpha,\beta}}\,\frac{\partial \mathrm{p(x,t)}}{\partial t} \tag{A.1.20}$$

### A.2 Flow in the Outer Reservoir

The flow equation for the outer reservoir in terms of pressure drop

$$\frac{\partial^2 \Delta p_o}{\partial x^2} = \frac{(\phi\, c_t)_o \mu}{k_{\alpha o}}\,\frac{\partial^{\alpha o}\Delta p_o}{\partial t^{\alpha o}} \tag{A.2.1}$$

In dimensionless form

$$\frac{\partial^2}{\partial(x_{HF}x_D)^2}\left(\frac{p_{OD}qB\mu}{2\pi k_{MF}h}\right)=\frac{(\phi\, c_t)_o\mu}{k_{\alpha o}}\frac{\partial^{\alpha o}\left(\frac{p_{OD}qB\mu}{2\pi k_{MF}h}\right)}{\partial\left(\frac{t_D x_{HF}^2(\phi\, c_t)_{MF}\mu}{k_{MF}}\right)^{\alpha o}} \tag{A.2.2}$$

$$\frac{1}{x_{HF}^2}\frac{\partial^2 p_{OD}}{\partial {x_D}^2}=\frac{(\phi\, c_t)_o}{(\phi\, c_t)_{MF}^{\alpha o}}\frac{k_{MF}^{\alpha o}\mu}{k_{\alpha o}\mu^{\alpha o}x_{HF}^{2\alpha}}\frac{\partial^{\alpha o}p_{OD}}{\partial t_D^{\alpha o}} \tag{A.2.3}$$

$$\frac{\partial^2 p_{OD}}{\partial {x_D}^2}=\frac{(\phi\, c_t)_o}{(\phi\, c_t)_{MF}^{\alpha o}}\frac{k_{MF}^{\alpha o}\mu x_{HF}^2}{k_{\alpha o}\mu^{\alpha o}x_{HF}^{2\alpha}}\frac{\partial^{\alpha o}p_{OD}}{\partial t_D^{\alpha o}} \tag{A.2.4}$$

$$\frac{\partial^2 p_{OD}}{\partial {x_D}^2}=\omega_{Ao}\lambda_{Ao}\frac{\partial^{\alpha o}p_{OD}}{\partial t_D^{\alpha o}} \tag{A.2.5}$$

$$\frac{\partial^2 p_{OD}}{\partial {x_D}^2}=M_{DA}\frac{\partial^{\alpha o}p_{OD}}{\partial t_D^{\alpha o}} \tag{A.2.6}$$

Applying the Laplace transformation

$$\frac{\partial^2 \bar{p}_{OD}(x_D,s)}{\partial {x_D}^2}-M_{DA}\{s^{\alpha o}\bar{p}_{OD}(x_D,s)-p_{OD}(x_D,0)\}=0 \tag{A.2.7}$$

Initial conditions for the outer reservoir

$$\Delta p_0(x,o)=0 \tag{A.2.8}$$

$$\frac{p_{OD(x_D,t_D=0)}qB\mu}{2\pi k_{MF}h}=0 \tag{A.2.9}$$

$$p_{OD(x_D,0)}=0 \tag{A.2.10}$$

For two parallel horizontal reservoirs, there is a no flow boundary at x = $x_e$

$$\frac{\partial \Delta p_o}{\partial x}_{|x=x_e}=0 \tag{A.2.11}$$

$$\frac{\partial(\frac{p_{OD}qB\mu}{2\pi k_{MF}h})}{\partial(x_{HF}x_D)}=0 \tag{A.2.12}$$

$$\left.\frac{\partial p_{oD}}{\partial x_D}\right|_{x_D=x_{eD}}=0 \tag{A.2.13}$$

$$\left.\frac{\partial \bar{p}_{OD}(x_D,s)}{\partial x_D}\right|_{x_D=x_{eD}}=0 \tag{A.2.14}$$

Due to the continuity of pressure, at the inner boundary of the outer reservoir

$$\Delta p_{0_{|x=x_{HF}}} = \Delta p_{MF_{|x=x_{HF}}} \tag{A.2.15}$$

$$p_{0D_{|x_D=1}} = p_{MFD_{|x_D=1}} \tag{A.2.16}$$

$$\bar{p}_{0D_{|x_D=1}} = \bar{p}_{MFD_{|x_D=1}} \tag{A.2.17}$$

From Eq. A.2.10 and Eq. A.2.7

$$\frac{\partial^2 \bar{p}_{OD}}{\partial {x_D}^2} - M_{DA} s^{\alpha o} \bar{p}_{OD} = 0 \tag{A.2.18}$$

The general solution of Eq. A.2.18

$$\bar{p}_{OD} = Aexp\left(-\sqrt{\beta_o} x_D\right) + Bexp(\sqrt{\beta_o} x_D) \tag{A.2.19}$$

$\beta_o = M_{DA} s^{\alpha o}$

Now, differentiating Eq. A.2.19 with respect to $x_D$

$$\frac{\partial \bar{p}_{OD}}{\partial x_D}_{|x_D=x_{eD}} = -\sqrt{\beta_o} Aexp\left(-\sqrt{\beta_o} x_{eD}\right) + \sqrt{\beta_o} Bexp(\sqrt{\beta_o} x_{eD}) = 0 \tag{A.2.20}$$

$$A = \frac{Bexp(\sqrt{\beta_o} x_{eD}}{exp\left(-\sqrt{\beta_o} x_{eD}\right)} \tag{A.2.21}$$

$$A = Bexp(2\sqrt{\beta_o} x_{eD}) \tag{A.2.22}$$

From Eq. A.2.19 and Eq. A.2.22

$$\bar{p}_{OD} = Bexp(\sqrt{\beta_o} x_{eD})\left((\exp(\sqrt{\beta_o}(x_{eD} - x_D) + \exp(-\sqrt{\beta_o}(x_{eD} - x_D))\right) \tag{A.2.23}$$

$$\bar{p}_{OD} = 2Bexp\left(\sqrt{\beta_o} x_{eD}\right) cosh\left(\sqrt{\beta_o}(x_{eD} - x_D)\right) \tag{A.2.24}$$

For the inner boundary condition

$$\bar{p}_{0D_{|x_D=1}} = 2Bexp\left(\sqrt{\beta_o} x_{eD}\right) cosh\left(\sqrt{\beta_o}(x_{eD} - x_D)\right) = \bar{p}_{MFD_{|x_D=1}} \tag{A.2.25}$$

$$B = \frac{\bar{p}_{MFD_{|x_D=1}}}{2exp\left(\sqrt{\beta_o} x_{eD}\right) cosh\left(\sqrt{\beta_o}(x_{eD} - 1)\right)} \tag{A.2.26}$$

From the Eq. A.2.24

$$\bar{p}_{OD} = \bar{p}_{MFD_{|x_D=1}} \frac{\cosh(\sqrt{\beta_o}(x_{eD} - x_D))}{\cosh(\sqrt{\beta_o}(x_{eD} - 1))} \tag{A.2.27}$$

### A.3 Flow in the Core Matrix

The governing equation for the spherical core matrix

$$\frac{1}{r^2}\frac{\partial}{\partial r}\left(r^2\,\frac{\partial \Delta p_{mc}}{\partial r}\right)=\frac{(\phi\, c_t)_{mc}\mu}{k_{mc}}\,\frac{\partial \Delta p_{mc}}{\partial t} \tag{A.3.1}$$

Initial conditions:

$$\Delta p_{mc}(r,0)=0 \tag{A.3.2}$$

$$p_{mcD}(r_{D,},t_D=0)=0 \tag{A.3.3}$$

Inner boundary condition:

$$\Delta p_{mc}(0,t_D)=finite \tag{A.3.4}$$

$$\bar{p}_{mcD}(0,s)=finite \tag{A.3.5}$$

Outer boundary condition:

$$\Delta p_{mc_{|r=r_{mc}}}=\Delta p_{fc_{|r=r_{mc}}} \tag{A.3.6}$$

$$\bar{p}_{mcD_{|r_D=r_{mcD}}}=\bar{p}_{mfD_{|r_D=r_{mcD}}} \tag{A.3.7}$$

Eq. A.3.1 in dimensionless form:

$$\frac{1}{r_D^2}\,\frac{\partial}{\partial r_D}\left(r_D\frac{\partial p_{mcD}}{\partial r_D}\right)=\frac{3\omega_{mc}}{\lambda_{mc}}\frac{\partial p_{mcD}}{\partial t_D} \tag{A.3.8}$$

Now let

$$w_{mcD}(r_D,t_D)=p_{mcD}(r_D,t_D)r_D \tag{A.3.9}$$

$$\bar{w}_{mcD}(r_D,s)=\bar{p}_{mcD}(r_D,s)r_D \tag{A.3.10}$$

From Eq. A.3. 8 and Eq. A.3.9

$$\frac{\partial^2 w_{mcD}}{\partial r_D^2}=\frac{3\omega_{mc}}{\lambda_{mc}}\,\frac{\partial w_{mcD}}{\partial t_D} \tag{A.3.11}$$

The initial and the boundary condition for $w_{mcD}$

$$\bar{w}_{mcD}(0,s)=0 \tag{A.3.12}$$

At inner boundary

$$w_{mcD}(r_{D,},t_D=0)=0 \tag{A.3.13}$$

$$\bar{w}_{mcD}(0,s)=0 \tag{A.3.14}$$

From the initial condition, Eq. A.3.12, from Eq. A.3.11

$$\frac{\partial^2 \bar{w}_{mcD}(r_D, s)}{\partial {r_D}^2} - \frac{3\omega_{mc}}{\lambda_{mc}} s\bar{w}_{mcD}(r_D, s) = 0 \tag{A.3.15}$$

The general solution of the Eq. A.3.15

$$\bar{w}_{mcD} = Aexp\left(-\sqrt{\alpha_{mc}} r_D\right) + Bexp(\sqrt{\alpha_{mc}} r_D) \tag{A.3.16}$$

Using the inner boundary condition (Eq.A.3.14):

$$\bar{w}_{mcD} = -2A \sinh(\sqrt{\alpha_{mc}} r_D) \tag{A.3.17}$$

From Eq.A.3.10 and Eq.A.3.17:

$$\bar{p}_{mcD}(r_D, s) = -\frac{2}{r_D} A \sinh(\sqrt{\alpha_{mc}} r_D) \tag{A.3.18}$$

Now at the outer boundary ($r_D = r_{mcD}$), from the Eq.A.3.7 and Eq.A.3.18

$$\bar{p}_{fcD} = -\frac{2}{r_{mcD}} A \sinh(\sqrt{\alpha_{mc}} r_{mcD}) \tag{A.3.19}$$

From Eq.A.3.18 and Eq.A.3.19

$$\bar{p}_{mcD}(r_D, t_D) = \frac{1}{r_D} \frac{\bar{p}_{fcD} r_{mcD} \sinh(\sqrt{\alpha_{mc}} r_D)}{\sinh(\sqrt{\alpha_{mc}} r_{mcD})} \tag{A.3.20}$$

### A.4 Flow in the fracture cake matrix

The governing flow equation in the fracture cake matrix

$$\frac{\partial^2 \Delta p_{cm}}{\partial \xi^2} = \frac{(\phi\, c_t)_{cm} \mu}{k_{cm}} \frac{\partial \Delta p_{cm}}{\partial t} \tag{A.4.1}$$

The initial condition

$$\Delta p_{cm}(\xi, o) = 0 \tag{A.4.2}$$

$$p_{cmD(\xi_D, 0)} = 0 \tag{A.4.3}$$

Boundary Conditions:

At the inner boundary

$$\left.\frac{\partial \Delta p_{cm}}{\partial \xi}\right|_{\xi=0} = 0 \tag{A.4.4}$$

$$\left.\frac{\partial \bar{p}_{cmD}}{\partial \xi_D}\right|_{\xi_D=0} = 0 \tag{A.4.5}$$

At the outer boundary of the cake matrix

$$\Delta p_{cm}\big|_{\xi=\frac{h_{cm}}{2}} = \Delta p_{fc}\big|_{\xi=\frac{h_{cm}}{2}} \tag{A.4.6}$$

$$\bar{p}_{cmD}{}_{|\xi_D=1} = \bar{p}_{fcD}{}_{|\xi_D=1} \tag{A.4.7}$$

The dimensionless form of Eq. A.4.1

$$\frac{\partial^2 p_{cmD}}{\partial {\xi_D}^2} - \frac{3\omega_{mc}}{\lambda_{cm}} \frac{\partial p_{cmD}}{\partial t_D} = 0 \tag{A.4.8}$$

Taking the Laplace transformation and using Eq. A.4.3

$$\frac{\partial^2 \bar{p}_{cmD}}{\partial {\xi_D}^2} - \frac{3\omega_{mc}}{\lambda_{cm}} s\bar{p}_{cmD}(\xi_D, s) = 0 \tag{A.4.9}$$

$$[\alpha_{cm} = \frac{3\omega_{mc}s}{\lambda_{cm}}]$$

The general solution of the Eq. A.4.9

$$\bar{p}_{cmD} = Aexp\left(-\sqrt{\alpha_{cm}}\xi_D\right) + Bexp(\sqrt{\alpha_{cm}}\xi_D) \tag{A.4.10}$$

Now for the inner boundary condition, the Eq. A.4.10 turns to be

$$\bar{p}_{cmD} = 2Bcosh\left(\sqrt{\alpha_{cm}s}\xi_D\right) \tag{A.4.11}$$

For the outer boundary condition (Eq. A.4.7)

$$B = \frac{\bar{p}_{fcD}}{2cosh\left(\sqrt{\alpha_{cm}}\right)}$$

Thus, the final pressure solution for the cake matrix

$$\bar{p}_{cmD} = \frac{\bar{p}_{fcD}cosh\left(\sqrt{\alpha_{cm}}\xi_D\right)}{cosh\left(\sqrt{\alpha_{cm}}\right)} \tag{A.4.12}$$

### A.5 Flow in Cake fracture

The one-dimensional flow equation:

$$\frac{\partial^2 \Delta p_{fc}}{\partial r^2} = \frac{(\phi\ c_t)_{fc}\mu}{k_{fc}} \frac{\partial \Delta p_{fc}}{\partial t} + \frac{\mu}{k_{fc}} q_{Source,cm} \tag{A.5.1}$$

$q_{Source,cm}$ is influx from the cake matrix to the unit volume of fracture at unit time. The source term can be evaluated as:

$$q_{Source,cm} = \frac{2k_{cm}}{\mu h_{cm}} \frac{\partial \Delta p_{cm}}{\partial \xi}\Big|_{\xi=\frac{h_{cm}}{2}} \tag{A.5.2}$$

Now Eq. A.5.1 with the source from cake matrix

$$\frac{\partial^2 \Delta p_{fc}}{\partial r^2} = \frac{(\phi\, c_t)_{fc}\mu}{k_{fc}} \frac{\partial \Delta p_{fc}}{\partial t} + \frac{2k_{cm}}{k_{fc}h_{cm}} \frac{\partial \Delta p_{cm}}{\partial \xi}\Big|_{\xi=\frac{h_{cm}}{2}} \tag{A.5.3}$$

The dimensionless form of the Eq. A.5.3

$$\frac{\partial^2 p_{fcD}}{\partial {r_D}^2} = \frac{3\omega_{fc}}{\lambda_{fc}} \frac{\partial p_{fcD}}{\partial t_D} + \lambda_{fc}^{'} \frac{\partial p_{cmD}}{\partial \xi_D}_{|\xi_D=1} \tag{A.5.4}$$

$$\frac{\partial^2 \bar{p}_{fcD}(r_D, s)}{\partial {r_D}^2} - \alpha_{fc}\left\{s\bar{p}_{fcD}(r_D, s) - p_{fcD}(r_D, 0)\right\} - \lambda_{fc}^{'} \frac{\partial \bar{p}_{cmD}(r_D, s)}{\partial \xi_D}_{|\xi_D=1} = 0 \tag{A.5.5}$$

Here, $\alpha_{fc} = \frac{3\omega_{fc}s}{\lambda_{fc}}$ that scales up the heterogeneity at the cake fracture only.

The dimensionless initial condition for the cake fracture

$$p_{fcD}(r_D, o) = 0 \tag{A.5.6}$$

At the inner boundary, there exist a flux continuity with the core matrix

$$q_{fc}(r_{mc}, t) = q_{mc}(r_{mc}, t) \tag{A.5.7}$$

The surface area ratio:

$$\frac{A_{mc}}{A_{fc}} = \frac{h_{fc} + h_{cm}}{h_{fc}} \tag{A.5.8}$$

Now from the Eq. A.5.7 with value of the surface ratio

$$\frac{\partial \Delta p_{fc}}{\partial r}_{|(r_{mc}, t)} = \frac{k_{mc}(h_{fc} + h_{cm})}{k_{fc}h_{fc}} \frac{\partial \Delta p_{mc}}{\partial r}_{|(r_{mc}, t)} \tag{A.5.9}$$

In dimensionless form after the Laplace transformation

$$\frac{\partial \bar{p}_{fcD}(r_D, s)}{\partial r_D}_{|(r_{mcD}, s)} = \frac{k_{mc}(h_{fc} + h_{cm})}{k_{fc}h_{fc}} \frac{\partial \bar{p}_{mcD}(r_D, s)}{\partial r_D}_{|(r_{mcD}, s)} \tag{A.5.10}$$

Differentiating Eq. A.3.20

$$\frac{\partial \bar{p}_{mcD}}{\partial r_D}_{|(r_D, s)} = \frac{\bar{p}_{fcD} r_{mcD}}{\sinh\left(\sqrt{\alpha_{mc}} r_{mcD}\right)} \left(\frac{1}{r_D} \cosh\left(\sqrt{\alpha_{mc}} r_D\right) \sqrt{\alpha_{mc}} - \sinh\left(\sqrt{\alpha_{mc}} r_D\right) \frac{1}{{r_D}^2}\right) \tag{A.5.11}$$

Evaluating at $r_D = r_{mcD}$

$$\frac{\partial \bar{p}_{mcD}}{\partial r_D}_{|(r_{mcD},s)} = \bar{p}_{fcD_{|r_{mcD}}}\{\sqrt{\alpha_{mc}}\coth\left(\sqrt{\alpha_{mc}}r_{mcD}\right) - \frac{1}{r_{mcD}}\} \quad \text{(A.5.12)}$$

From the Eq. A.5.10 and Eq. A.5.12

$$\frac{\partial \bar{p}_{fcD}}{\partial r_D}_{|(r_{mcD},s)} = \bar{p}_{fcD_{|r_{mcD}}}\beta_{mc} \quad \text{(A.5.13)}$$

Here, $\beta_{mc} = \frac{k_{mc}(h_{fc}+h_{cm})}{k_{fc}h_{fc}}\left\{\sqrt{\alpha_{mc}}\coth\left(\sqrt{\alpha_{mc}}r_{mcD}\right) - \frac{1}{r_{mcD}}\right\}$

The outer boundary condition for the cake fracture due to the pressure continuity

$$\Delta p_{fc}\Big|_{r=\frac{y_f}{2}} = \Delta p_{mf}\Big|_{r=\frac{y_f}{2}} \quad \text{(A.5.14)}$$

In dimensionless form and in Laplace domain

$$\bar{p}_{fcD_{|r_D=1}}(r_D,s) = \bar{p}_{mfD_{|r_D=1}}(r_D,s) \quad \text{(A.5.15)}$$

Now differentiating the Eq. A.4.12

$$\frac{\partial \bar{p}_{cmD}}{\partial \xi_D}_{|(\xi_D,s)} = \frac{\bar{p}_{fcD}sinh\left(\sqrt{\alpha_{cm}}\xi_D\right)\sqrt{\alpha_{cm}}}{cosh\left(\sqrt{\alpha_{cm}}\right)} \quad \text{(A.5.16)}$$

Evaluating at $\xi_D = 1$

$$\frac{\partial \bar{p}_{cmD}}{\partial \xi_D}_{|(\xi_D=1,s)} = \bar{p}_{fcD_{|\xi_D=1}}\sqrt{\alpha_{cm}}\tanh\left(\sqrt{\alpha_{cm}}\right) \quad \text{(A.5.17)}$$

Substitute Eq. A.5.6 and Eq. A.5.17 in the Eq. A.5.5

$$\frac{\partial^2 \bar{p}_{fcD}}{\partial {r_D}^2} - \left(\alpha_{fc} + \lambda_{fc}^{'}\sqrt{\alpha_{cm}}\tanh\left(\sqrt{\alpha_{cm}}\right)\right)\bar{p}_{fcD}(r_D,s) = 0 \quad \text{(A.5.18)}$$

Assuming that $\bar{p}_{fcD} \neq f(\xi)$

$$\frac{\partial^2 \bar{p}_{fcD}}{\partial {r_D}^2} - \alpha'_{fc}\bar{p}_{fcD} = 0 \quad \text{(A.5.19)}$$

Here, $\alpha_{fc}^{'} = \alpha_{fc} + \lambda'_{fc}\sqrt{\alpha_{cm}}\tanh\left(\sqrt{\alpha_{cm}}\right)$

The general solution of the Eq. A.5.19

$$\bar{p}_{fcD} = Aexp\left(-\sqrt{\alpha'_{fc}}r_D\right) + Bexp\left(\sqrt{\alpha'_{fc}}r_D\right) \quad \text{(A.5.20)}$$

From the Eq. A.5.20

$$\frac{\partial \bar{p}_{fcD}}{\partial r_D}_{|(r_{D=}r_{mcD},s)} = -\sqrt{\alpha'_{fc}}Aexp\left(-\sqrt{\alpha'_{fc}}r_{mcD}\right) + \sqrt{\alpha'_{fc}}Bexp\left(\sqrt{\alpha'_{fc}}r_{mcD}\right) \quad \text{(A.5.21)}$$

Substitute the Eq. A.5.21 and Eq. A.5.20 in the Eq. A.5.13

$$-\sqrt{\alpha'_{fc}}Aexp\left(-\sqrt{\alpha'_{fc}}r_{mcD}\right)+\sqrt{\alpha'_{fc}}Bexp(\sqrt{\alpha'_{fc}}r_{mcD}) = \beta_{mc}\left\{Aexp\left(-\sqrt{\alpha'_{fc}}r_{mcD}\right)+Bexp(\sqrt{\alpha'_{fc}}r_{mcD})\right\} \quad \text{(A.5.22)}$$

$$A = B\left(\frac{\sqrt{\alpha'_{fc}}-\beta_{mc}}{\sqrt{\alpha'_{fc}}+\beta_{mc}}\right)exp(2\sqrt{\alpha'_{fc}}r_{mcD}) \quad \text{(A.5.23)}$$

Substitute the value of A in the Eq. A.5.20

$$\bar{p}_{fcD} = Bexp(\sqrt{\alpha'_{fc}}r_{mcD})\left\{\left(\frac{\sqrt{\alpha'_{fc}}-\beta_{mc}}{\sqrt{\alpha'_{fc}}+\beta_{mc}}\right)exp\left(\sqrt{\alpha'_{fc}}(r_{mcD}-r_D)\right) + exp\left(-\sqrt{\alpha'_{fc}}(r_{mcD}-r_D)\right)\right\} \quad \text{(A.5.24)}$$

Using the outer boundary condition (Eq. A.5.15) in the Eq. A.5.24

$$B = \frac{\bar{p}_{mfD_{|r_D=1}}}{exp(\sqrt{\alpha'_{fc}}sr_{mcD})\left\{\left(\frac{\sqrt{\alpha'_{fc}}-\beta_{mc}}{\sqrt{\alpha'_{fc}}+\beta_{mc}}\right)exp\left(\sqrt{\alpha'_{fc}}(r_{mcD}-1)\right)+exp\left(-\sqrt{\alpha'_{fc}}(r_{mcD}-1)\right)\right\}} \quad \text{(A.5.25)}$$

From the Eq. A.5.24 and Eq. A.5.25

$$\bar{p}_{fcD}$$

$$= \bar{p}_{mfD_{|r_D=1}} \frac{\left(\frac{\sqrt{\alpha'_{fc}} - \beta_{mc}}{\sqrt{\alpha'_{fc}} + \beta_{mc}}\right) exp\left(\sqrt{\alpha'_{fc}}(r_{mcD} - r_D)\right) + exp\left(-\sqrt{\alpha'_{fc}}(r_{mcD} - r\right.}{\left(\frac{\sqrt{\alpha'_{fc}} - \beta_{mc}}{\sqrt{\alpha'_{fc}} + \beta_{mc}}\right) exp\left(\sqrt{\alpha'_{fc}}(r_{mcD} - 1)\right) + exp\left(-\sqrt{\alpha'_{fc}}(r_{mcD} - 1\right.} \quad (A.5.26)$$

$$\bar{p}_{fcD} = \bar{p}_{mfD_{|r_D=1}} \frac{1}{\beta_{fc}} \left\{ \left(\frac{\sqrt{\alpha'_{fc}} - \beta_{mc}}{\sqrt{\alpha'_{fc}} + \beta_{mc}}\right) exp\left(\sqrt{\alpha'_{fc}}(r_{mcD} - r_D)\right) + exp\left(-\sqrt{\alpha'_{fc}}(r_{mcD} - r_D)\right) \right\} \quad (A.5.27)$$

$$Here, \beta_{fc} = \left(\frac{\sqrt{\alpha'_{fc}} - \beta_{mc}}{\sqrt{\alpha'_{fc}} + \beta_{mc}}\right) exp\left(\sqrt{\alpha'_{fc}}(r_{mcD} - 1)\right) + exp\left(-\sqrt{\alpha'_{fc}}(r_{mcD} - 1)\right)$$

### A.6 Flow in the Micro-fracture

According to Swaan O (1976), at the transient condition the flow from the matrix block to the half of the volume of fracture at unit time is

$$q_{Source,fc} = \frac{2k_{fc}h_{fc}}{\mu h_{mf}(h_{cm} + h_{fc})} \frac{\partial \Delta p_{fc}}{\partial r}\Big|_{r=\frac{y_f}{2}} \quad (A.6.1)$$

The fluid flow equation for the micro-fracture

$$\frac{\partial^2 \Delta p_{mf}}{\partial z^2} = \frac{(\phi\, c_t)_{mf}\mu}{k_{mf}} \frac{\partial \Delta p_{mf}}{\partial t} + \frac{\mu}{k_{mf}} q_{Source,fc} \quad (A.6.2)$$

With the Source term

$$\frac{\partial^2 \Delta p_{mf}}{\partial z^2} = \frac{(\phi\, c_t)_{mf}\mu}{k_{mf}} \frac{\partial \Delta p_{mf}}{\partial t} + \frac{2k_{fc}h_{fc}}{k_{mf}h_{mf}(h_{cm}+h_{fc})} \frac{\partial \Delta p_{fc}}{\partial r}\Big|_{r=\frac{y_f}{2}} \tag{A.6.3}$$

The dimensionless form of the Eq. A.6.3

$$\frac{\partial^2 p_{mfD}}{\partial {z_D}^2} = \frac{3\omega_{mf}}{\lambda_{mf}} \frac{\partial p_{mfD}}{\partial t_D} + \lambda_{fcf} \frac{\partial p_{fcD}}{\partial r_D}_{|r_D=1} \tag{A.6.4}$$

Initial condition for the micro-fracture

$$\Delta p_{mf}(z, o) = 0 \tag{A.6.5}$$

$$p_{mfD}(z_D, o) = 0 \tag{A.6.6}$$

The inner boundary conditions

$$\frac{\partial \Delta p_{mf}}{\partial z}_{|z=0,t} = 0 \tag{A.6.7}$$

$$\frac{\partial \bar{p}_{mfD}(z,s)}{\partial z_D}_{|z_D=o,s} = 0 \tag{A.6.8}$$

The outer boundary conditions

$$\Delta p_{mf}\Big|_{z=\frac{L_f}{2}} = \Delta p_{MF}\Big|_{z=\frac{L_f}{2}} \tag{A.6.9}$$

$$\bar{p}_{mfD}{}_{|z_D=1,s} = \bar{p}_{MFD}{}_{|z_D=1,s} \tag{A.6.10}$$

Differentiating Eq. A.5.27

$$\frac{\partial \bar{p}_{fcD}}{\partial r_D}_{|(r_D,s)} = -\bar{p}_{mfD}{}_{|r_D=1} \frac{1}{\beta_{fc}} \left\{ \left( \frac{\sqrt{\alpha'_{fc}} - \beta_{mc}}{\sqrt{\alpha'_{fc}} + \beta_{mc}} \right) \sqrt{\alpha'_{fc}} exp\left( \sqrt{\alpha'_{fc}} (r_{mcD} - r_D) \right) - \sqrt{\alpha'_{fc}} exp\left( -\sqrt{\alpha'_{fc}} (r_{mcD} - r_D) \right) \right\} \tag{A.6.11}$$

$$\frac{\partial \bar{p}_{fcD}}{\partial r_D}_{|(r_D=1)} = -\bar{p}_{mfD_{|r_D=1}} \frac{1}{\beta_{fc}} \left\{ \left( \frac{\sqrt{\alpha'_{fc}} - \beta_{mc}}{\sqrt{\alpha'_{fc}} + \beta_{mc}} \right) \sqrt{\alpha'_{fc}} exp\left( \sqrt{\alpha'_{fc}} (r_{mcD} - 1) \right) - \sqrt{\alpha'_{fc}} exp\left( -\sqrt{\alpha'_{fc}} (r_{mcD} - 1) \right) \right\} \quad \text{(A.6.12)}$$

$$\frac{\partial \bar{p}_{fcD}}{\partial r_D}_{|(r_D=1)} = -\bar{p}_{mfD_{|r_D=1}} \beta'_{fc} \quad \text{(A.6.13)}$$

$$Here, \beta'_{fc} = \frac{1}{\beta_{fc}} \left\{ \left( \frac{\sqrt{\alpha'_{fc}} - \beta_{mc}}{\sqrt{\alpha'_{fc}} + \beta_{mc}} \right) \sqrt{\alpha'_{fc}} exp\left( \sqrt{\alpha'_{fc}} (r_{mcD} - 1) \right) - \sqrt{\alpha'_{fc}} exp\left( -\sqrt{\alpha'_{fc}} (r_{mcD} - 1) \right) \right\}$$

Using Eq. A.6.6 and Eq. A.6.13 in Eq. A.6.4 in Laplace domain

$$\frac{\partial^2 \bar{p}_{mfD}}{\partial {z_D}^2} - \left( \frac{3\omega_{mf} s}{\lambda_{mf}} - \beta'_{fc} \lambda_{fcf} \right) \bar{p}_{mfD} = 0 \quad \text{(A.6.14)}$$

$Assuming, \overline{\Delta p}_{mfD} \neq f(r)]$

$$\frac{\partial^2 \bar{p}_{mfD}}{\partial {z_D}^2} - \beta_{mf} \bar{p}_{mfD} = 0 \quad \text{(A.6.15)}$$

$$Here, \beta_{mf} = \frac{3\omega_{mf} s}{\lambda_{mf}} - \beta'_{fc} \lambda_{fcf}$$

The general solution of the Eq. A.6.15

$$\bar{p}_{mfD} = Aexp\left( -\sqrt{\beta_{mf}} z_D \right) + Bexp\left( \sqrt{\beta_{mf}} z_D \right) \quad \text{(A.6.16)}$$

Apply the inner boundary condition (Eq. A.6.8)

$$A=B \tag{A.6.17}$$

$$\bar{p}_{mfD} = 2Bcosh\left(\sqrt{\beta_{mf}}z_D\right) \tag{A.6.18}$$

The outer boundary condition yields

$$B = \frac{\bar{p}_{MFD_{|z_D=1}}}{2cosh\left(\sqrt{\beta_{mf}}\right)} \tag{A.6.19}$$

Thus, the final pressure solution for the micro-fracture is

$$\bar{p}_{mfD} = \bar{p}_{MFD_{|z_D=1}} \frac{cosh\left(\sqrt{\beta_{mf}}z_D\right)}{cosh\left(\sqrt{\beta_{mf}}\right)} \tag{A.6.20}$$

### A.7 Flow in the Macro-fracture

The flow equation:

$$\frac{\partial^2 \Delta p_{MF}}{\partial x^2} + \frac{\partial^2 \Delta p_{MF}}{\partial y^2} = \frac{(\phi\, c_t)_{MF}\mu}{k_{MF}} \frac{\partial \Delta p_{MF}}{\partial t} + \frac{\mu}{k_{MF}} q_{Source,mf} \tag{A.7.1}$$

The source term from the micro fracture to macro fracture is $q_{Source,mf}$ . Under the transient flow condition transient flow, the flow from unit volume of the micro-fracture at unit time

$$q_{Source,mf} = \frac{k_{mf}}{\frac{L_f}{2}\mu} \frac{\partial \Delta p_{mf}}{\partial z}\Big|_{z=\frac{L_f}{2}} \tag{A.7.2}$$

From the Eq. A.7.1 and Eq. A.7.2

$$\frac{\partial^2 \Delta p_{MF}}{\partial x^2} + \frac{\partial^2 \Delta p_{MF}}{\partial y^2} - \frac{2}{L_f}\frac{k_{mf}}{k_{MF}} \frac{\partial \Delta p_{mf}}{\partial z}\Big|_{z=\frac{L_f}{2}} = \frac{(\phi\, c_t)_{MF}\mu}{k_{MF}} \frac{\partial \Delta p_{MF}}{\partial t} \tag{A.7.3}$$

Integrating Eq. A.7.3 with respect to x

$$\begin{gathered}\int_0^{x_{HF}} \left(\frac{\partial^2 \Delta p_{MF}}{\partial x^2}\right) \partial x + \int_0^{x_{HF}} \left(\frac{\partial^2 \Delta p_{MF}}{\partial y^2}\right) \partial x - \\ \int_0^{x_{HF}} \left(\frac{2}{L_f}\frac{k_{mf}}{k_{MF}} \frac{\partial \Delta p_{mf}}{\partial z}\Big|_{z=\frac{L_f}{2}}\right) \partial x = \int_0^{x_{HF}} \left(\frac{(\phi\, c_t)_{MF}\mu}{k_{MF}} \frac{\partial \Delta p_{MF}}{\partial t}\right) \partial x\end{gathered} \tag{A.7.4}$$

Assuming the pseudo-function assumption:

$$\frac{\partial \Delta p_{MF}}{\partial y} \neq f(x)$$

$$\frac{\partial \Delta p_{mf}}{\partial z} \neq f(x)$$

By using these relation in Eq. A.7.4

$$\frac{1}{x_{HF}}\frac{\partial \Delta p_{MF}}{\partial x} + \frac{\partial^2 \Delta p_{MF}}{\partial y^2} - \frac{2}{L_f}\frac{k_{mf}}{k_{MF}}\frac{\partial \Delta p_{mf}}{\partial z}\Big|_{z=\frac{L_f}{2}} = \frac{(\phi\, c_t)_{MF}\mu}{k_{MF}}\frac{\partial \Delta p_{MF}}{\partial t} \tag{A.7.5}$$

In dimensionless form

$$\frac{\partial p_{MFD}}{\partial x_D} + \frac{\partial^2 p_{MFD}}{\partial {y_D}^2} - \frac{\lambda_{mf}}{3}\frac{\partial p_{mfD}}{\partial z_D}_{|z_D=1} = \frac{\partial p_{MFD}}{\partial t_D} \tag{A.7.6}$$

After Laplace transformation

$$\frac{\partial \bar{p}_{MFD}}{\partial x_D} + \frac{\partial^2 \bar{p}_{MFD}}{\partial {y_D}^2} - \frac{\lambda_{mf}}{3}\frac{\partial \bar{p}_{mfD}}{\partial z_D}_{|z_D=1} = s\bar{p}_{MFD} - p_{MFD_{|t_D=0}} \tag{A.7.7}$$

The initial condition for the macro-fracture

$$\Delta p_{MF}(x, y, o) = p_i \tag{A.7.8}$$

$$p_{MFD(x_D, y_D, t_D=0)} = 0 \tag{A.7.9}$$

Inner boundary condition in the $x$ direction

$$q_0(x_{HF}, y, t) = q_{MF}(x_{HF}, y, t) \tag{A.7.10}$$

$$\frac{k_{\alpha o}(h_{MF} + L_f)}{\mu}\frac{\partial^{1-\alpha o}}{\partial t^{1-\alpha o}}\left(\frac{\partial \Delta p_0}{\partial x}\right)_{x=x_{HF}} = \frac{k_{MF}h_{MF}}{\mu}\left(\frac{\partial \Delta p_{MFD}}{\partial x}\right)_{x=x_{HF}} \tag{A.7.11}$$

In dimensionless form

$$\begin{aligned}&\left(\frac{\partial p_{MFD}}{\partial x_D}\right)_{x_D=1}\\ &= \frac{k_{\alpha o}(h_{MF} + L_f)}{k_{MF}h_{MF}}\left(\frac{(\phi\, c_t)_{MF}\mu x_{HF}^2}{k_{MF}}\right)^{\alpha o-1}\frac{\partial^{1-\alpha o}}{\partial {t_D}^{1-\alpha o}}\left(\frac{\partial p_{0D}}{\partial x_D}\right)_{x_D=1}\end{aligned} \tag{A.7.12}$$

In Laplace domain

$$\left(\frac{\partial \bar{p}_{MFD}(x,y,s)}{\partial x_D}\right)_{x_D=1} = C_{OMF}\left(\frac{(\phi\, c_t)_{MF}\mu x_{HF}^2}{k_{MF}}\right)^{\alpha o-1} s^{1-\alpha o}\left(\frac{\partial \bar{p}_{oD}(x,y,s)}{\partial x_D}\right)_{x_D=1} \quad \text{(A.7.13)}$$

Here, $C_{OMF} = \frac{k_{\alpha o}(h_{MF}+L_f)}{k_{MF}h_{MF}}$

Differentiating the Eq. A.2.27

$$\left(\frac{\partial \bar{p}_{oD}}{\partial x_D}\right) = \bar{p}_{MFD_{|x_D=1}} \frac{1}{\cosh(\sqrt{\beta_o}(x_{eD}-1))} - \sqrt{\beta_o}\sinh(\sqrt{\beta_o}(x_{eD} - x_D)) \quad \text{(A.7.14)}$$

$$\left(\frac{\partial \bar{p}_{oD}}{\partial x_D}\right)_{x_D=1} = -\bar{p}_{MFD_{|x_D=1}}\sqrt{\beta_o}\tanh\left(\sqrt{\beta_o}(x_{eD}-1)\right) \quad \text{(A.7.15)}$$

$$\left(\frac{\partial \bar{p}_{oD}}{\partial x_D}\right)_{x_D=1} = -\bar{p}_{MFD_{|x_D=1}}\beta_{OMF} \quad \text{(A.7.16)}$$

Substituting the value of Eq. A.7.16 in the Eq. A.7.13

$$\left(\frac{\partial \bar{p}_{MFD}}{\partial x_D}\right)_{x_D=1} = -C_{OMF}\left(\frac{(\phi\, c_t)_{MF}\mu x_{HF}^2}{k_{MF}}\right)^{\alpha o-1} s^{1-\alpha o}\beta_{OMF}\bar{p}_{MFD_{|x_D=1}} \quad \text{(A.7.17)}$$

$$\left(\frac{\partial \bar{p}_{MFD}}{\partial x_D}\right)_{x_D=1} = -\beta_{OMFD}\bar{p}_{MFD_{|x_D=1}} \quad \text{(A.7.18)}$$

Differentiating the Eq. A.6.20

$$\frac{\partial \bar{p}_{mfD}}{\partial z_D}_{|z_D=1} = \bar{p}_{MFD_{|z_D=1}}\sqrt{\beta_{mf}}\tanh\left(\sqrt{\beta_{mf}}\right) \quad \text{(A.7.19)}$$

Using the A.7.9, A.7.18, A.7.19 in A.7.7

$$-\beta_{OMFD}\bar{p}_{MFD_{|x_D=1}} + \frac{\partial^2 \bar{p}_{MFD}}{\partial {y_D}^2} - \frac{\lambda_{mf}}{3}\sqrt{\beta_{mf}}\tanh\left(\sqrt{\beta_{mf}}\right)\bar{p}_{MFD_{|z_D=1}} - s\overline{\Delta p}_{MFD} = 0 \quad \text{(A.7.20)}$$

According to the pseudo-function assumption $\bar{p}_{MFD}$ is not the function of micro-fracture and outer reservoir. So, it can be assumed that $\bar{p}_{MFD_{|x_D=1}} = \bar{p}_{MFD_{|z_D=1}} = \bar{p}_{MFD}$.

Therefore, A.7.20 gives

$$\frac{\partial^2 \bar{p}_{MFD}}{\partial {y_D}^2} - \beta_{MF}\bar{p}_{MFD} = 0 \tag{A.7.21}$$

Here $\beta_{MF} = \beta_{OMFD} + \frac{\lambda_{mf}}{3}\sqrt{\beta_{mf}}\tanh\left(\sqrt{\beta_{mf}}\right) + s$

The general solution of the Eq. A.7.21

$$\bar{p}_{MFD} = Aexp\left(-\sqrt{\beta_{MF}}y_D\right) + Bexp\left(\sqrt{\beta_{MF}}y_D\right) \tag{A.7.22}$$

In the inner boundary of the $y$ axis, there is a no flow boundary. So

$$\frac{\partial \Delta p_{MF}}{\partial y}_{|y=y_e} = 0 \tag{A.7.23}$$

$$\frac{\partial \bar{p}_{MFD}(x_D, y_D, s)}{\partial y_D}_{|y_D=y_{eD},s} = 0 \tag{A.7.24}$$

Pressure continuity at the outer reservoir yields

$$\Delta p_{MF}{}_{|y=\frac{w}{2}} = \Delta p_{HF}{}_{|y=\frac{w}{2}} \tag{A.7.25}$$

$$\bar{p}_{MFD}{}_{|y_D=\frac{w_D}{2}} = \bar{p}_{HFD}{}_{|y_D=\frac{w_D}{2}} \tag{A.7.26}$$

Now from the Eq. A.7.22

$$\frac{\partial \bar{p}_{MFD}}{\partial y_D}_{|y_D=y_{eD},s} = 0 \tag{A.7.27}$$

$$= -\sqrt{\beta_{MF}}Aexp\left(-\sqrt{\beta_{MF}}y_{eD}\right) + \sqrt{\beta_{MF}}Bexp\left(\sqrt{\beta_{MF}}y_{eD}\right)$$

$$A = Bexp\left(2\sqrt{\beta_{MF}}y_{eD}\right) \tag{A.7.28}$$

From the Eq. A.7.22 and A.7.28

$$\bar{p}_{MFD} = Bexp\left(\sqrt{\beta_{MF}}y_{eD}\right)2\cosh\left(\sqrt{\beta_{MF}}(y_{eD} - y_D)\right) \tag{A.7.29}$$

Using the outer boundary condition

$$B = \frac{\bar{p}_{HFD}{}_{|y_D=\frac{w_D}{2}}}{2exp\left(\sqrt{\beta_{MF}}y_{eD}\right)\cosh\left(\sqrt{\beta_{MF}}(y_{eD} - \frac{w_D}{2})\right)} \tag{A.7.30}$$

The final pressure solution for the macro-fracture is derived from the Eq. A.7.29 and Eq. A.7.30

$$\bar{p}_{MFD} = \bar{p}_{HFD}{}_{|y_D=\frac{w_D}{2}}\frac{\cosh\left(\sqrt{\beta_{MF}}(y_{eD} - y_D)\right)}{\cosh\left(\sqrt{\beta_{MF}}(y_{eD} - \frac{w_D}{2})\right)} \tag{A.7.31}$$

**A.8 Flow in the Hydraulic fracture**

Eq. A.1.20 is the characteristics equation for the fluid flow in the hydraulic fracture. The governing equation is

$$\frac{\partial}{\partial x}\left(\frac{k_\beta}{\mu}\frac{\partial^\beta \Delta p_{HF}}{\partial x^\beta}\right)+\frac{\partial}{\partial y}\left(\frac{k_\beta}{\mu}\frac{\partial^\beta \Delta p_{HF}}{\partial y^\beta}\right)=(\phi\, c_t)_{HF}\,\frac{\partial \Delta p_{HF}}{\partial t} \tag{A.8.1}$$

$$\frac{\partial}{\partial x}\left(\frac{\partial^\beta \Delta p_{HF}}{\partial x^\beta}\right)+\frac{\partial}{\partial y}\left(\frac{\partial^\beta \Delta p_{HF}}{\partial y^\beta}\right)=\frac{(\phi\, c_t)_{HF}\mu}{k_\beta}\,\frac{\partial \Delta p_{HF}}{\partial t} \tag{A.8.2}$$

Integrating the Eq. A.8.2 along the y axis

$$\int_0^{\frac{w}{2}}\left(\frac{\partial}{\partial x}\left(\frac{\partial^\beta \Delta p_{HF}}{\partial x^\beta}\right)\right)\partial y+\int_0^{\frac{w}{2}}\left(\frac{\partial}{\partial y}\left(\frac{\partial^\beta \Delta p_{HF}}{\partial y^\beta}\right)\right)\partial y=\int_0^{\frac{w}{2}}\left(\frac{(\phi\, c_t)_{HF}\mu}{k_\beta}\,\frac{\partial \Delta p_{HF}}{\partial t}\right)\partial y \tag{A.8.3}$$

Pseudo-function assumption

$$\frac{\partial^\beta \Delta p_{HF}}{\partial x^\beta}\neq f(y) \tag{A.8.4}$$

That implies

$$\frac{\partial}{\partial x}\left(\frac{\partial^\beta \Delta p_{HF}}{\partial x^\beta}\right)+\frac{2}{w}\left(\frac{\partial^\beta \Delta p_{HF}}{\partial y^\beta}\right)_{y=\frac{w}{2}}=\frac{(\phi\, c_t)_{HF}\mu}{k_\beta}\,\frac{\partial \Delta p_{HF}}{\partial t} \tag{A.8.5}$$

The Dimensionless form of the Eq. A.8.5

$$\frac{\partial}{\partial x_D}\left(\frac{\partial^\beta p_{HFD}}{\partial {x_D}^\beta}\right)+\frac{2}{w_D}\left(\frac{\partial^\beta p_{HFD}}{\partial {y_D}^\beta}\right)_{y_D=\frac{w_D}{2}}=\omega_{HF}\lambda_{AF}\frac{\partial p_{HFD}}{\partial t_D} \tag{A.8.6}$$

$$\frac{\partial}{\partial x_D}\left(\frac{\partial^\beta p_{HFD}}{\partial {x_D}^\beta}\right)+\frac{2}{w_D}\left(\frac{\partial^\beta p_{HFD}}{\partial {y_D}^\beta}\right)_{y_D=\frac{w_D}{2}}=M_{DAHF}\frac{\partial p_{HFD}}{\partial t_D} \tag{A.8.7}$$

Initial Condition for the hydraulic fracture

$$\Delta p_{HF}(x,y,o)=0 \tag{A.8.8}$$

$$p_{HFD}(x_D,y_D,o)=0 \tag{A.8.9}$$

At the outer boundary of $y$ axis, there is a continuity of flux between the hydraulic fracture and the macro-fracture

$$q_{HF}\left(y=\frac{w}{2},t\right)=q_{MF}\left(y=\frac{w}{2},t\right) \tag{A.8.10}$$

$$\left(\frac{\partial^{\beta}\Delta p_{HF}}{\partial y^{\beta}}\right)_{y=\frac{w}{2}} = \frac{k_{MF}h_{MF}}{k_{\beta}(h_{MF}+L_f)}\left(\frac{\partial \Delta p_{MF}}{\partial y}\right)_{y=\frac{w}{2}} \tag{A.8.11}$$

$$\left(\frac{\partial^{\beta} p_{HFD}}{\partial {y_D}^{\beta}}\right)_{y_D=\frac{w_D}{2}} = \lambda'_{AF}\left(\frac{\partial p_{MFD}}{\partial y_D}\right)_{y_D=\frac{w_D}{2}} \tag{A.8.12}$$

$$\left(\frac{\partial^{\beta} \bar{p}_{HFD}}{\partial {y_D}^{\beta}}\right)_{y_D=\frac{w_D}{2}} = \lambda'_{AF}\left(\frac{\partial \bar{p}_{MFD}}{\partial y_D}\right)_{y_D=\frac{w_D}{2}} \tag{A.8.13}$$

From the Eq. A.7.31

$$\left(\frac{\partial \bar{p}_{MFD}}{\partial y_D}\right)_{y_D=\frac{w_D}{2}} = -\sqrt{\beta_{MF}}\tanh\left(\sqrt{\beta_{MF}}(y_{eD}-\frac{w_D}{2})\right)\bar{p}_{HFD}|_{y_D=\frac{w_D}{2}} \tag{A.8.14}$$

Substituting the Eq. A.8.14 in Eq. A.8.13

$$\left(\frac{\partial \bar{p}_{HFD}}{\partial {y_D}^{\beta}}\right)_{y_D=\frac{w_D}{2}} = -\lambda'_{AF}\sqrt{\beta_{MF}}\tanh\left(\sqrt{\beta_{MF}}(y_{eD}-\frac{w_D}{2})\right)\bar{p}_{HFD}|_{y_D=\frac{w_D}{2}} \tag{A.8.15}$$

$$\left(\frac{\partial \bar{p}_{HFD}}{\partial {y_D}^{\beta}}\right)_{y_D=\frac{w_D}{2}} = -\beta_{MHF}\bar{p}_{HFD}|_{y_D=\frac{w_D}{2}} \tag{A.8.16}$$

Laplace transformation of Eq. A.8.7

$$\frac{\partial}{\partial x_D}\left(\frac{\partial^{\beta}\bar{p}_{HFD}(x,y,s)}{\partial {x_D}^{\beta}}\right)+\frac{2}{w_D}\left(\frac{\partial^{\beta}\bar{p}_{HFD}(x,y,s)}{\partial {y_D}^{\beta}}\right)_{y_D=\frac{w_D}{2}} = M_{DAHF}\left(s\bar{p}_{HFD}-p_{HFD}(x,y,0)\right) \tag{A.8.17}$$

Using Eq. A.8.9 and Eq. A.8.16 in Eq. A.8.17

$$\frac{\partial}{\partial x_D}\left(\frac{\partial^{\beta}\bar{p}_{HFD}}{\partial {x_D}^{\beta}}\right)-\frac{2}{w_D}\beta_{MHF}\bar{p}_{HFD}|_{y_D=\frac{w_D}{2}} = M_{DAHF}s\bar{p}_{HFD} \tag{A.8.18}$$

Linear flow assumption implies that the magnitude of the macro-fracture pressure is independent of the location at the macro-fracture.

$$\frac{\partial}{\partial x_D}\left(\frac{\partial^{\beta}\bar{p}_{HFD}}{\partial {x_D}^{\beta}}\right)-\beta_{HF}\bar{p}_{HFD}=0 \tag{A.8.19}$$

Here $\beta_{HF}=\frac{2}{w_D}\beta_{MHF}+M_{DAHF}s$

The Laplace transformation of the Eq. A.8.19 for the space is

$$\tilde{s}\left[\tilde{s}^{\beta}\bar{\bar{p}}(s,\tilde{s})-\tilde{s}^{\beta-1}\bar{p}_{HFD}(0,s)\right]-\left(\frac{\partial^{\beta}\bar{p}_{HFD}(x_D,s)}{\partial {x_D}^{\beta}}\right)_{x_D=0}-\beta_{HF}\bar{\bar{p}}(s,\tilde{s}) \tag{A.8.20}$$

$$=0$$

$$[\tilde{s}^{\beta+1}\overline{\overline{\Delta p}}(s,\tilde{s})-\tilde{s}^{\beta}\overline{\Delta p}_{HFD}(0,s)-\left(\frac{\partial\overline{\Delta p}_{HFD}(x_D,s)}{\partial {x_D}^{\beta}}\right)_{x_D=0}-\beta_{HF}\overline{\overline{\Delta p}}(s,\tilde{s})$$

$$=0$$

$$\overline{\overline{\Delta p}}(s,\tilde{s})\left(\tilde{s}^{\beta+1}-\beta_{HF}\right)-\tilde{s}^{\beta}\overline{\Delta p}_{HFD}(0,s)-\left(\frac{\partial\overline{\Delta p}_{HFD}(x_D,s)}{\partial {x_D}^{\beta}}\right)_{x_D=0}=0]$$

$$\bar{\bar{p}}(s,\tilde{s})=\frac{\tilde{s}^{\beta}}{\tilde{s}^{\beta+1}-\beta_{HF}}\bar{p}_{HFD}(0,s)+\frac{1}{\tilde{s}^{\beta+1}-\beta_{HF}}\left(\frac{\partial^{\beta}\bar{p}_{HFD}(x_D,s)}{\partial {x_D}^{\beta}}\right)_{x_D=0} \tag{A.8.21}$$

$$=0$$

From the definition of the Mittag-Leffler function

$$\mathcal{L}\left[x^{\beta-1}E_{\alpha,\beta}(ax^{\alpha})\right]=\frac{s^{\alpha-\beta}}{s^{\alpha}-a} \tag{A.8.22}$$

Inverting the Eq. A.8.21 with properties of A.8.22

$$\bar{p}_{HFD}(x_D,s)=\bar{p}_{HFD}(0,s)E_{\beta+1}\left(\beta_{HF}{x_D}^{\beta+1}\right)+{x_D}^{\beta}E_{\beta+1,\beta+1}(\beta_{HF}{x_D}^{\beta+1})\left(\frac{\partial\bar{p}_{HFD}(x_D,s)}{\partial {x_D}^{\beta}}\right)_{x_D=0} \tag{A.8.23}$$

Constant flow rate at the inner boundary at the $x$ direction gives

$$u=-\frac{k_{\beta}}{\mu}\left(\frac{\partial^{\beta}\Delta p_{HF}}{\partial x^{\beta}}\right)_{x=0} \tag{A.8.24}$$

An integration is done to determine the total flow

$$\int_0^{\frac{w}{2}}\int_0^{\frac{h}{2}}u\,\partial z\partial y=-\frac{k_{\beta}}{\mu}\int_0^{\frac{w}{2}}\int_0^{\frac{h}{2}}\left(\frac{\partial^{\beta}\Delta p_{HF}}{\partial x^{\beta}}\right)_{x=0}\partial z\partial y \tag{A.8.25}$$

$$\frac{q}{4*2}=-\frac{k_{\beta}}{\mu}\frac{w}{2}\frac{h}{2}\left(\frac{\partial^{\beta}\Delta p_{HF}}{\partial x^{\beta}}\right)_{x=0} \tag{A.8.26}$$

In dimensionless form

$$\left(\frac{\partial^{\beta} p_{HFD}}{\partial {x_D}^{\beta}}\right)_{x_D=0} = -\frac{\pi k_{MF} {x_{HF}}^{\beta}}{Bwk_{\beta}} \tag{A.8.27}$$

$$\left(\frac{\partial^{\beta} \bar{p}_{HFD}}{\partial {x_D}^{\beta}}\right)_{x_D=0} = -\frac{\pi}{c_{AFD} s} \tag{A.8.28}$$

This inner boundary condition is substituted in the Eq. A.8.23

$$\begin{aligned} \bar{p}_{HFD}(x_D, s) = {} & \bar{p}_{HFD}(0, s) E_{\beta+1}\left(\beta_{HF} {x_D}^{\beta+1}\right) \\ & - \frac{\pi}{c_{AFD} s} {x_D}^{\beta} E_{\beta+1,\beta+1}(\beta_{HF} {x_D}^{\beta+1}) \end{aligned} \tag{A.8.29}$$

Due to a no-flow boundary at the tip of the hydraulic fracture

$$\frac{\partial \Delta p_{HF}}{\partial x}_{|x=x_{HF},t} = 0 \tag{A.8.30}$$

$$\frac{\partial \bar{p}_{HFD}}{\partial x_D}_{|x_D=1,s} = 0 \tag{A.8.31}$$

Using the derivative properties of the Mittag-Leffler function (Hombole *et. al.*, 2011)

$$\frac{d}{dx_D}\left[{x_D}^{\beta} E_{\beta+1,\beta+1}(\beta_{HF} {x_D}^{\beta+1})\right] = {x_D}^{\beta-1} E_{\beta+1,\beta}\left(\beta_{HF} {x_D}^{\beta+1}\right) \tag{A.8.32}$$

From Fomin *et. al.*, 2010

$$\frac{d}{dx}\left[E_{\beta+1}(\beta_{HF} {x_D}^{\beta+1})\right] = \beta_{HF} {x_D}^{\beta} E_{\beta+1,\beta+1}(\beta_{HF} {x_D}^{\beta+1}) \tag{A.8.33}$$

Through the Eq. A.8.29, Eq. A.8.32 and Eq. A.8.33

$$\frac{\partial \bar{p}_{HFD}}{\partial x_D}_{|x_D=1,s} = \bar{p}_{HFD}(0, s) \beta_{HF} E_{\beta+1,\beta+1}(\beta_{HF}) - \frac{\pi}{c_{AFD} s} E_{\beta+1,\beta}(\beta_{HF}) = 0 \tag{A.8.34}$$

$$\bar{p}_{HFD}(0, s) = \frac{\pi E_{\beta+1,\beta}(\beta_{HF})}{c_{AFD} s \beta_{HF} E_{\beta+1,\beta+1}(\beta_{HF})} \tag{A.8.35}$$

Substitute Eq. A.8.35 in Eq. A.8.29

$$\begin{aligned} \bar{p}_{HFD}(x_D, s) = \frac{\pi}{c_{AFD} s} \Bigg\{ & \frac{E_{\beta+1,\beta}(\beta_{HF})}{\beta_{HF} E_{\beta+1,\beta+1}(\beta_{HF})} E_{\beta+1}\left(\beta_{HF} {x_D}^{\beta+1}\right) \\ & - {x_D}^{\beta} E_{\beta+1,\beta+1}\left(\beta_{HF} {x_D}^{\beta+1}\right) \Bigg\} \end{aligned} \tag{A.8.36}$$

This is the expression for the dimensionless hydraulic fracture pressure for the constant terminal rate flow.

At $x_D = 0$ the hydraulic fracture pressure will be the bottom-hole pressure

$$\bar{p}_{wD}(x_D, s) = \frac{\pi}{c_{AFD} s}\left\{\frac{E_{\beta+1,\beta}(\beta_{HF})}{\beta_{HF} E_{\beta+1,\beta+1}(\beta_{HF})}\right\} \tag{A.8.37}$$

$E_{\beta+1}(0) \approx 1$

This is the expression for the dimensionless bottom-hole pressure for the constant terminal rate flow.

# Appendix B

# Derivation of the Flow Solution for A Rectangular Matrix Block

The governing flow equation for the matrix block

$$\frac{\partial^2 \Delta p_m}{\partial \zeta^2} = \frac{(\phi\, c_t)_m \mu}{k_{mc}} \frac{\partial \Delta p_m}{\partial t} \tag{B.1}$$

Dimensionless initial Condition

$$p_{mD(\zeta_D,0)} = 0 \tag{B.2}$$

Dimensionless inner boundary condition

$$\frac{\partial p_{cmD}}{\partial \zeta_D}_{|\zeta_D=0} = 0 \tag{B.3}$$

$$\frac{\partial \bar{p}_{cmD}}{\partial \zeta_D}_{|\zeta_D=0} = 0 \tag{B.4}$$

Dimensionless outer boundary condition

$$\Delta p_m\Big|_{\zeta=\frac{y_f}{2}} = \Delta p_{mf}\Big|_{\zeta=\frac{y_f}{2}} \tag{B.5}$$

$$\bar{p}_{mD_{|\zeta_D=1}} = \bar{p}_{mfD_{|\zeta_D=1}} \tag{B.6}$$

Eq. B.1 in dimensionless form

$$\frac{\partial^2 p_{mD}}{\partial \zeta_D{}^2} - \frac{3\omega_m}{\lambda_m} \frac{\partial p_{mD}}{\partial t_D} = 0 \tag{B.7}$$

Eq. B.7 in Laplace domain with initial condition

$$\frac{\partial^2 \bar{p}_{mD}}{\partial \zeta_D{}^2} - \alpha_m \bar{p}_{mD}(\zeta_D, s) = 0 \tag{B.8}$$

Here $\alpha_m = \frac{3\omega_m s}{\lambda_m}$

The general Solution

$$\bar{p}_{mD} = A exp\left(-\sqrt{\alpha_m}\zeta_D\right) + B exp\left(\sqrt{\alpha_m}\zeta_D\right) \tag{B.9}$$

Applying the boundary condition (Eq. B. 4 and Eq. B.6), the pressure solution is derived

$$\bar{p}_{mD} = \frac{\bar{p}_{mfD} cosh\left(\sqrt{\alpha_m}\zeta_D\right)}{cosh\left(\sqrt{\alpha_m}\right)} \tag{B.10}$$

A source of flux is transferred to the micro-fracture at $\zeta = \frac{y_f}{2}$ at transient flow condition and evaluated as

$$q_{Source,m} = \frac{k_m}{\frac{y_f}{2}\mu} \frac{\partial \Delta p_m}{\partial \zeta}\Big|_{\zeta=\frac{y_f}{2}} \tag{B.11}$$

The flow equation in the micro-fracture with the source term

$$\frac{\partial^2 \Delta p_{mf}}{\partial z^2} = \frac{(\phi\, c_t)_{mf}\mu}{k_{mf}} \frac{\partial \Delta p_{mf}}{\partial t} + \frac{k_m}{k_{mf}} \frac{2}{y_f} \frac{\partial \Delta p_m}{\partial \zeta}\Big|_{\zeta=\frac{y_f}{2}} \tag{B.12}$$

Dimensionless form of Eq. B.12

$$\frac{\partial^2 p_{mfD}}{\partial {z_D}^2} = \frac{3\omega_{mf}}{\lambda_{mf}} \frac{\partial p_{mfD}}{\partial t_D} + \lambda'_{mf} \frac{\partial p_{mD}}{\partial \zeta_D}_{|\zeta=1} \tag{B.13}$$

Differentiating the Eq. B.10

$$\frac{\partial \bar{p}_{mD}}{\partial \xi_D}_{|\xi_D=1} = \bar{p}_{mfD}\sqrt{\alpha_m}\tanh\left(\sqrt{\alpha_m}\right) \tag{B.14}$$

Transforming the Eq. B.13 in Laplace domain and using the initial condition and Eq. B.14

$$\frac{\partial^2 \bar{p}_{mfD}}{\partial {z_D}^2} - \frac{3\omega_{mf} s}{\lambda_{mf}} \bar{p}_{mfD} - \beta_m \bar{p}_{mfD_{|\xi_D=1}} = 0 \tag{B.15}$$

Here, $\beta_m = \lambda'_{mf}\sqrt{\alpha_m}\tanh\left(\sqrt{\alpha_m}\right)$

$$\frac{\partial^2 \bar{p}_{mfD}}{\partial {z_D}^2} - \beta'_{mf}\bar{p}_{mfD} = 0 \tag{B.16}$$

$Here, \beta'_{mf} = \frac{3\omega_{mf} s}{\lambda_{mf}} + \beta_m$

The solution of the Eq. B.16 is follows the same procedure through the Eq. A.616 to Eq. A.6.20 and is applying the same boundary condition (Eq. A.6.8 and Eq. A.6.10). The final solution is given as

$$\bar{p}_{mfD} = \bar{p}_{MFD_{|z_D=1}} \frac{cosh\left(\sqrt{\beta'_{mf}} z_D\right)}{cosh\left(\sqrt{\beta'_{mf}}\right)} \tag{B.17}$$

# Appendix C

## Derivation of the Pressure Solution for a Two-Dimensional Linear Flow in the Hydraulic Fracture

The flow equation in the macro-fracture is the same as in Appendix A (Eq. A.7.31)

$$\overline{\Delta p}_{MFD} = \overline{\Delta p}_{HFD}|_{y_D=\frac{w_D}{2}} \frac{\cosh\left(\sqrt{\beta_{MF}}(y_{eD}-y_D)\right)}{\cosh\left(\sqrt{\beta_{MF}}(y_{eD}-\frac{w_D}{2})\right)} \tag{C.1}$$

The characteristics equation for a two-dimensional flow in the hydraulic fracture

$$\frac{\partial}{\partial x}\left(\frac{\partial \Delta p_{HF}}{\partial x}\right)+\frac{\partial}{\partial y}\left(\frac{\partial \Delta p_{HF}}{\partial y}\right)=\frac{(\phi\, c_t)_{HF}\mu}{k_{HF}}\,\frac{\partial \Delta p_{HF}}{\partial t} \tag{C.2}$$

Integrating Eq. C.2 along the $y$ axis from $0\ to\ \frac{w}{2}$ and applying the pseudo-function assumption gives

$$\frac{\partial}{\partial x}\left(\frac{\partial \Delta p_{HF}}{\partial x}\right)+\frac{2}{w}\left(\frac{\partial \Delta p_{HF}}{\partial y}\right)_{y=\frac{w}{2}}=\frac{(\phi\, c_t)_{HF}\mu}{k_{HF}}\,\frac{\partial \Delta p_{HF}}{\partial t} \tag{C.3}$$

Converting the Eq. C.3 in dimensionless form

$$\frac{\partial}{\partial x_D}\left(\frac{\partial p_{HFD}}{\partial x_D}\right)+\frac{2}{w_D}\left(\frac{\partial p_{HFD}}{\partial y_D}\right)_{y_D=\frac{w_D}{2}}=\frac{(\phi\, c_t)_{HF}}{(\phi\, c_t)_{MF}}\frac{k_{MF}}{k_{HF}}\frac{\partial p_{HFD}}{\partial t_D} \tag{C.4}$$

$$\frac{\partial}{\partial x_D}\left(\frac{\partial p_{HFD}}{\partial x_D}\right)+\frac{2}{w_D}\left(\frac{\partial p_{HFD}}{\partial y_D}\right)_{y_D=\frac{w_D}{2}}=\eta_{HFD}\frac{\partial p_{HFD}}{\partial t_D} \tag{C.5}$$

Initial condition

$$\Delta p_{HF}(x,y,o)=0 \tag{C.6}$$

$$p_{HFD}(x_D,y_D,o)=0 \tag{C.7}$$

At the outer boundary ($y=\frac{w}{2}$) the flux is continuous as it is in macro-fracture

$$\frac{k_{HF}}{\mu}\left(\frac{\partial \Delta p_{HF}}{\partial y}\right)_{y=\frac{w}{2}}=\frac{k_{MF}h_{MF}}{\mu(h_{MF}+L_f)}\left(\frac{\partial \Delta p_{MF}}{\partial y}\right)_{y=\frac{w}{2}} \tag{C.8}$$

$$\left(\frac{\partial p_{HFD}}{\partial y_D}\right)_{y_D=\frac{w_D}{2}}=\frac{k_{MF}h_{MF}}{k_{HF}(h_{MF}+L_f)}\left(\frac{\partial p_{MFD}}{\partial y_D}\right)_{y_D=\frac{w_D}{2}} \tag{C.9}$$

$$\left(\frac{\partial p_{HFD}}{\partial y_D}\right)_{y_D=\frac{w_D}{2}} = \lambda'_{HF}\left(\frac{\partial p_{MFD}}{\partial y_D}\right)_{y_D=\frac{w_D}{2}} \quad \text{(C.10)}$$

$$\left(\frac{\partial \bar{p}_{HFD}(x_D, y_D, s)}{\partial y_D}\right)_{y_D=\frac{w_D}{2}} = \lambda'_{HF}\left(\frac{\partial \bar{p}_{MFD}(x_D, y_D, s)}{\partial y_D}\right)_{y_D=\frac{w_D}{2}} \quad \text{(C.11)}$$

Differentiate Eq. C.1 with respect to $y_D$

$$\left(\frac{\partial \bar{p}_{MFD}}{\partial y_D}\right)_{y_D=\frac{w_D}{2}} = -\sqrt{\beta_{MF}}\tanh\left(\sqrt{\beta_{MF}}(y_{eD} - \frac{w_D}{2})\right)\bar{p}_{HFD}|_{y_D=\frac{w_D}{2}} \quad \text{(C.12)}$$

From the Eq. C.11 and C.12

$$\left(\frac{\partial \bar{p}_{HFD}}{\partial y_D}\right)_{y_D=\frac{w_D}{2}} = -\beta'_{MHF}\bar{p}_{HFD}|_{y_D=\frac{w_D}{2}} \quad \text{(C.13)}$$

$Here, \beta'_{MHF} = \lambda'_{HF}\sqrt{\beta_{MF}}\tanh\left(\sqrt{\beta_{MF}}(y_{eD} - \frac{w_D}{2})\right)$

Transforming the Eq. C.5 in Laplace domain and using the Eq. C.7

$$\frac{\partial^2 \bar{p}_{HFD}(x_D, y_D, s)}{\partial {x_D}^2} + \frac{2}{w_D}\left(\frac{\partial \bar{p}_{HFD}(x_D, y_D, s)}{\partial y_D}\right)_{y_D=\frac{w_D}{2}} = \eta_{HFD} s\bar{p}_{HFD}(x_D, y_D, s) \quad \text{(C.14)}$$

From the Eq. C.13 and Eq. C.14

$$\frac{\partial^2 p_{HFD}}{\partial {x_D}^2} - \frac{2}{w_D}\beta'_{MHF}\bar{p}_{HFD}|_{y_D=\frac{w_D}{2}} = \eta_{HFD} s\bar{p}_{HFD} \quad \text{(C.15)}$$

$$\frac{\partial^2 p_{HFD}}{\partial {x_D}^2} - \beta'_{HF}\bar{p}_{HFD} = 0 \quad \text{(C.16)}$$

Here, $\beta'_{HF} = \frac{2}{w_D}\beta'_{MHF} + \eta_{HFD} s$

The general solution of Eq. C.16

$$\bar{p}_{HFD} = Aexp\left(-\sqrt{\beta'_{HF}}x_D\right) + Bexp(\sqrt{\beta'_{HF}}x_D) \quad \text{(C.17)}$$

In the inner boundary of $x$ direction, there exists a constant flow rate at the well. Thus, the inner boundary condition at Laplace domain

$$\left(\frac{\partial \bar{p}_{HFD}}{\partial x_D}\right)_{x_D=0} = -\frac{\pi k_{MF} x_{HF}}{Bwk_{HF} s} \quad \text{(C.18)}$$

$$\left(\frac{\partial \bar{p}_{HFD}}{\partial x_D}\right)_{x_D=0} = -\frac{\pi}{c_{HFD}s} \tag{C.19}$$

The outer boundary in the $x$ direction is the tip of the hydraulic-fracture. A no-flow boundary at the tip of the fracture implies

$$\frac{\partial \Delta p_{HF}}{\partial x}_{|x=x_{HF},t} = 0 \tag{C.20}$$

$$\frac{\partial \bar{p}_{HFD}}{\partial x_D}_{|x_D=1,s} = 0 \tag{C.21}$$

Using the outer boundary condition in the Eq. C.17 gives

$$A = Bexp(2\sqrt{\beta'_{HF}}) \tag{C.22}$$

From the Eq. C.17 and Eq. C.22

$$\bar{p}_{HFD} = Bexp(\sqrt{\beta'_{HF}})\left(exp\left(\sqrt{\beta'_{HF}}(1-x_D\right) + exp\left(-\sqrt{\beta'_{HF}}(1-x_D\right)\right) \tag{C.23}$$

Applying the inner boundary condition (Eq.C.19) in Eq. C.23 yields

$$B = \frac{\pi}{2c_{HFD}s\sqrt{\beta'_{HF}}exp(\sqrt{\beta'_{HF}})sinh\left(\sqrt{\beta'_{HF}}\right)} \tag{C.24}$$

The final pressure solution for the hydraulic fracture is derived from the Eq. C.23 and C.24

$$\bar{p}_{HFD} = \frac{\pi \cosh\left(\sqrt{\beta'_{HF}}(1-x_D\right)}{c_{HFD}s\sqrt{\beta'_{HF}}sinh\left(\sqrt{\beta_{MF}}\right)} \tag{C.25}$$

This is the expression for the dimensionless hydraulic fracture pressure for the constant terminal rate during a conventional flow in the two-dimension of the fracture.

At $x_D = 0$ the hydraulic fracture pressure will be the bottom-hole pressure.

$$\bar{p}_{wD} = \frac{\pi}{c_{HFD}s\sqrt{\beta'_{HF}}tanh\left(\sqrt{\beta'_{HF}}\right)} \tag{C.26}$$

# Appendix D

## Dimensionless Parameters and Model Parameters for The Comparative Study

$$p_D = \frac{2\pi k_{\alpha,\beta} h \Delta p}{qB\mu}$$

$$t_D = \frac{k_{\alpha,\beta} t}{x_e^2 \phi\, c_t \mu}$$

$$\eta = \frac{k_{\alpha,\beta}}{\phi\, c_t \mu}$$

$$x_D = \frac{x}{x_e}$$

$$\lambda_{\alpha,\beta} = \frac{x_e {x_e}^{\beta}}{\eta \left(\frac{x_e^2 \phi\, c_t \mu}{k_{\alpha,\beta}}\right)^{\alpha}}$$

$$z_D = \frac{z}{\frac{L_{nf}}{2}}$$

$$\omega_m = \frac{(\phi\, c_t)_m}{(\phi\, c_t)_{nf}}$$

$$\lambda_m = \frac{12 x_e^2 k_m}{{L_{nf}}^2 k_{nf}}$$

$$\alpha_m = \frac{3\omega_m s}{\lambda_m}$$

$$y_D = \frac{y}{\frac{y_e}{2}}$$

$$y_{eD} = \frac{y_e}{x_e}$$

$$\lambda_{mf} = \frac{y_e^2 k_m}{{L_{nf}}^2 k_{nf}}$$

$$\alpha_{nf} = \frac{y_{eD}^2 s}{4} + \lambda_{mf}\sqrt{\alpha_m}\tanh\left(\sqrt{\alpha_m}\right)$$

$$\omega_{HF} = \frac{(\phi\, c_t)_{HF}}{(\phi\, c_t)_{nf}}$$

$$k_{HFD} = \frac{k_{HF}}{k_{nf}}$$

$$\lambda_{HF} = \frac{12x_e^2 k_{nf}}{{y_e}^2 k_{MF}}$$

$$c_{AD} = \frac{Bk_{HF}hw}{\pi k_{nf} h_f x_e}$$

$$\alpha_{HF} = \frac{\omega_{HF}}{k_{HFD}} s + \frac{\lambda_{HF}}{3}\sqrt{\alpha_{nf}}\tanh\left(\sqrt{\alpha_{nf}}\right)$$